A CATALOG OF FALLOUT PATTERNS

S. M. Greenfield

R. R. Rapp

P. A. Walters

RM-1676-AEC

16 April 1956

RESEARCH MEMORANDUM

This is a working paper. It may be expanded, modified, or withdrawn at any time.

The RAND Corporation
SANTA MONICA • CALIFORNIA

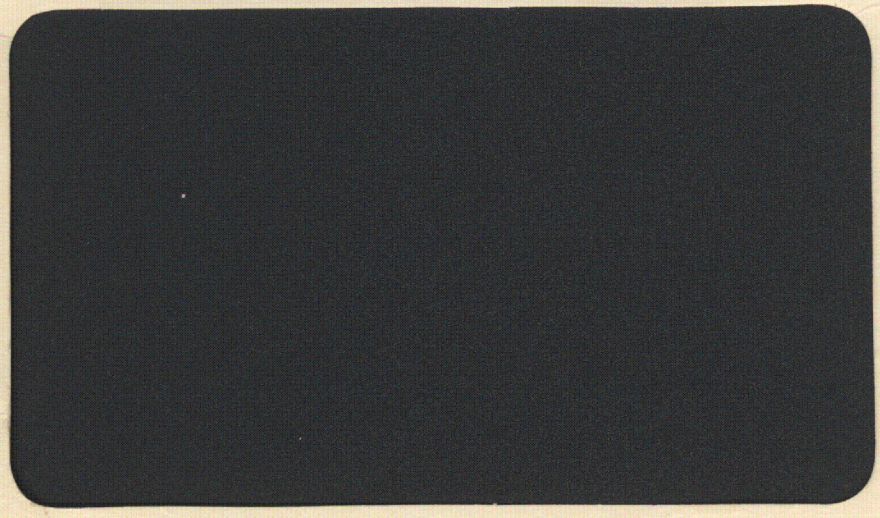

Prepared Under Contract With
The U. S. Atomic Energy Commission Contract No. AT(11-1)-135

RESEARCH MEMORANDUM

A CATALOG OF FALLOUT PATTERNS

S. M. Greenfield

R. R. Rapp

P. A. Walters

RM-1676-AEC

16 April 1956

Assigned to NO NUKES
— JACKSON BROWNE

This is a working paper. It may be expanded, modified, or withdrawn at any time.

The RAND Corporation
1700 MAIN ST. • SANTA MONICA • CALIFORNIA

SUMMARY

In the event of a massive nuclear attack, the combined fallout from quantities of surface-burst nuclear weapons must be considered as a serious hazard over an extended area. This report presents one method for rapidly estimating the fallout from such an attack. It is essentially an analog method and consists of 26 carefully computed fallout patterns together with instructions for matching them approximately to a given yield and wind condition. A brief outline of the basic computational model is given, and possible sources of errors of estimates are discussed.

CONTENTS

Explanatory Figures

Pattern Figures

The 26 pattern figures occupy pages 15 through 92 and are arranged, for each case (place and date) in order of (a) hodograph of winds, (b) dose rate, and (c) dosage.

I. INTRODUCTION

In the past few years it has become increasingly evident that the fallout of radioactive material from an atomic cloud due to a surface burst must be considered a serious hazard. The physical process by which debris is distributed on the ground has been studied in considerable detail by many agencies, and several models have been proposed which satisfactorily reproduce the observed results. It should be noted that these models are considered "satisfactory" in that they reproduce the observed results within the limits of accuracy of the observations. It is recognized that these limits of accuracy can be as high as a factor of two. Falling within these rather broad limits are to be found everything from purely "idealized" patterns which follow a strict, but arbitrary, rule of size and shape and are simply pointed in the direction of a "mean" wind, to an extremely detailed physical model of the fallout which takes into account all possible variations in the actual wind structure.

It is not the purpose of this report to ascertain which philosophy of approach is correct, since advantages and disadvantages exist at both ends of the spectrum. It is the feeling at RAND, however, that in reality no two patterns should be exactly alike, and that the purely idealized patterns do not allow wind variations in space and time to play the important roles they play in actually determining the final pattern. At the same time, it is recognized that the RAND model, which does give some of this required detail, was designed primarily to be a research tool. As such, this model is somewhat cumbersome for routine use.

During our study of this phenomenon we have had occasion to compute the fallout due to several hypothetical bomb yields over a relatively wide range of wind conditions. This is by no means a complete set of possible conditions, but in the past we have found that with some astuteness one could match the wind conditions that prevail in a specific problem with one for which a computation has been made, and could make an adjustment for yield (over a limited range) by a simple change of scale. Such an analog method would allow one to retain the gross effects of the wind variations without resorting to a laborious computing process for each new case. The analog method outlined briefly above is discussed in more detail in Section IV.

II. THE RAND MODEL FOR FALLOUT COMPUTATION

To illustrate the detail that goes into the computation of a fallout pattern using the RAND model, it might be well to outline briefly the model itself.

The basic ballistic equation that applies to any object falling through the atmosphere and affected by the wind at all levels is given, in component form, as follows:

$$X = \sum_h \frac{V_x(h)}{w\,(r,h)} \Delta h$$

$$Y = \sum_h \frac{V_y(h)}{w(r,h)} \Delta h$$

where X and Y are the distances traveled in the component directions; $V_x(h)$ and $V_y(h)$ are the velocity components at a given altitude h; $w(r,h)$ is the vertical-fall velocity applicable to a given object of known size, shape, and density existing at a given altitude h; and Δh is the altitude increment in which $w(r,h)$ and $V(h)$ are considered to remain constant.

It is conceivable that if one were able to describe the spatial distribution of radioactive materials in an atomic cloud from a surface burst completely as to activity, size, and shape, and, furthermore, could describe in terms of well-ordered continuous functions the wind and fall velocity variation with height, then one could compute the ultimate ground position of all the material. This, however, is impractical, mainly because none of the above-mentioned quantities or distributions are known to the required degree of accuracy. As a result, one is forced to make assumptions

and approximations. These assumptions and approximations constitute the chief source of differences among the majority of the proposed fallout computational models. The basic assumptions that constitute the RAND model are as follows:

1. Particles are assumed to be smooth spheres with a density of 2.5 gm/cm^3.
2. Radioactive particles are assumed distributed between the mushroom and the stem so as to place 90 per cent of the total activity in the mushroom.
3. The distribution of activity and particle size is assumed to be uniform for all altitudes in the stem.
4. Although the activity distribution with particle size is assumed uniform for all altitudes in the mushroom, the density of the activity in the mushroom is adjusted so as to be distributed in the vertical proportional to the air density (i.e., the total activity in the mushroom falls off exponentially with altitude).
5. No horizontal variation in distribution is assumed in either the stem or the mushroom.
6. It is assumed that the vertical velocities of these particles are given by an aerodynamic law which takes into account drag and hence varies with altitude. (See Fig. A.)
7. It is assumed that gross fission products decay proportionally with $t^{-1.2}$.
8. It is finally assumed that the distribution of activity with particle size in the stem and mushroom is as given in Fig. B.

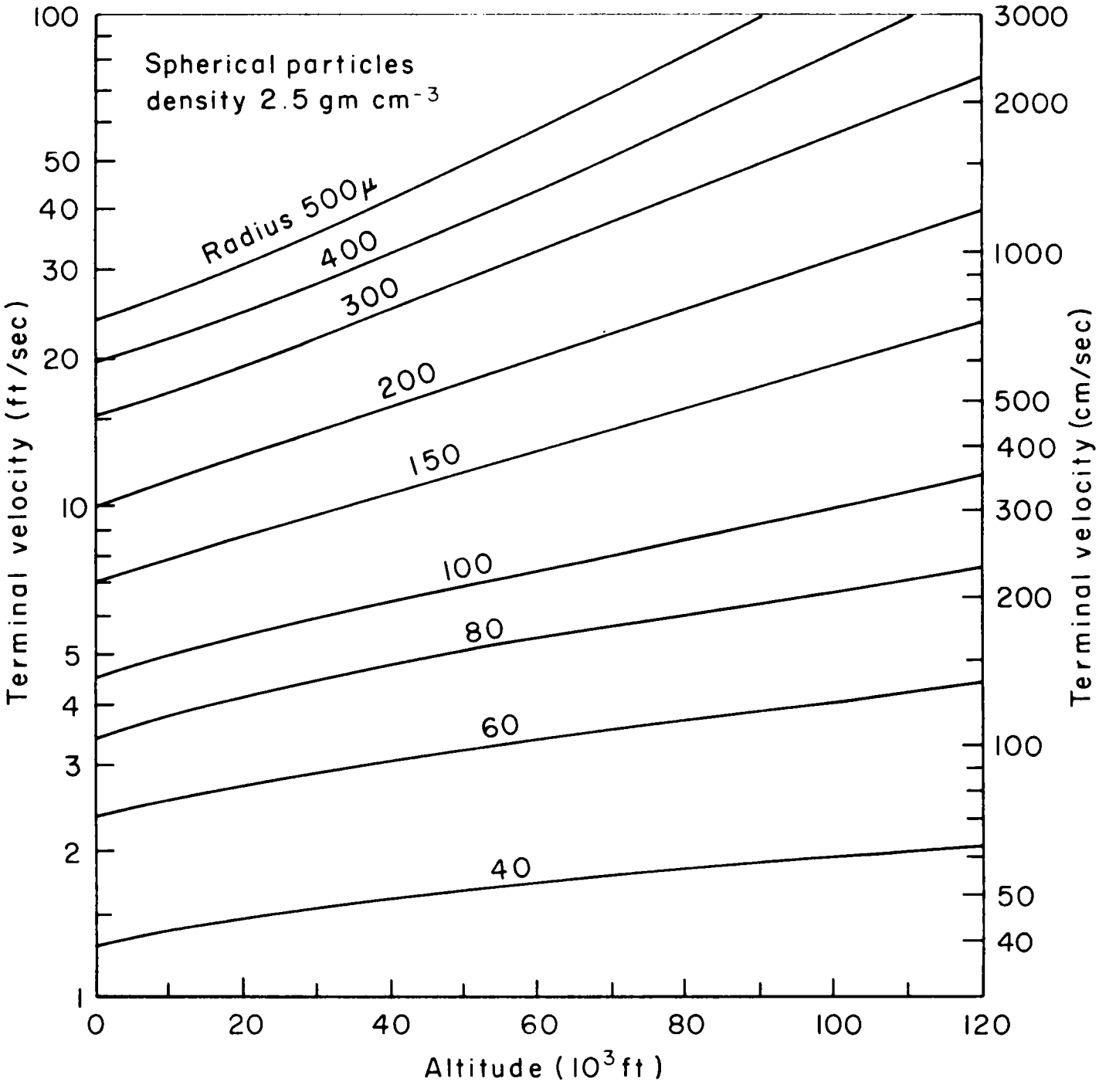

Fig. A — Fall velocities of spherical particles computed by aerodynamic drag law

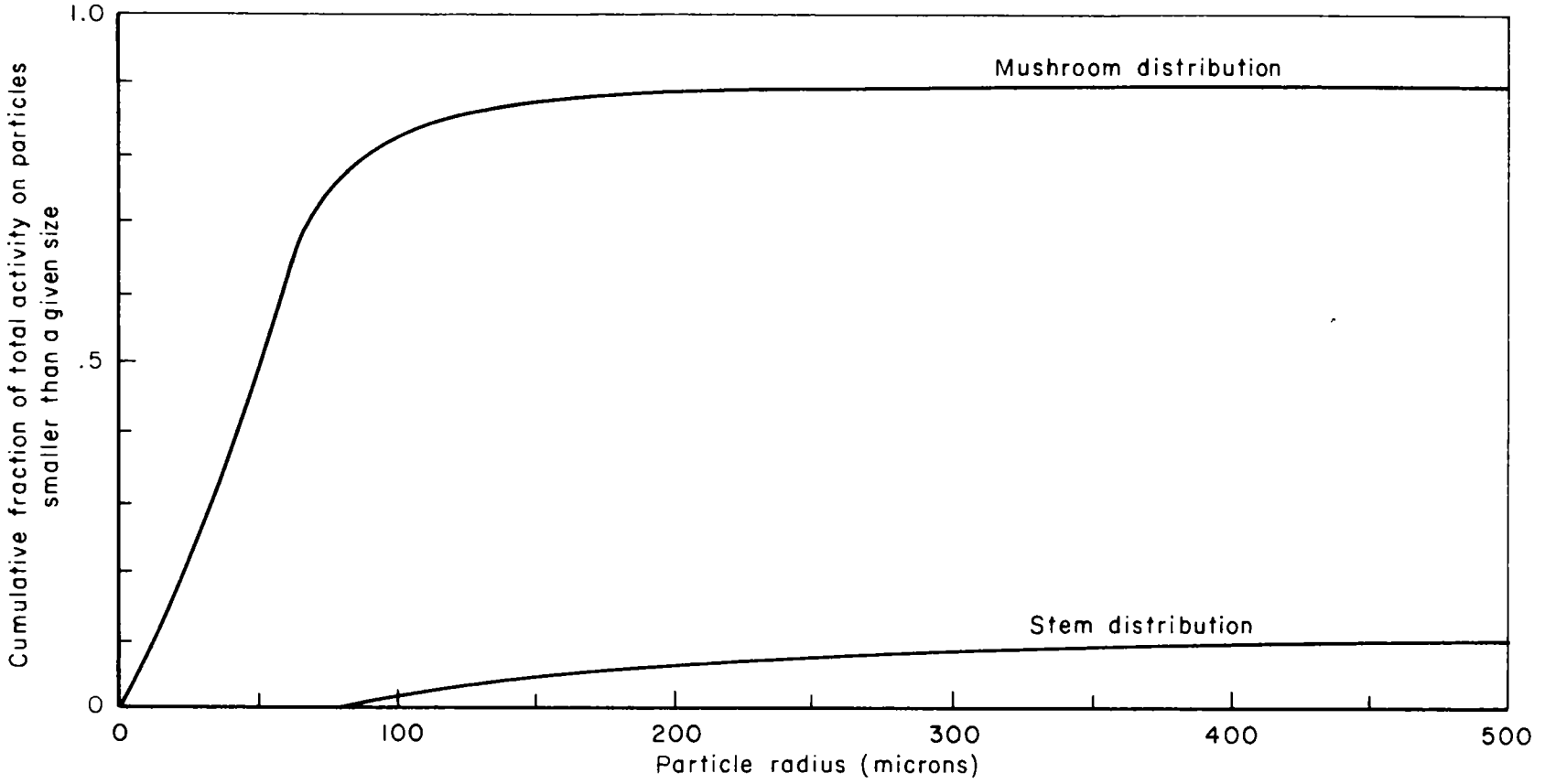

Fig. B — Assumed cumulative distribution of activity with particle size for RAND model

It should be noted that although the above conditions are listed as assumptions, it is felt from an analysis of the available test data, and from the degree to which computations based on the RAND model approximate observed fallout that they have a well-founded basis in fact.

These conditions, when compared with the empirically derived data which relate the dimensions of an atomic cloud to the yield of the weapon, provide one with a framework for computing the radioactive fallout. Approximations are made to continuous distributions by dividing the atmosphere into 1000-ft layers, and the particle sizes into 100 increments, each of which contains an equal fraction of the activity. Summation of the deposition of material is performed on an IBM 701 electronic digital computer, and densities of material and, hence, activities are computed for selected points in the pattern. These points (numbering some 200) are chosen so as to give a good sample of all possible points in the pattern, and allow one to draw a contoured pattern of the fallout. In this connection the number of selected points in any one location is directly proportional to the steepness of the gradient of radioactivity.

It can be seen that by setting V_x or V_y equal to 1 in the above equation, one has an expression for the time it takes a particle to reach the ground. Combining this with the computational method described, fallout can be computed as a function of time, with the pattern for any one time representing only contributions from material that has reached the ground by that time.

III. THE CONTENTS OF THE CATALOG

The method outlined above was used to compute the 52 patterns presented in this catalog. These patterns represent 22 different wind situations, and each is presented with an individual plot for H + 24 hours integrated dose and one for H + 24 hours dose rate. The discrepancy between number of patterns and number of wind situations is due to the fact that in four cases the same winds were used for two different yields.

Time lines are drawn on each dose-rate pattern, but apply equally well for the dosage patterns. The time lines represent the approximate time when the peak dose rate occurred, and as such, in combination with the two patterns, should allow one to extend the value, as given, both forward and backward in time. It should be noted that although the model is capable of handling time and space variations of the wind, all cases presented in this catalog are based on a point wind. This implies that as the time of fall of material increases the pattern departs from reality.

For clarity, the area surrounding ground zero has been doubled in scale and in each case is presented as an inset. Wind hodographs are presented for each case and are plotted for 5000-ft increments of altitude. The weapon yields represented in this catalog are 100 and 400 KT, and 1 and 5 MT.

IV. USING THE CATALOG

As stated previously, this catalog is slanted towards use in an analog method of predicting fallout patterns. It might be well at this point to run through an illustrative example of how one might match a given wind distribution with one included in this report.

Let us suppose that for a given point we have information on wind speeds and directions for several altitudes. This may not be a complete hodograph, but by weighting the levels appropriately and interpolating between points, we can finally produce a structure like the one in Fig. C. In the example given, information was available for the 500-, 100-, and 50-Mb levels, and these winds are given weights of 7, 5, and 4, respectively. Looking through the catalog one finds that the hodograph for Detroit, Michigan, on June 15, 1954 (Fig. 20a), comes closest to matching our example in terms of vector lengths and general shape. It is apparent, however, that not only are the two hodographs oriented in different directions but, although the major turning point comes at the proper level ($\sim$60,000 ft), they turn in opposite directions. However, if one rotates the Detroit hodograph 180° around the East-West axis (producing a mirror image) and then turns it counterclockwise through an angle of 10°, relatively good agreement is achieved, as shown in Fig. D. It is felt, therefore, that a similar manipulation with the patterns made from the Detroit wind structure (Figs. 20b and 20c) would approximate the fallout picture due to the sample hodograph. In like manner other wind structures can be fitted to catalog examples.

During the course of our study, we have had occasion to examine the areas enclosed by various contours of patterns due to several weapon yields and different wind structures. If the area is normalized by dividing it by the yield, and this area-yield ratio is plotted against contour value, a

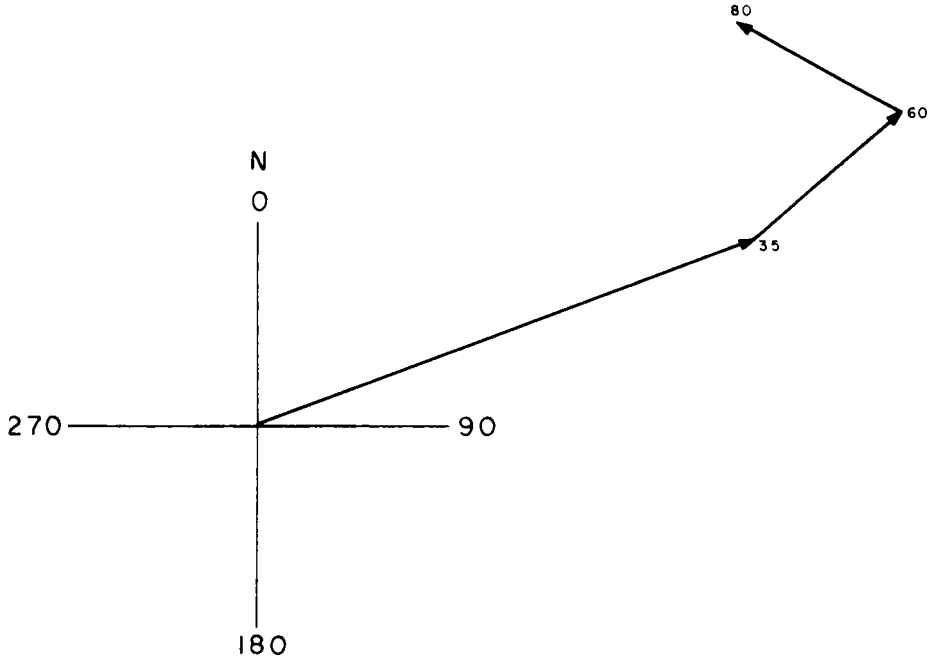

Scale: 1 mm = 2 knots

Fig. C — Sample hodograph constructed with information from three levels

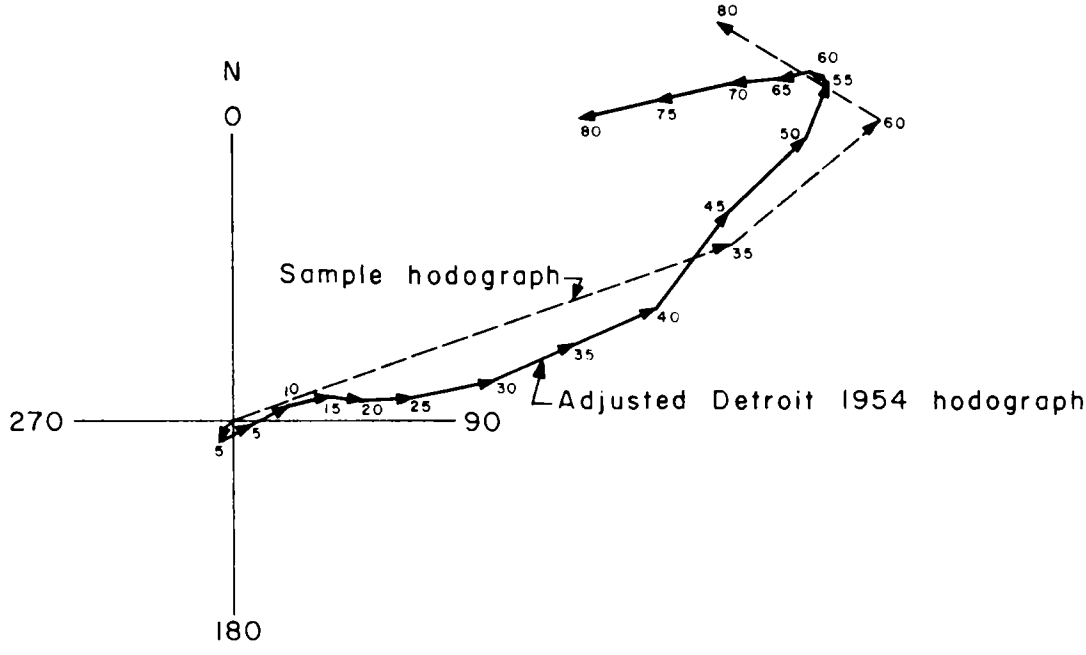

Scale: 1 mm = 2 knots

Fig. D—Comparison of sample hodograph with adjusted Detroit 1954 hodograph

graph as shown in Fig. E is obtained. Although the envelope enclosing all the plots is admittedly rather broad, there is some evidence that the broadness is caused by the wind variations. For at least a small range of yields (at least over an order-of-magnitude variation), and under similar wind conditions, it appears that the area within a pattern can be scaled linearly with the ratio of yields. If this assumption is true, then we can conceive of scaling the linear dimension of a pattern in proportion to the square root of the ratio of the yields, and hence we have a tool for extending the usefulness of this catalog.

NOTE

An index of wind-structure patterns is provided on a foldout page at the end of this report (p. 93) as an easy-aid in locating the desired hodograph in the text. The patterns are drawn approximately to scale and are arranged by weapon yields. The index should be folded out into view and the user's sample wind structure matched with one or more of the patterns. Then the text hodograph that best fits the sample can be found readily by turning to the pages indicated beneath the patterns.

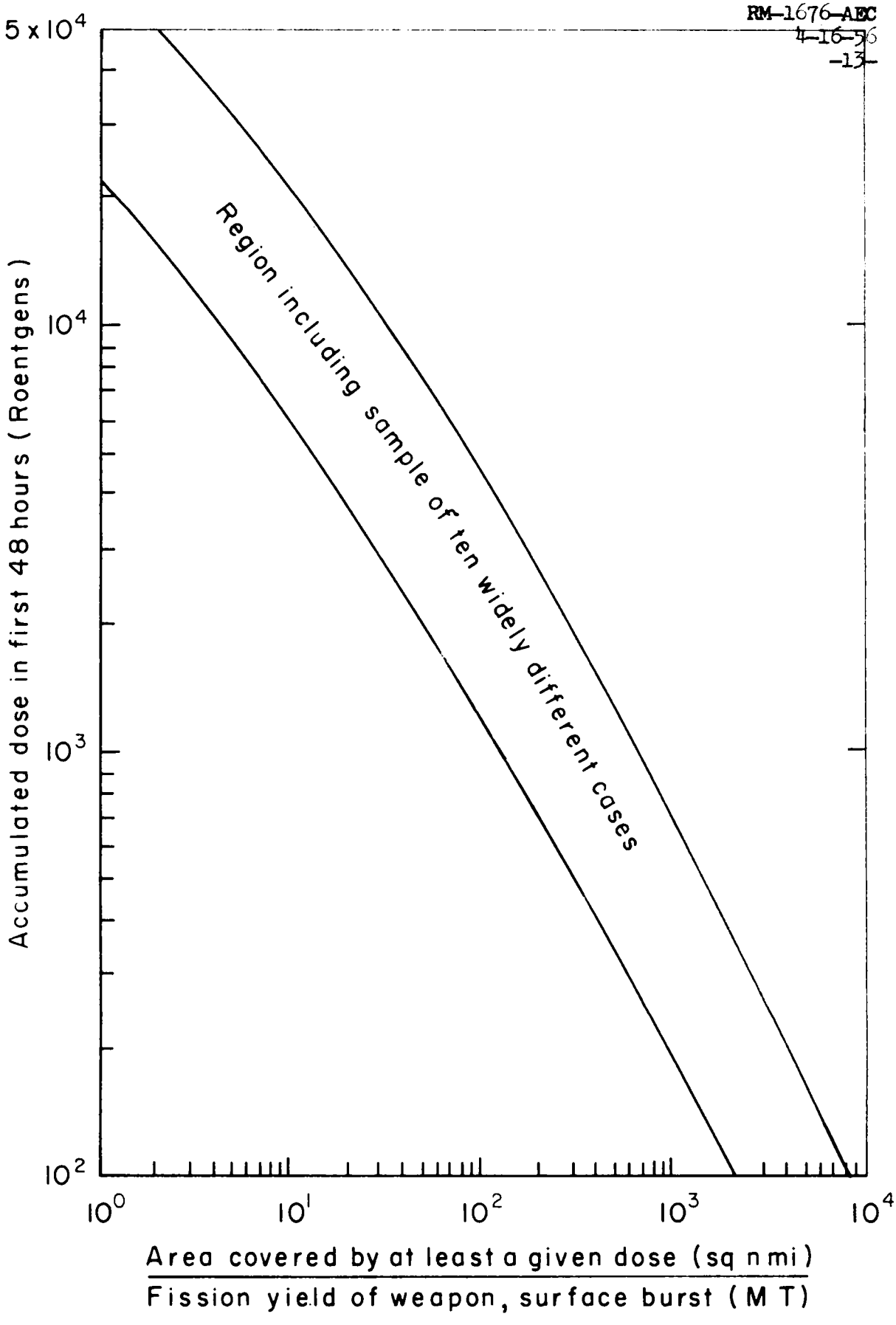

Fig. E — Approximate scaling relationship between 48-hr dose rate and normalized area

V. CONCLUSIONS

We wish to emphasize that this catalog does not represent a complete and final solution to all the problems of fallout. The catalog does not contain a representative sample of wind conditions, the model is at best an approximation, and the analogies can never be perfect. However, we are publishing this catalog in the hope that it will give many people the realization that fallout is a phenomenon dependent largely upon the weather and therefore is extremely variable in its location and intensity. Further, we feel that the application of these patterns to specific problems, in the manner we have outlined, can effect considerable saving of time and effort in estimating fallout effects.

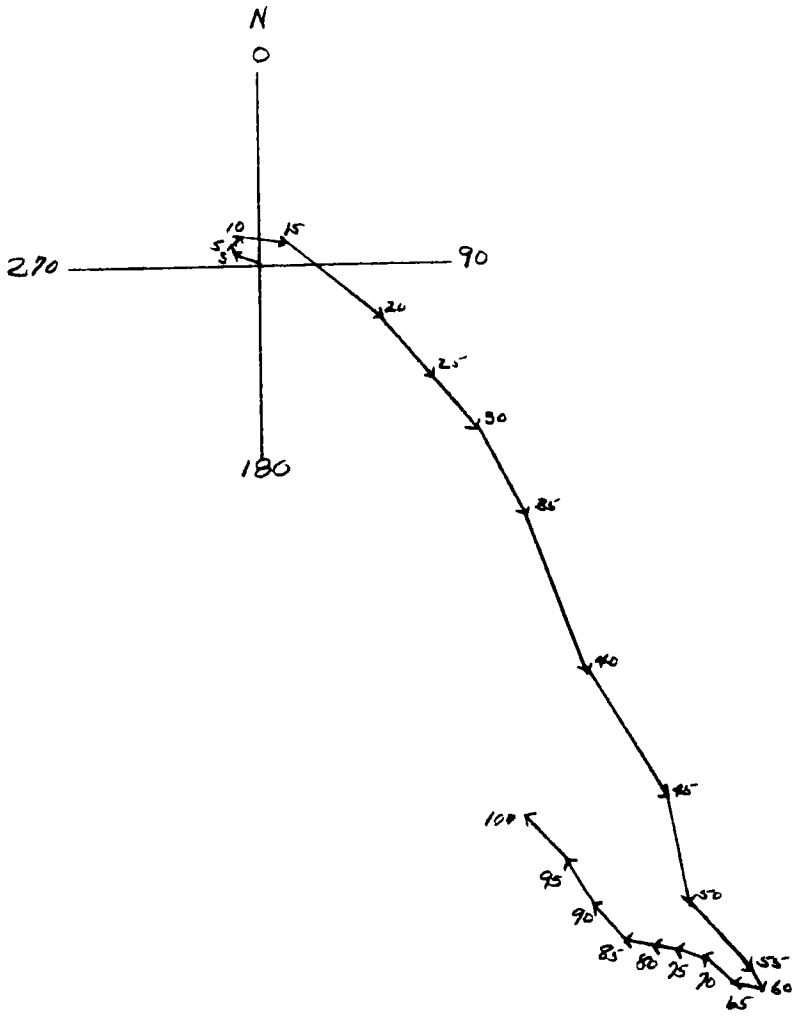

Scale:
1MM = 2 KNOTS

Fig. 1a Hodograph of winds at Chicago, Illinois on June 15, 1953

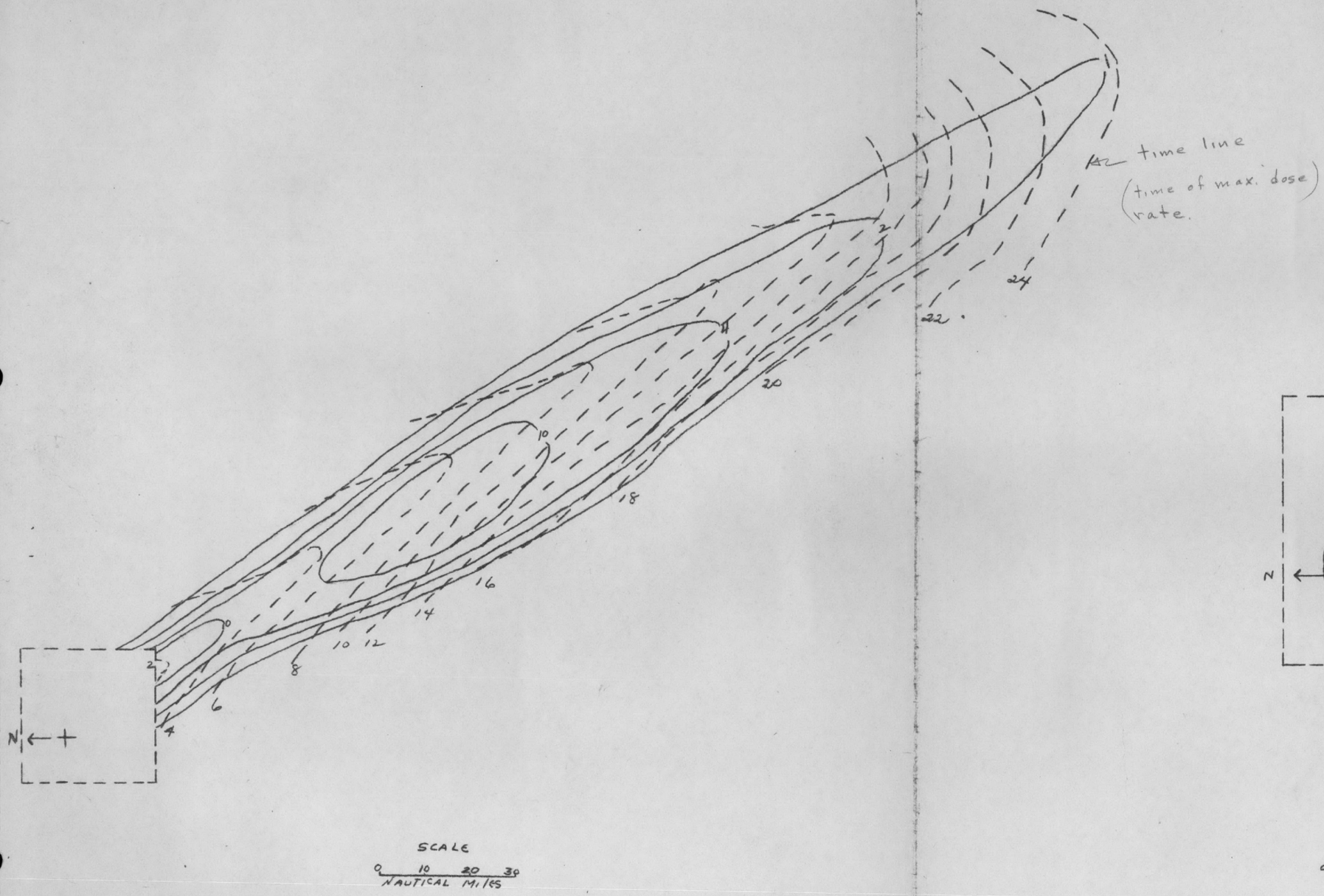

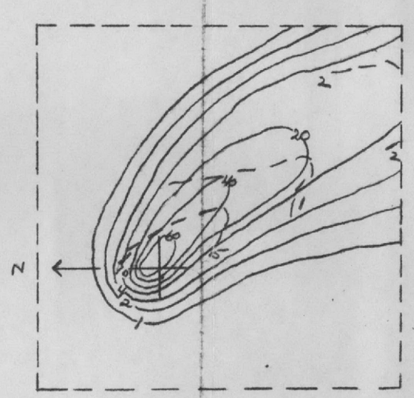

Fig. 1b Dose rate at 24 hours due to a 5 MT device detonated at Chicago, Illinois on June 15, 1953 with approximate mean arrival times.

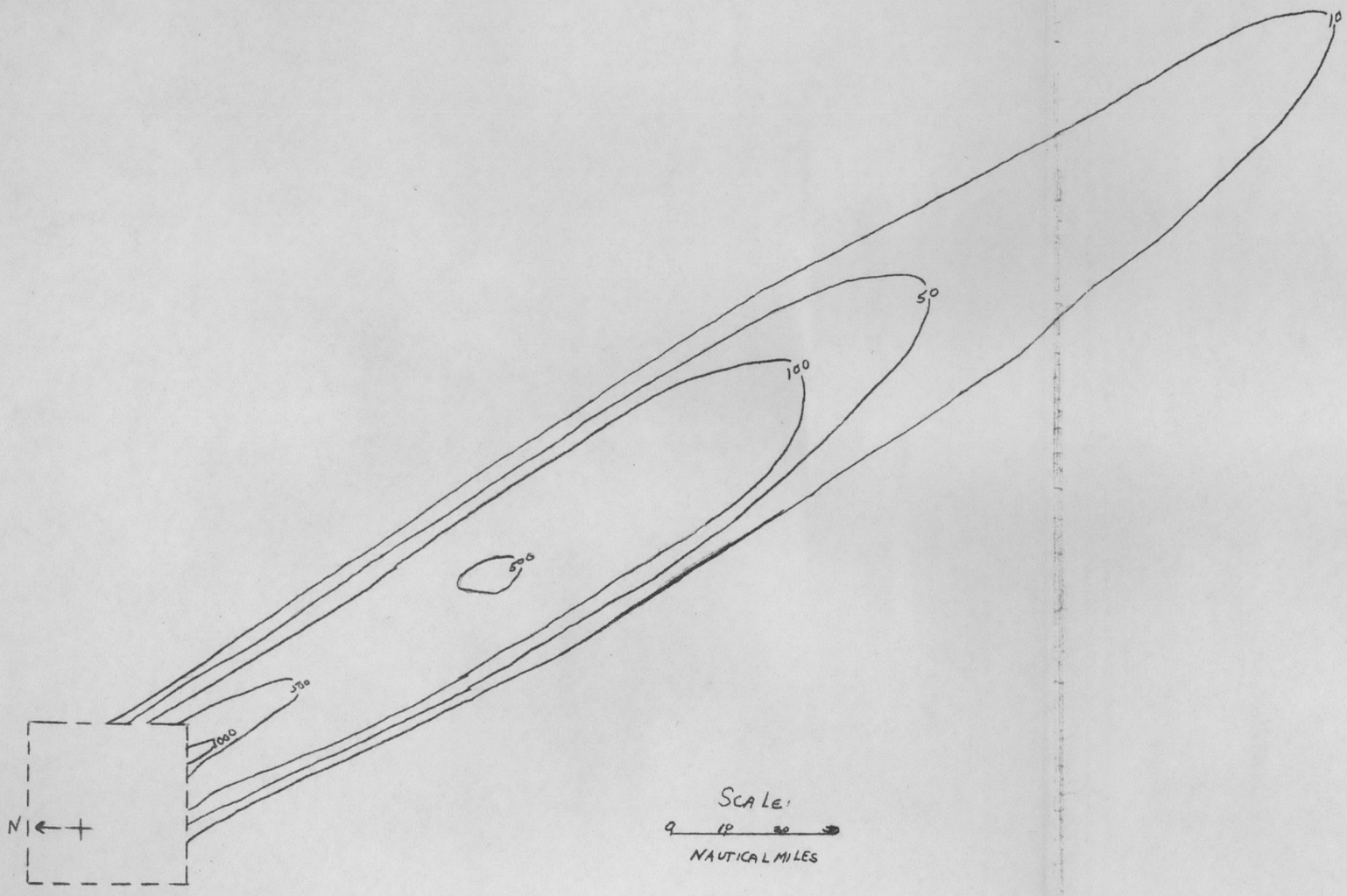

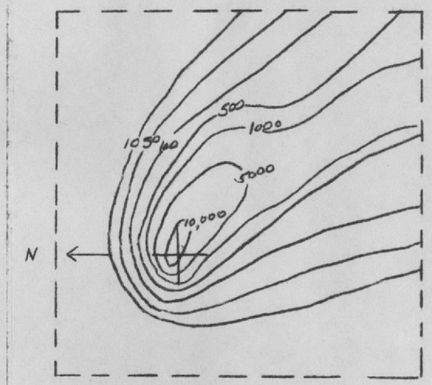

Fig. 1c Dosage from time of arrival to 24 hrs. due to a 5 MT device detonated at Chicago, Illinois on June 15, 1953.

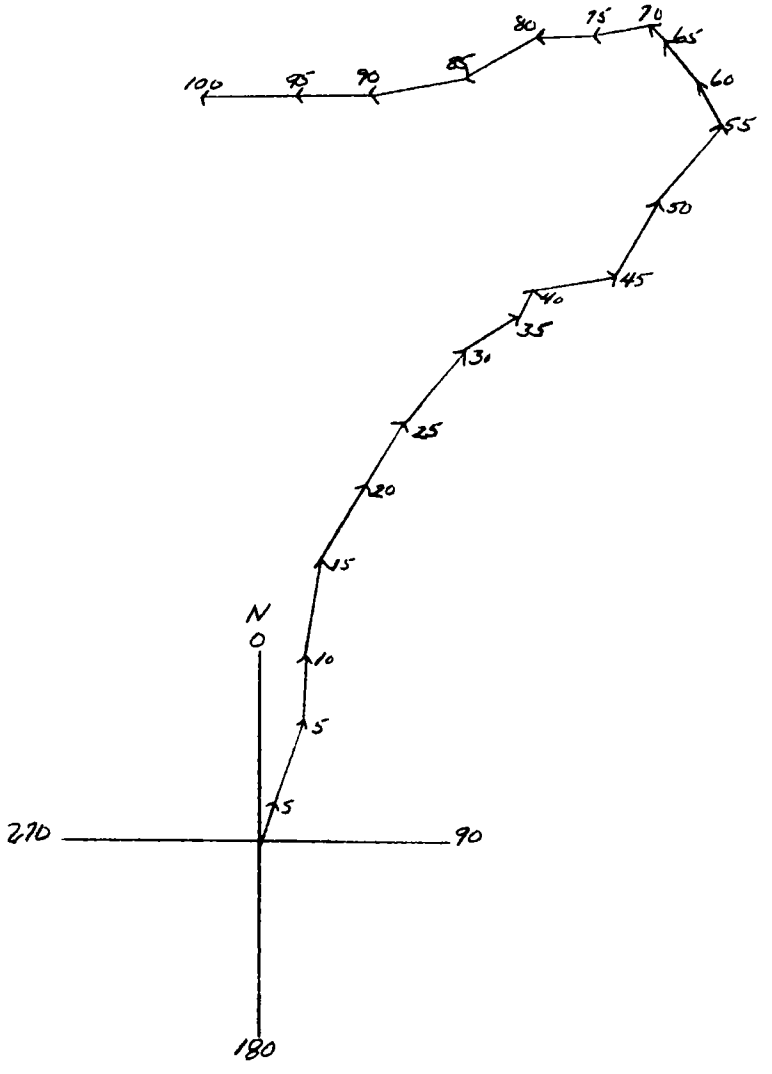

SCALE:
1MM=2 KNOTS

Fig. 2a Hodograph of winds at Chicago, Illinois on June 15, 1954

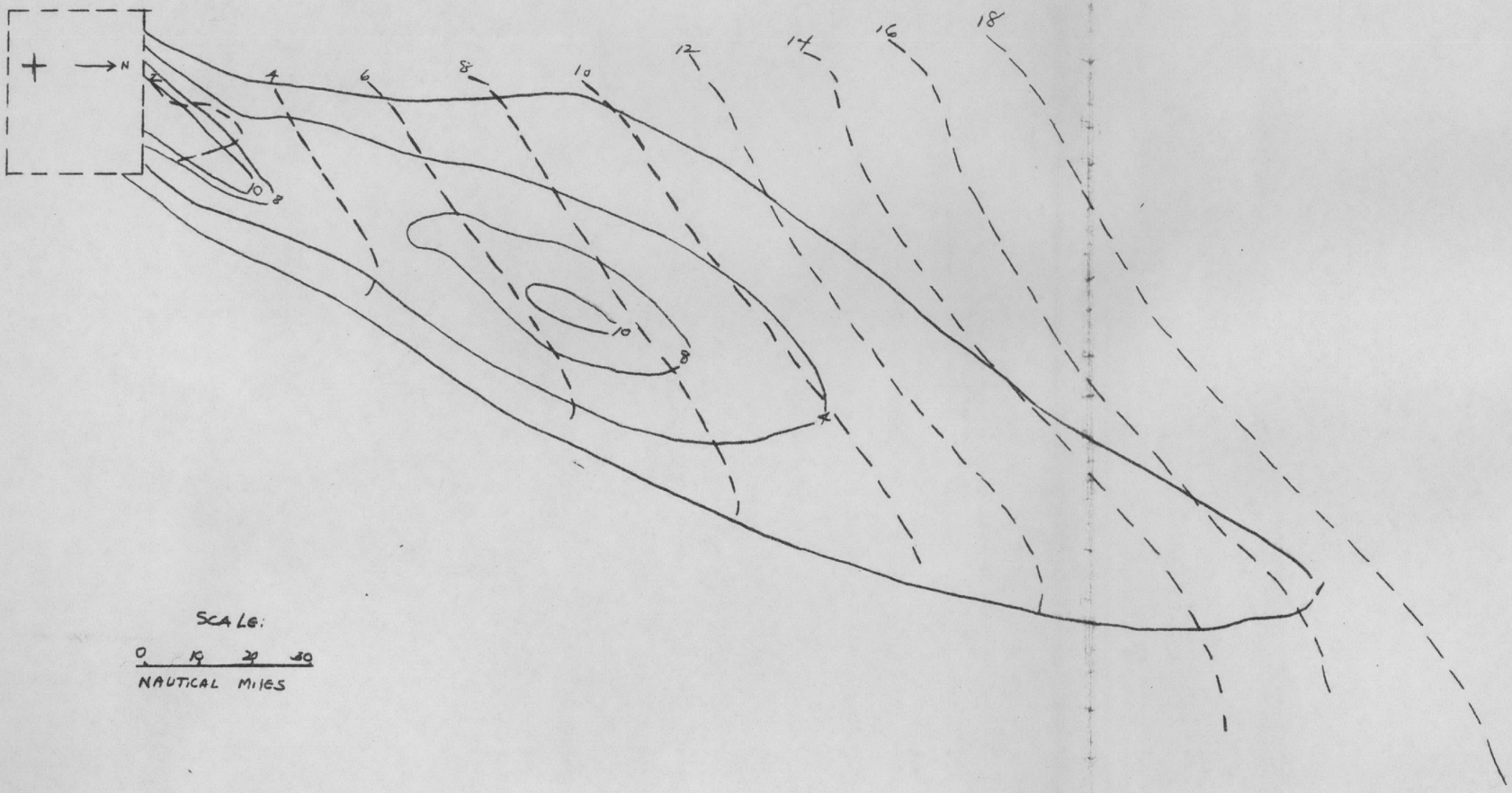

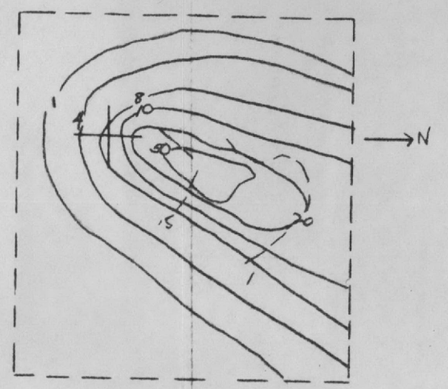

Fig. 2b Dose rate at 24 hours due to a 5 MT device detonated at Chicago, Illinois on June 15, 1954 with approximate mean arrival times.

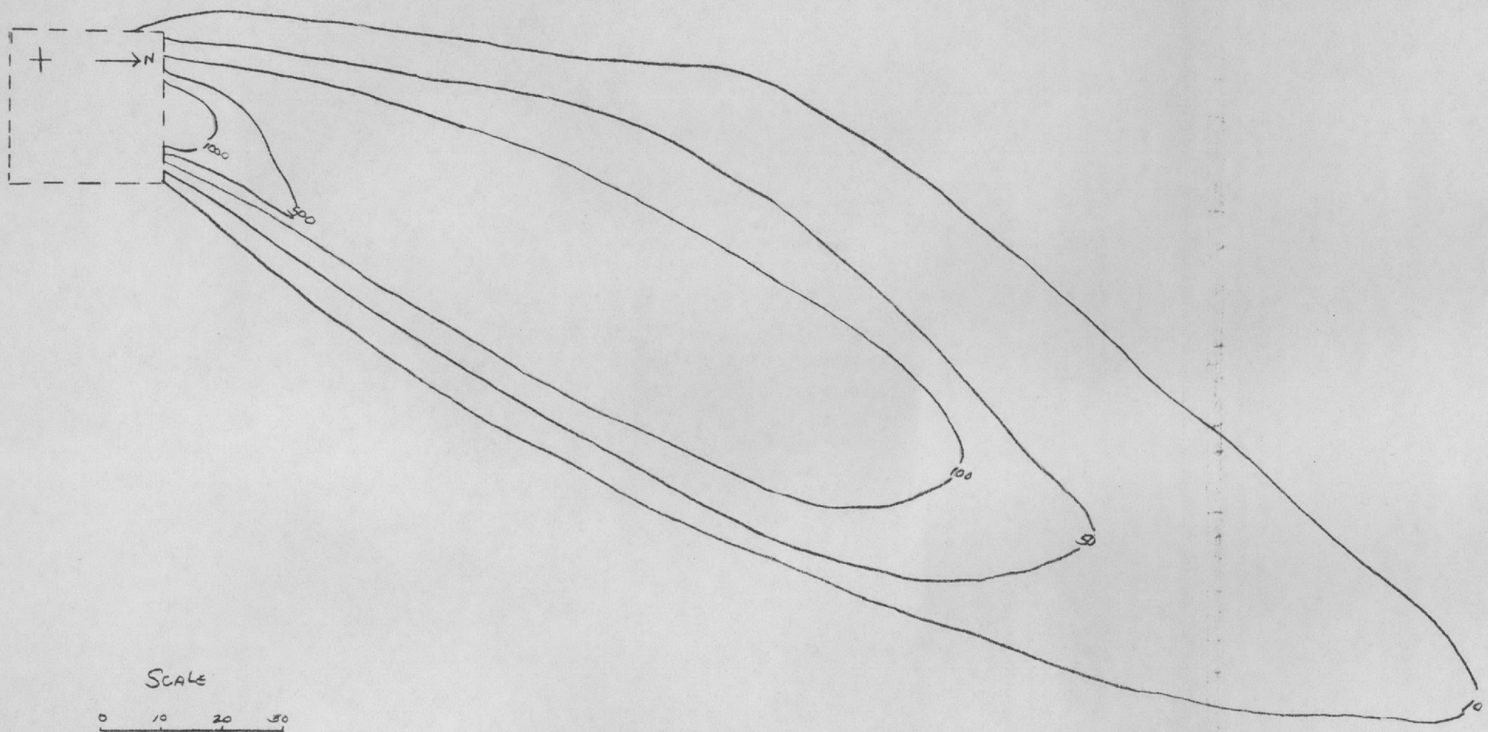

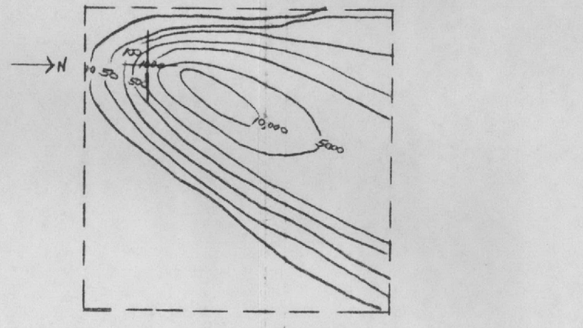

Fig. 2c Dosage from time of arrival to 24 hrs. due to a 5 MT device detonated at Chicago, Illinois on June 15, 1954.

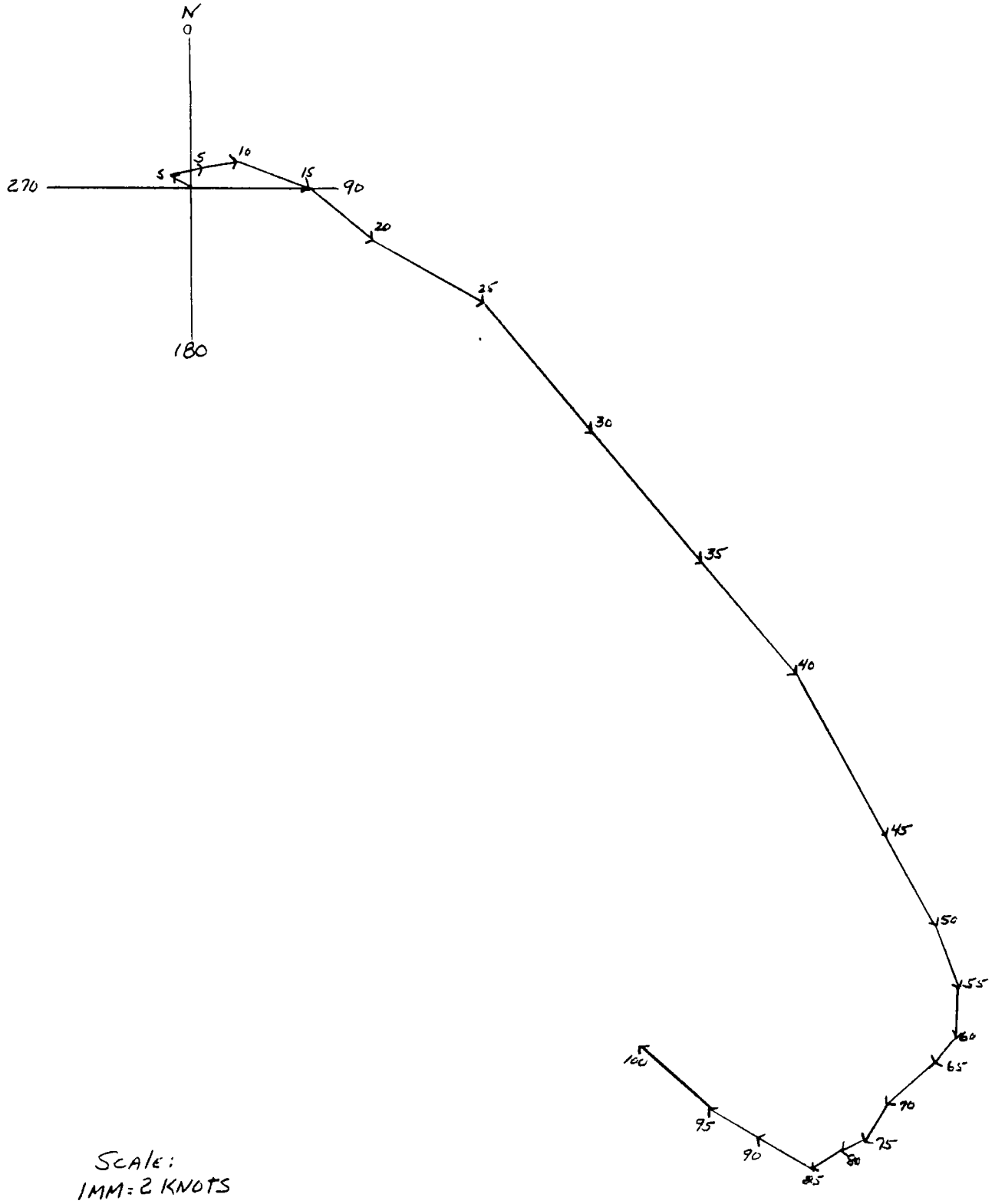

Fig. 3a Hodograph of winds at New York, New York on June 15, 1954

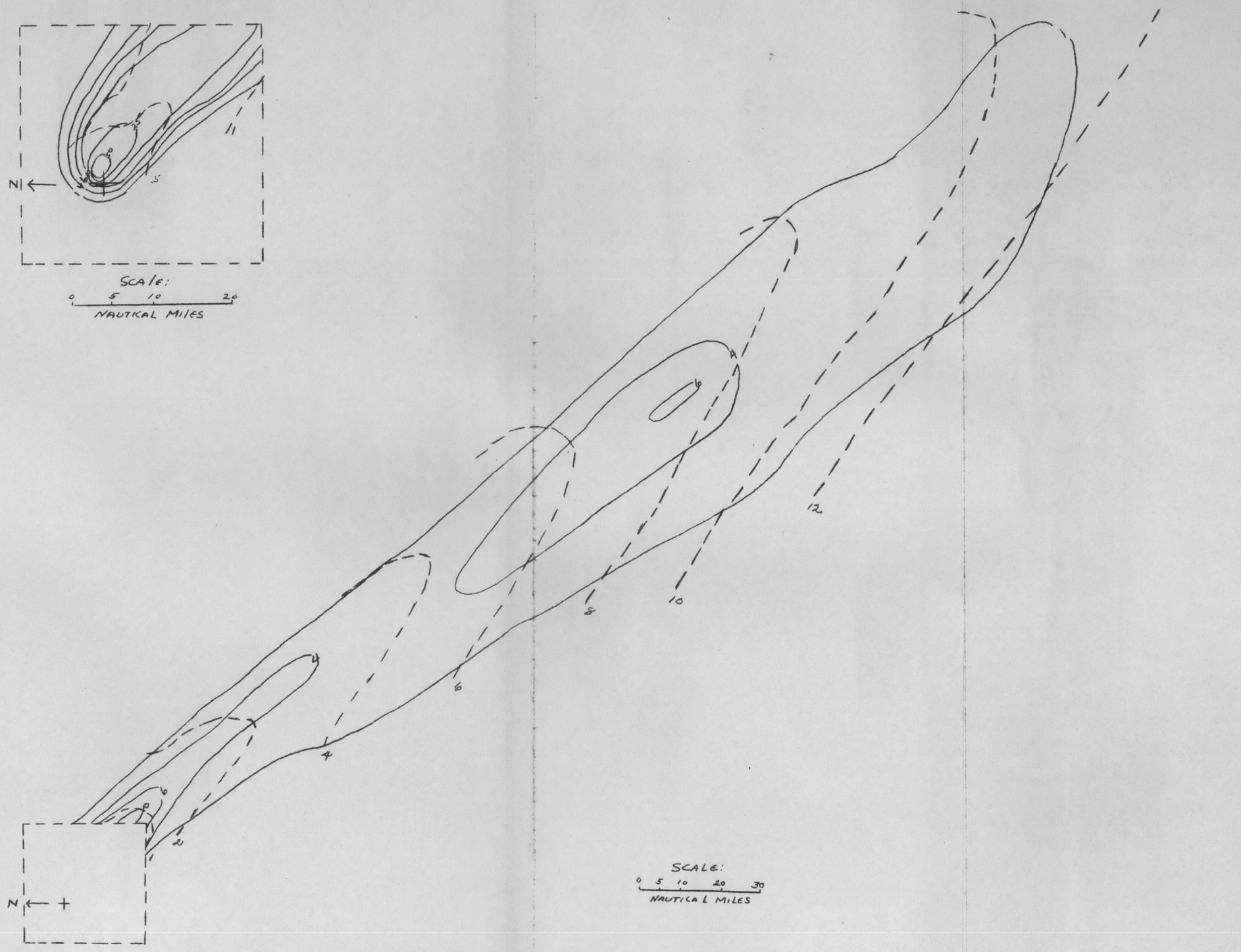

Fig. 3b Dose rate at 24 hrs. due to a 5 MT device detonated at New York, New York on June 15, 1954 with approximate mean arrival times.

SCALE:
0 5 10 20
NAUTICAL MILES

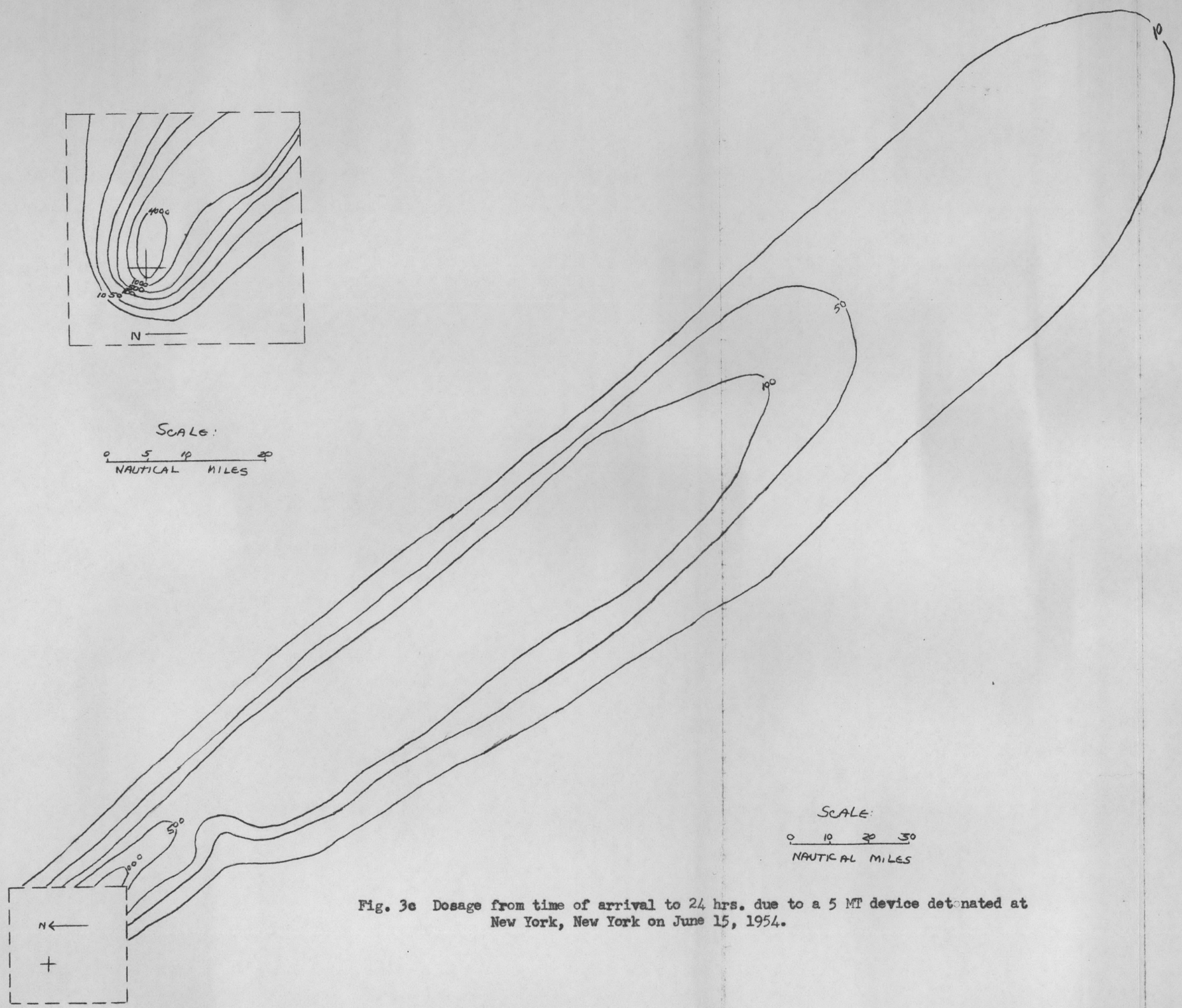

SCALE:
0 10 20 30
NAUTICAL MILES

Fig. 3c Dosage from time of arrival to 24 hrs. due to a 5 MT device detonated at New York, New York on June 15, 1954.

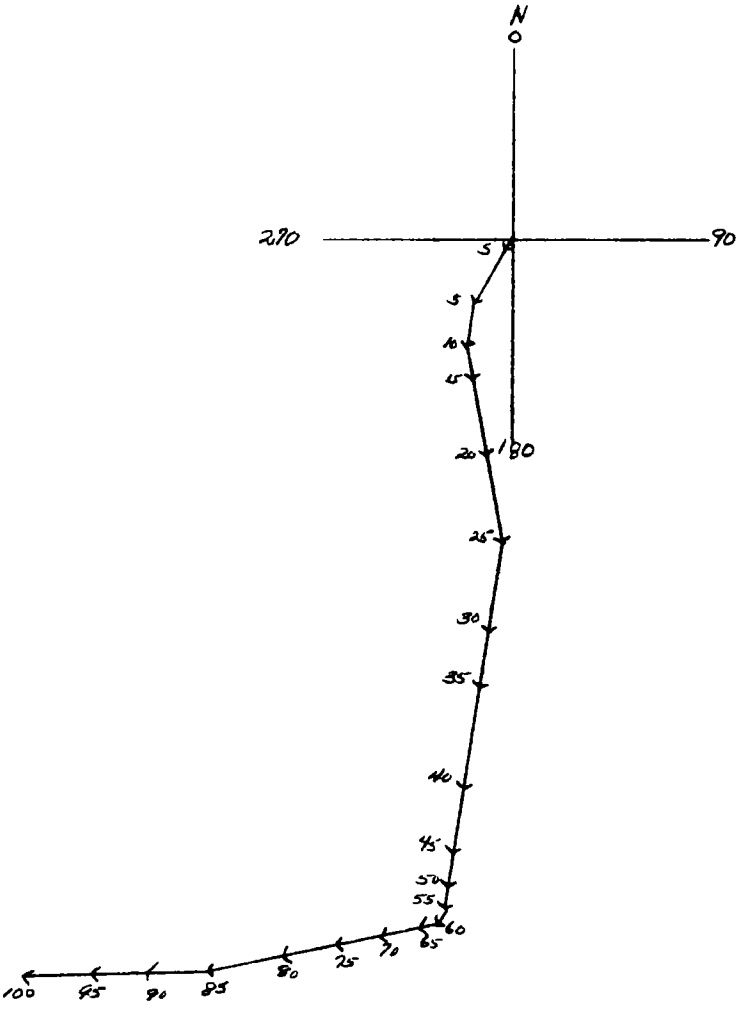

SCALE:
1MM = 2 KNOTS

Fig. 4a Hodograph of winds at New York, New York on June 15, 1953

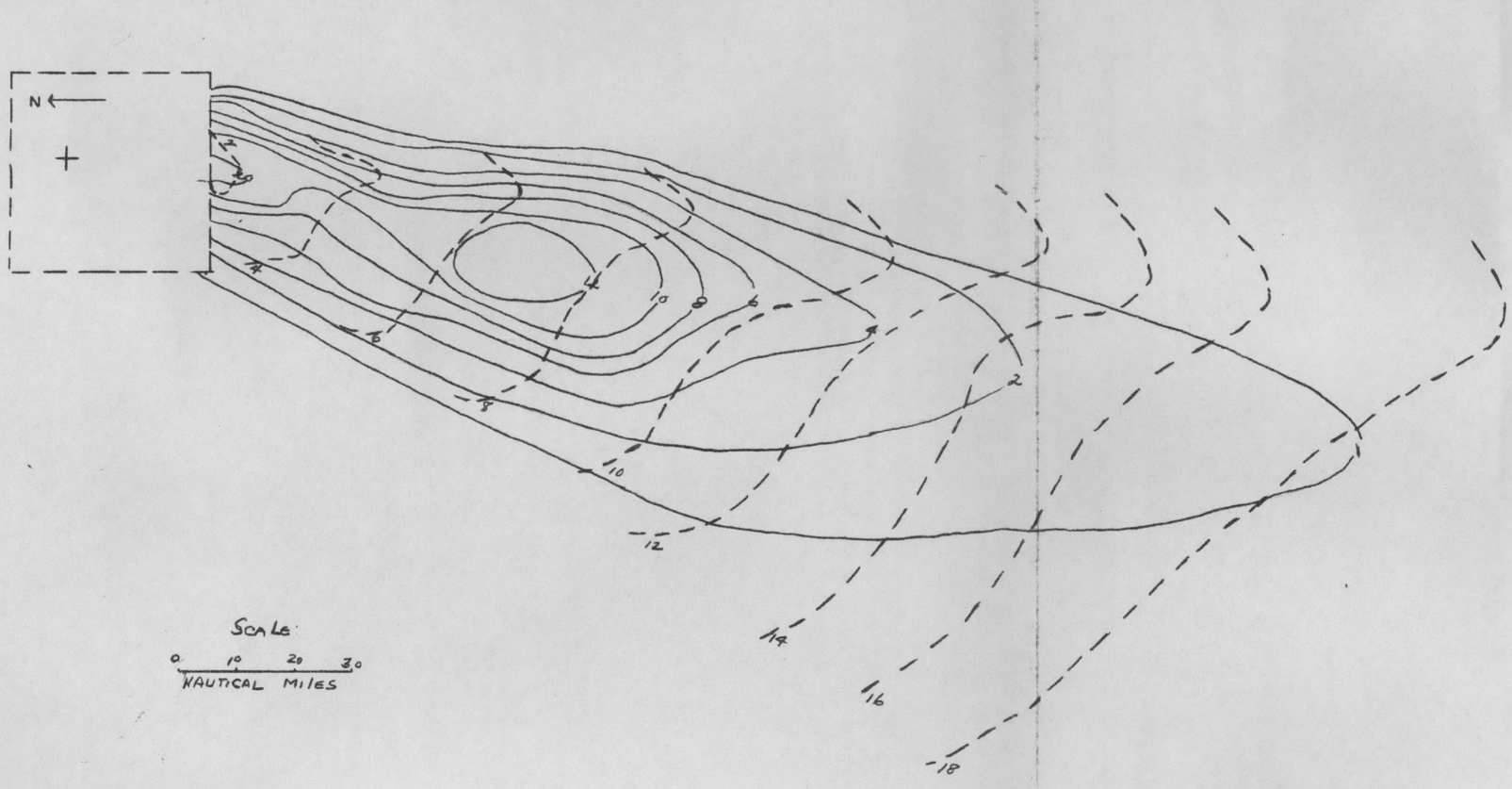

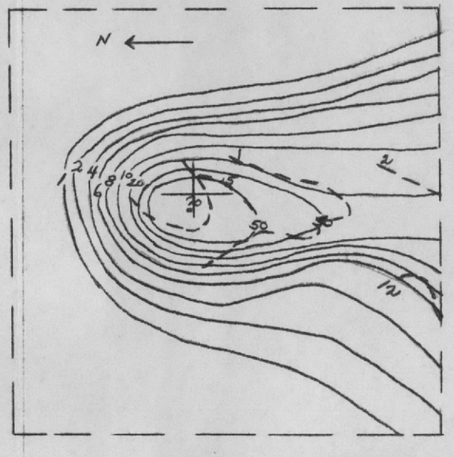

Fig. 4b Dose rate at 24 hours due to a 5 MT device detonated at New York New York on June 15, 1953 with approximate mean arrival times.

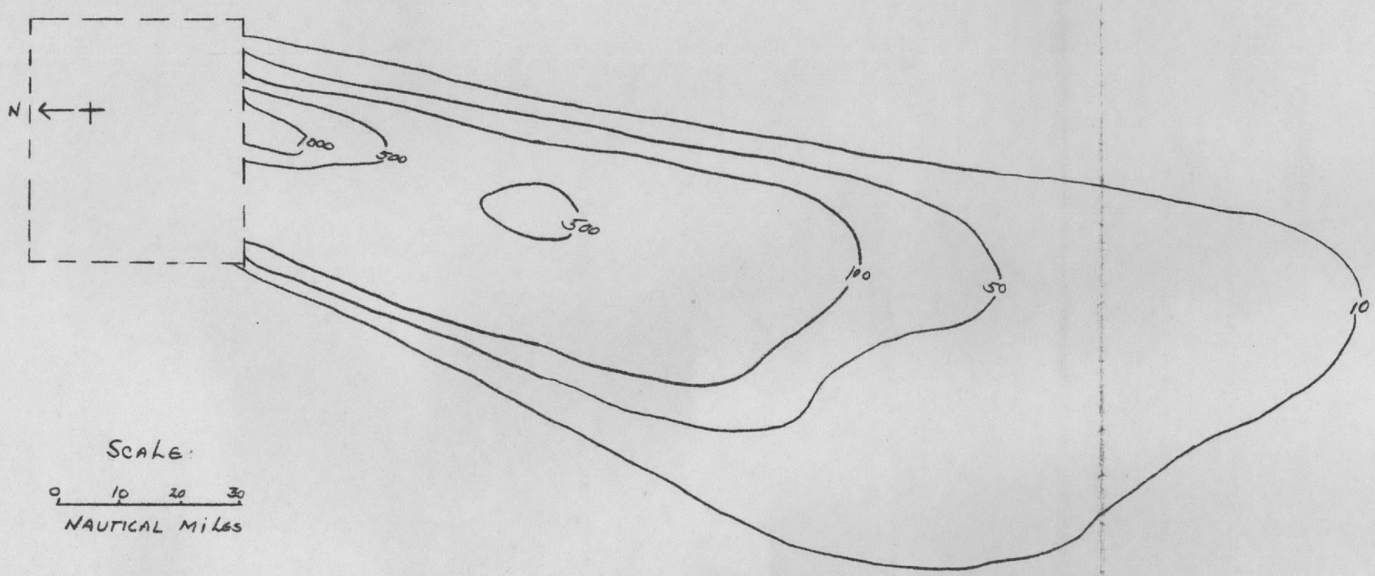

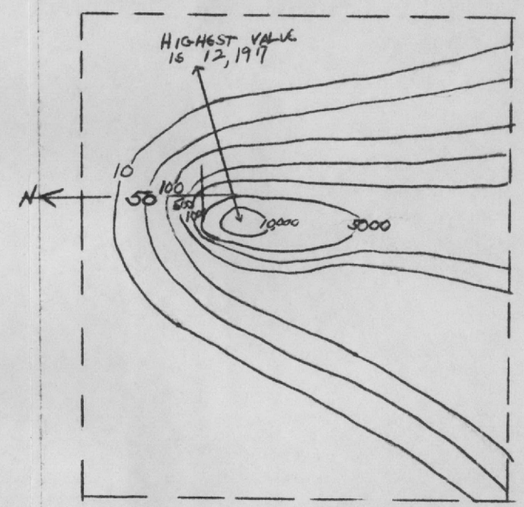

Fig. 4c Dosage from time of arrival to 24 hrs. due to a 5 MT device detonated at New York, New York on June 15, 1953.

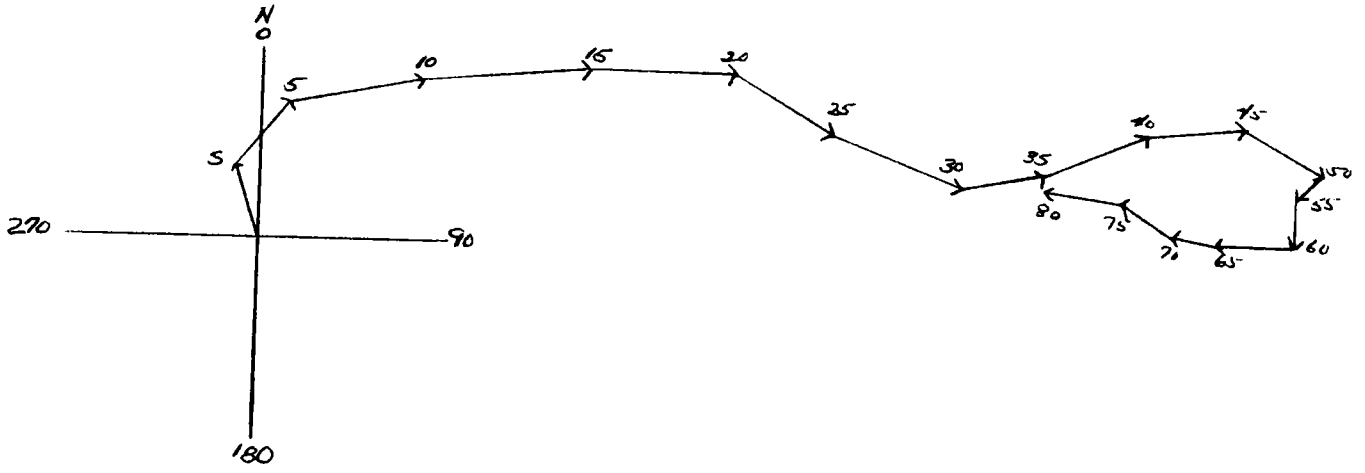

Scale:
1MM = 2 KNOTS

Fig. 5a Hodograph of winds at Kansas City, Missouri on June 15, 1953

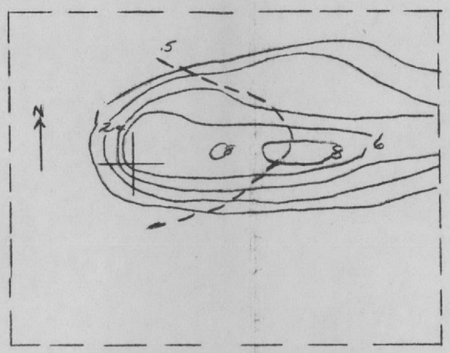

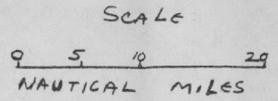

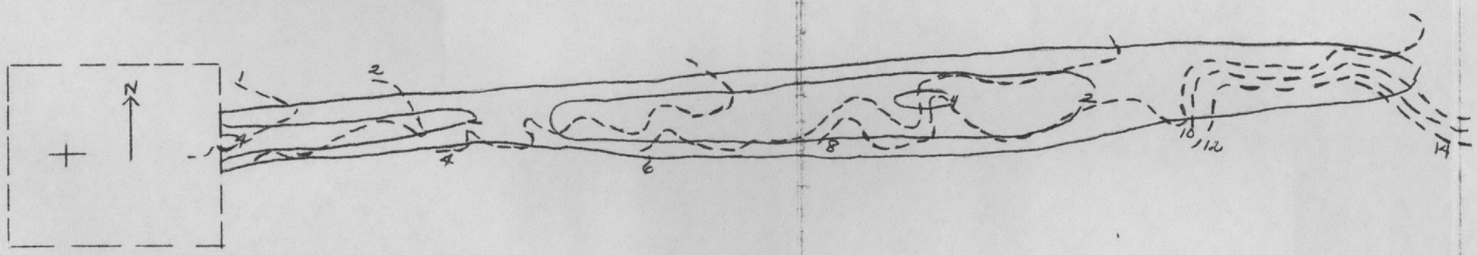

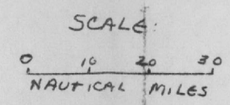

Fig. 5b Dose rate at 24 hours due to a 1 MT device detonated at Kansas City, Missouri on June 15, 1953 with approximate mean arrival times.

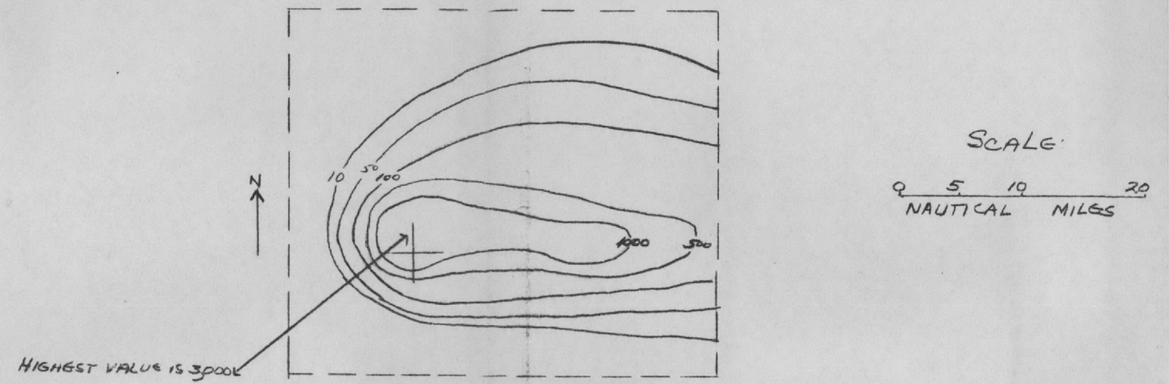

SCALE
0 5 10 20
NAUTICAL MILES

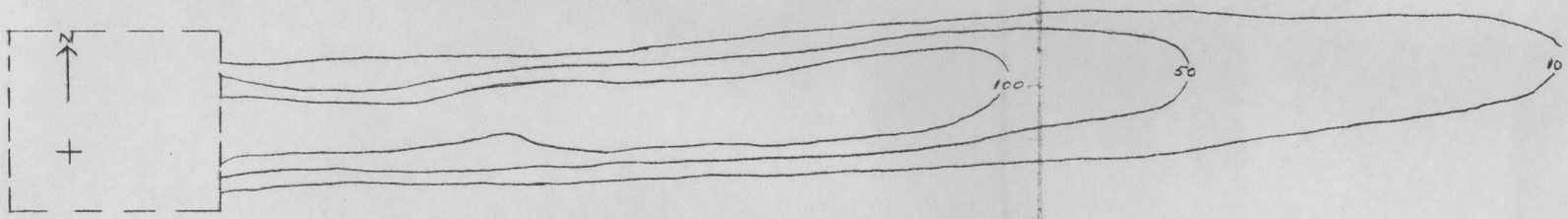

SCALE:
0 10 20 30
NAUTICAL MILES

Fig. 5e Dosage from time of arrival to 24 hrs. due to a 1 MT device detonated at Kansas City, Missouri on June 15, 1953.

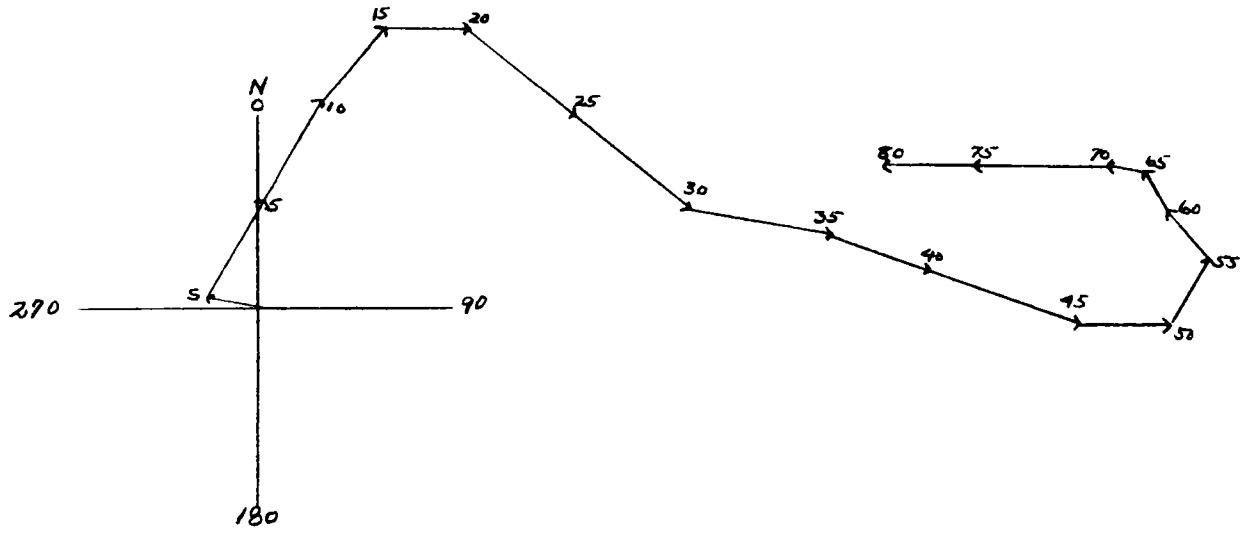

Scale;
1MM = 2 KNOTS

Fig. 6a Hodograph of winds at Kansas City, Missouri on June 15, 1954

RM-1676-AEC
4/16/56
-30-

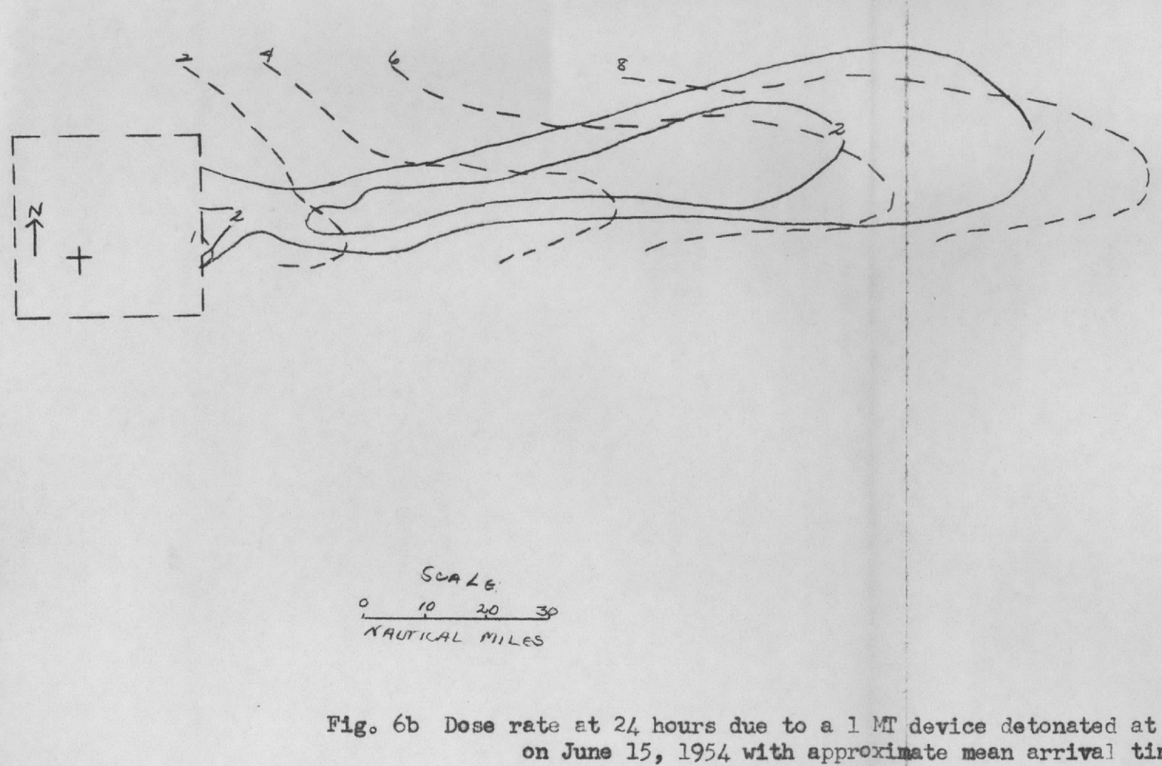

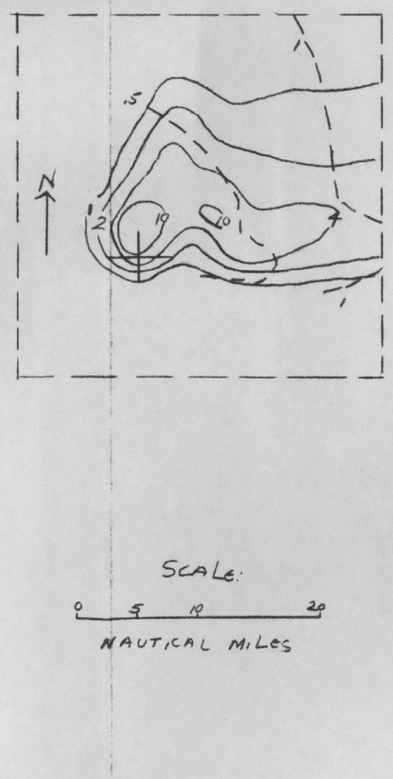

Fig. 6b Dose rate at 24 hours due to a 1 MT device detonated at Kansas City, Missouri on June 15, 1954 with approximate mean arrival times.

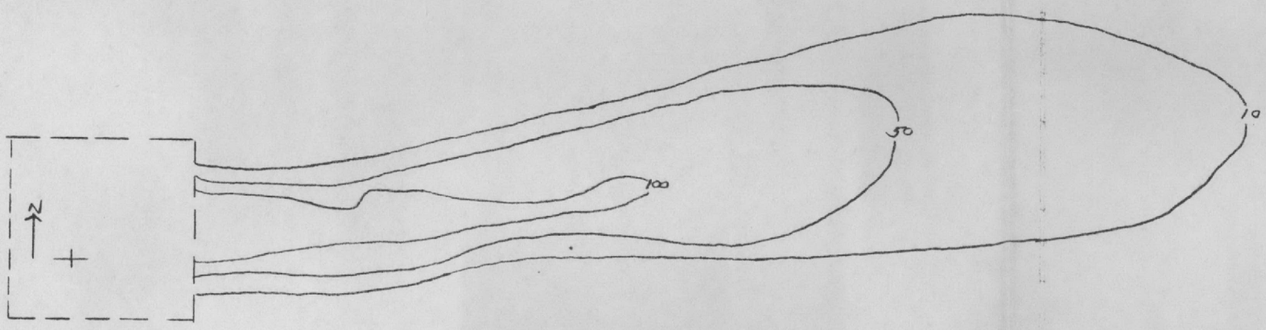

SCALE:
0 10 20 30
NAUTICAL MILES

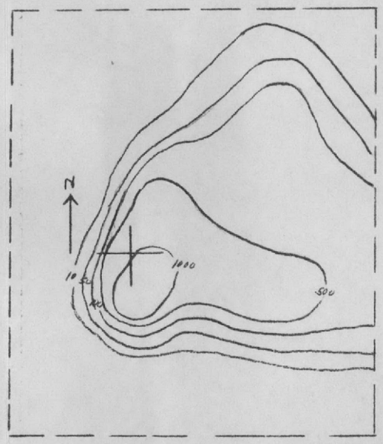

SCALE
0 5 10 20
NAUTICAL MILES

Fig. 6c Dosage from time of arrival to 24 hrs. due to a 1 MT device detonated at Kansas City, Missouri on June 15, 1954.

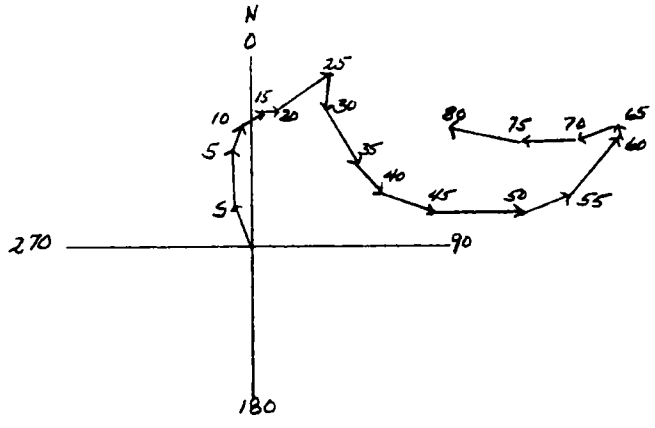

Fig. 7a Hodograph of winds at Houston, Texas on June 15, 1954

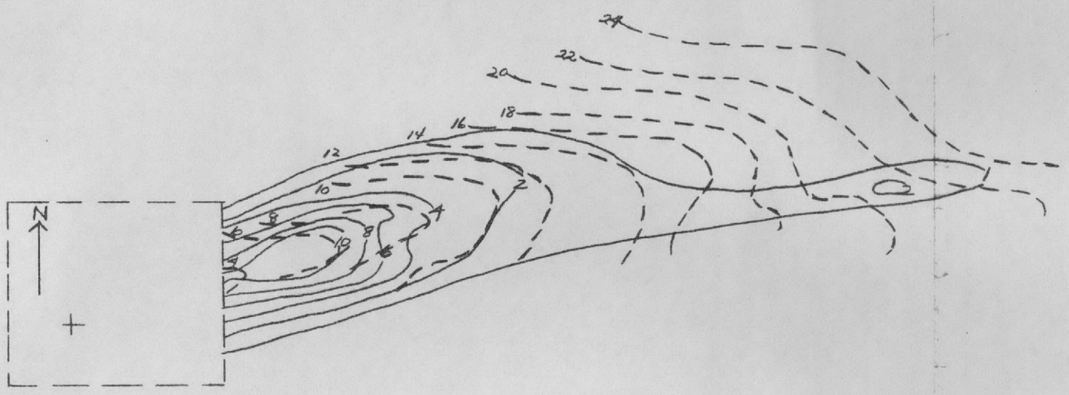

SCALE
0 10 20 30
NAUTICAL MILES

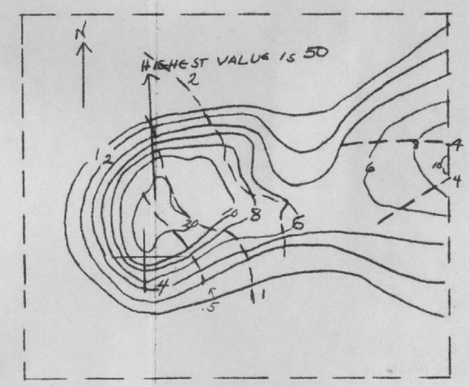

SCALE
0 5 10 20
NAUTICAL MILES

Fig. 7b Dose rate at 24 hours due to a 1 MT device detonated at Houston, Texas on June 15, 1954 with approximate mean arrival times.

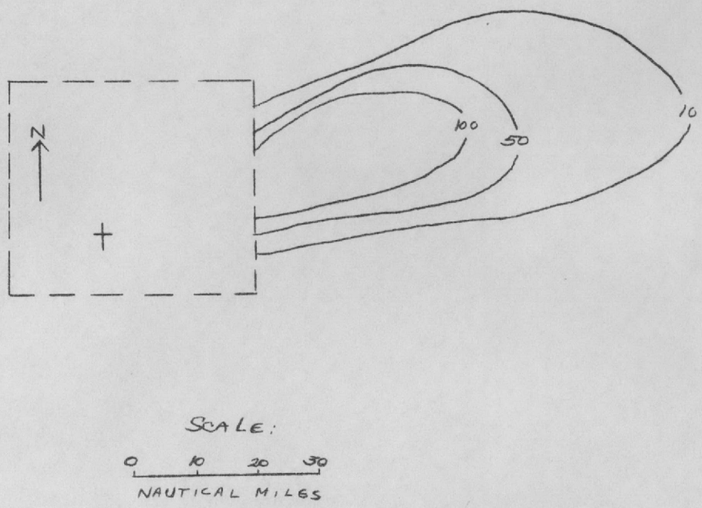

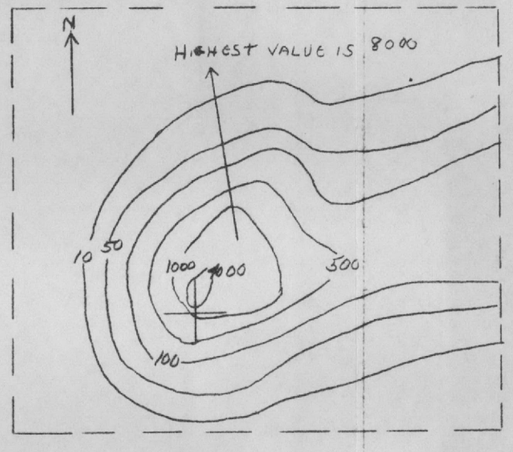

Fig. 7c Dosage from time of arrival to 24 hrs. due to a 1 MT device detonated at Houston, Texas on June 15, 1954.

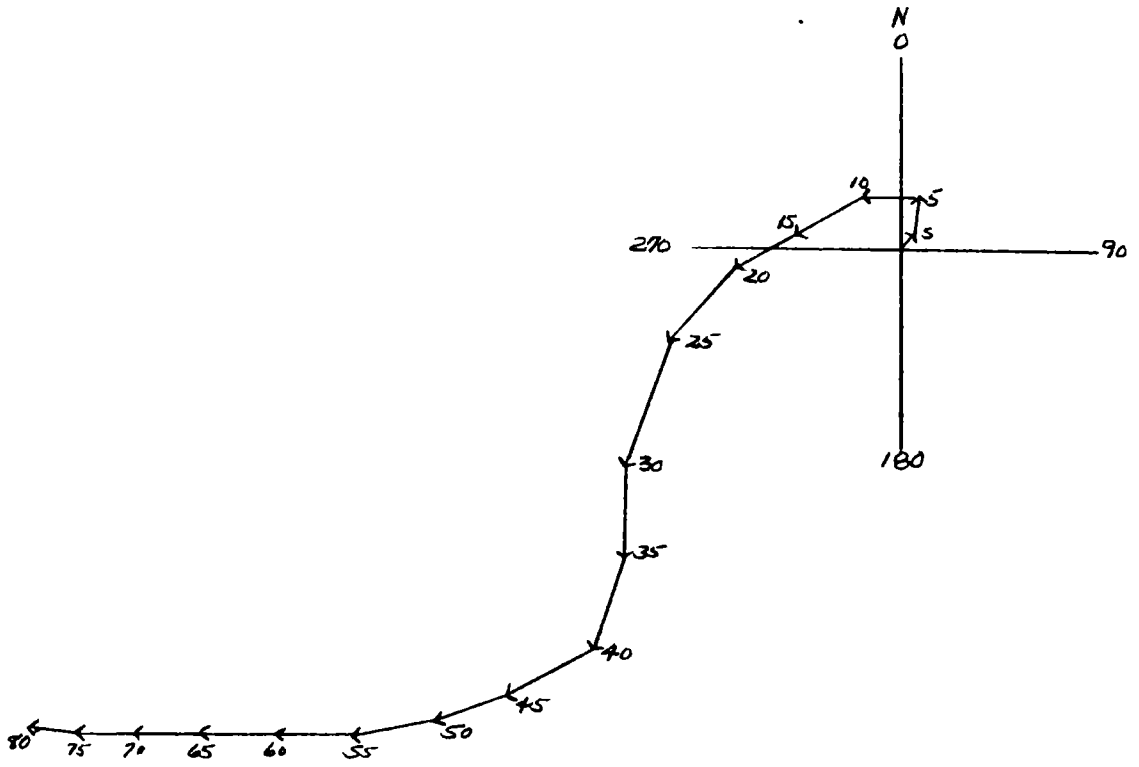

Fig. 8a Hodograph of winds at Houston, Texas on June 15, 1953.

SCALE:
1 MM = 2 KNOTS

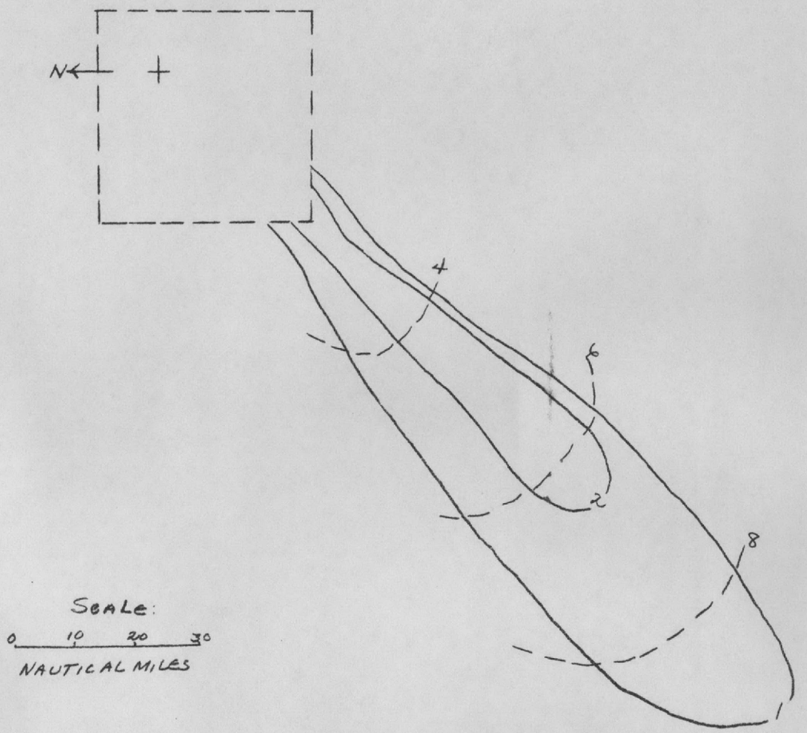

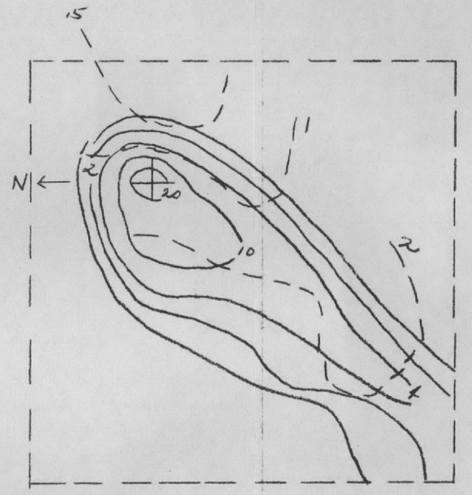

Fig. 8b Dose rate at 24 hours due to a 1 MT device detonated at Houston, Texas on June 15, 1953 with approximate mean arrival times.

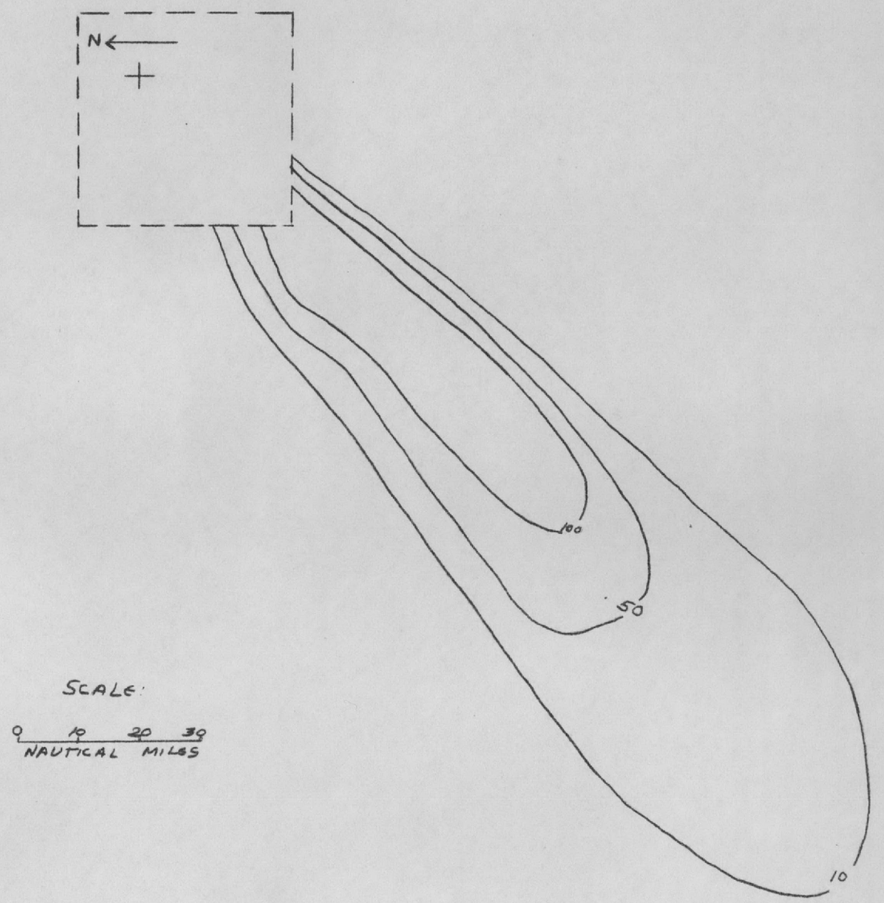

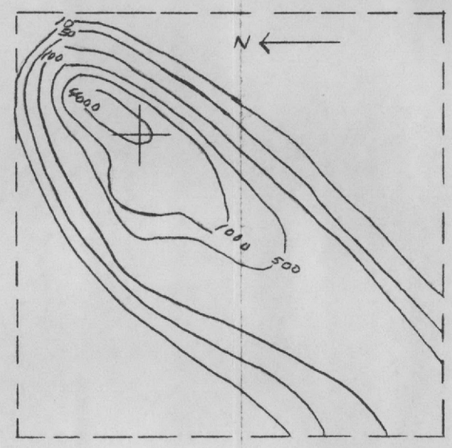

Fig. 8c Dosage from time of arrival to 24 hrs. due to a 1 MT device detonated at Houston, Texas on June 15, 1953.

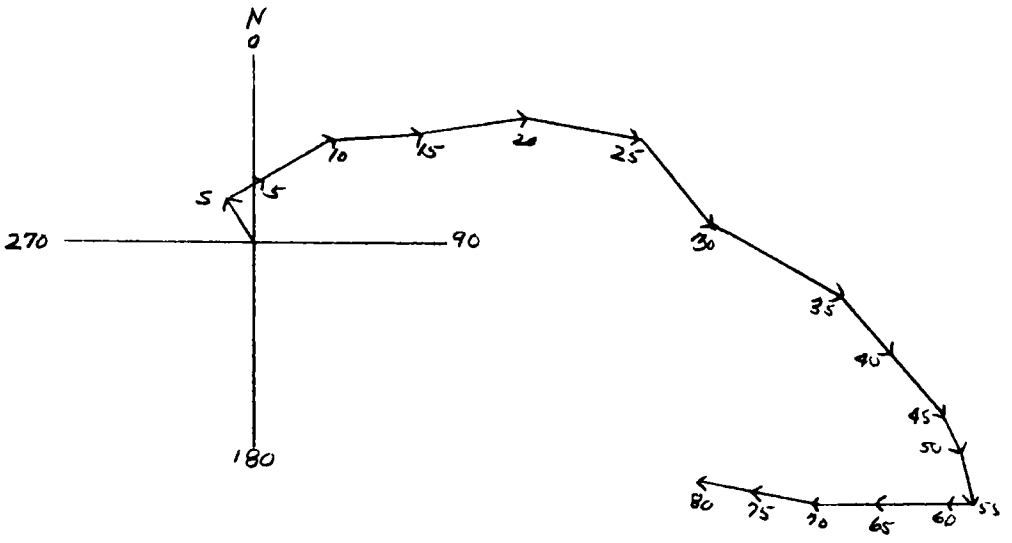

Scale:
1MM = 2 KNOTS

Fig. 9a Hodograph of winds at St. Louis, Missouri on June 15, 1953

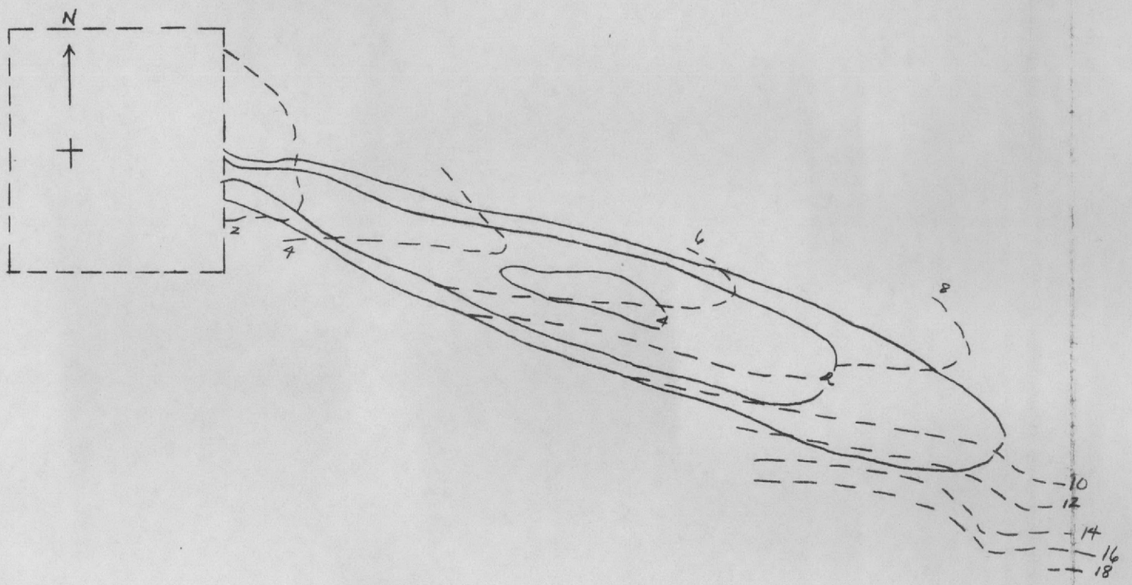

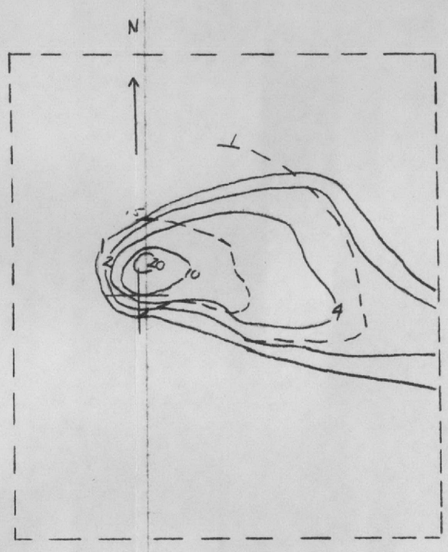

Fig. 9b Dose rate at 24 hours due to a 1 MT device detonated at St. Louis, Missouri on June 15, 1953 with approximate mean arrival times.

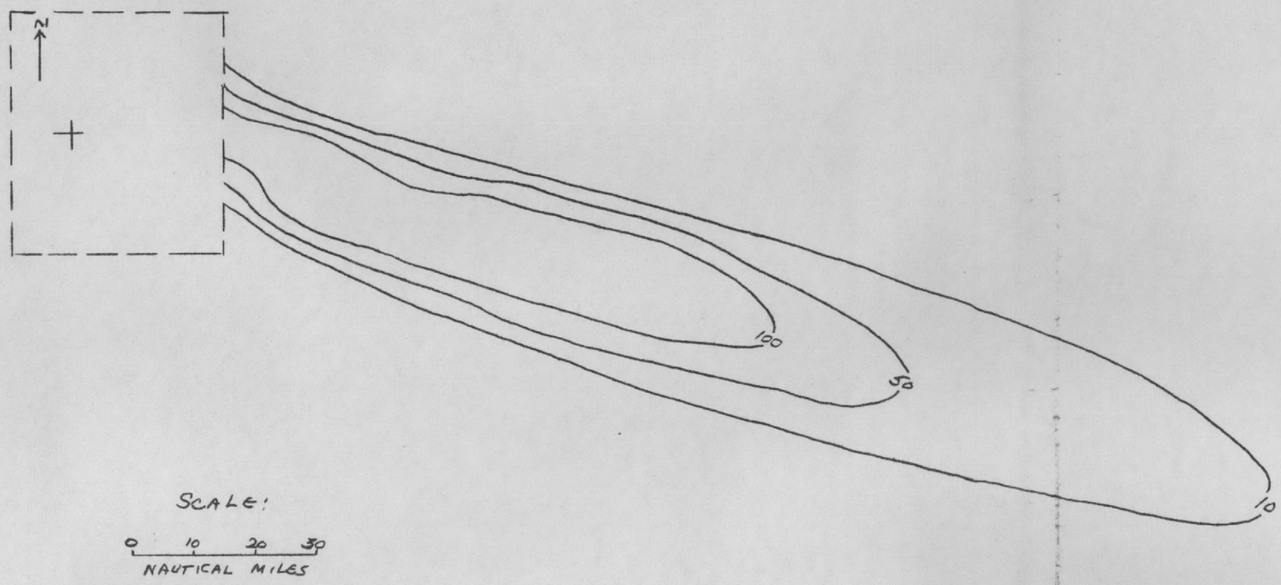

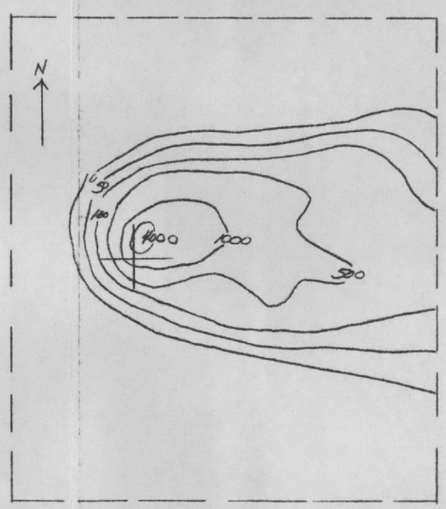

Fig. 9c Dosage from time of arrival to 24 hrs. due to a 1 MT device detonated at St. Louis, Missouri on June 15, 1953.

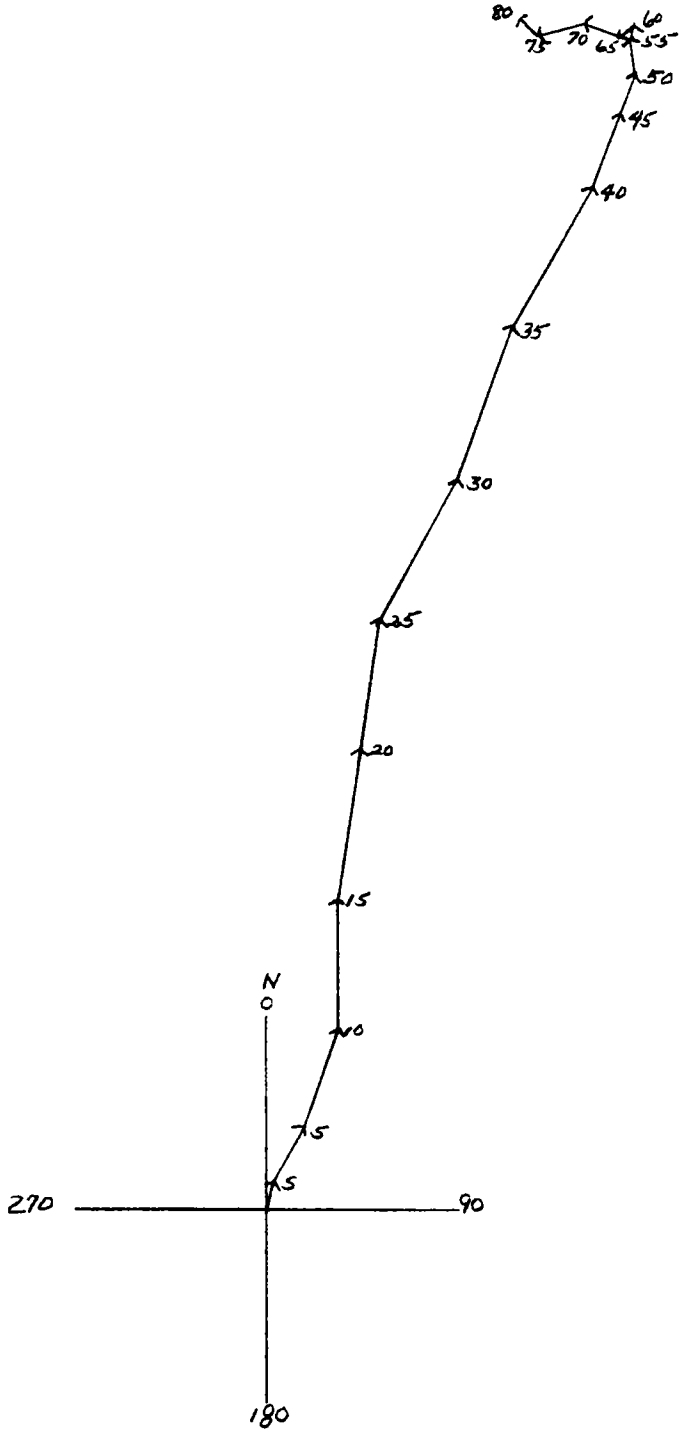

Fig. 10a Hodograph of winds at St. Louis, Missouri on June 15, 1954

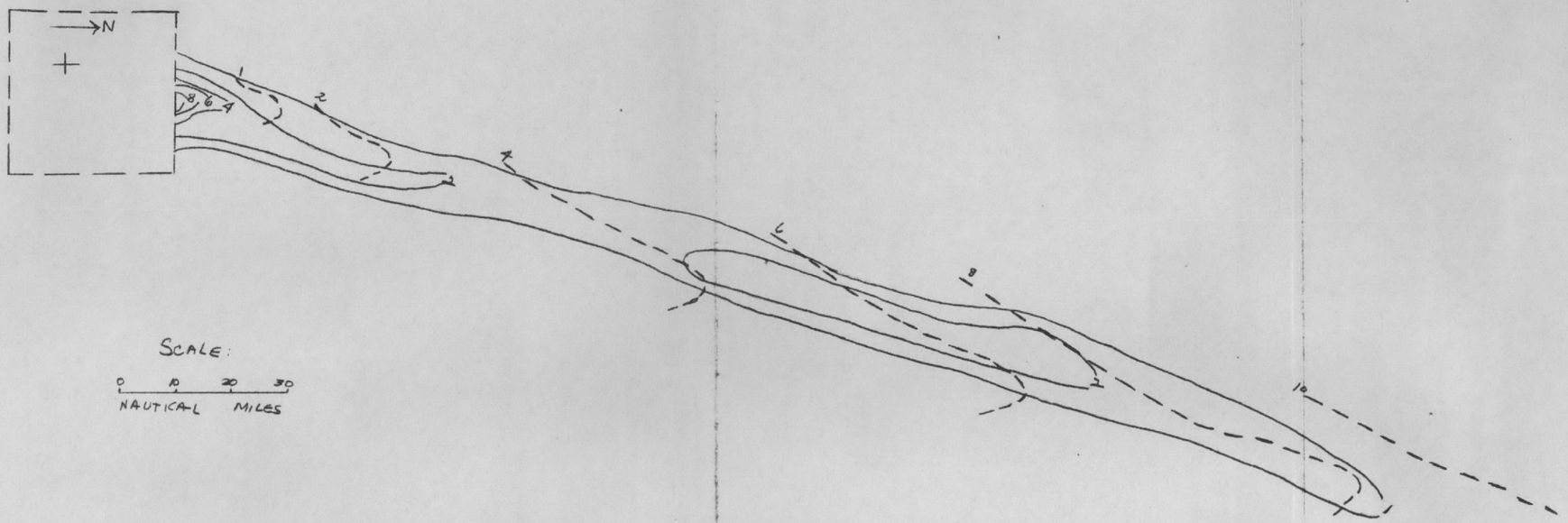

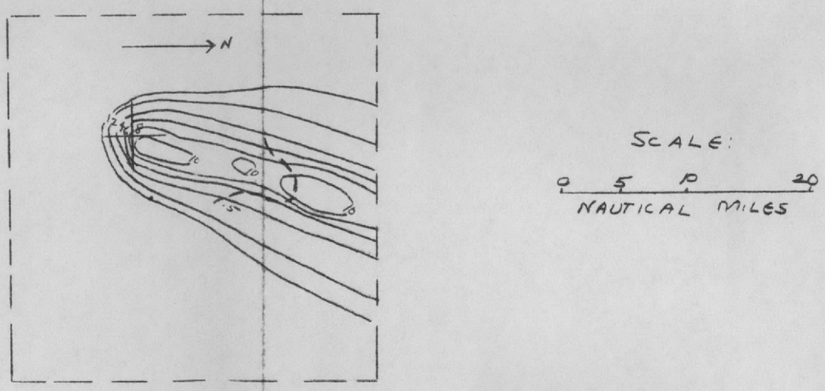

Fig. 10b Dose rate at 24 hours due to a 1 MT device detonated at St. Louis, Missouri on June 15, 1954 with approximate mean arrival times.

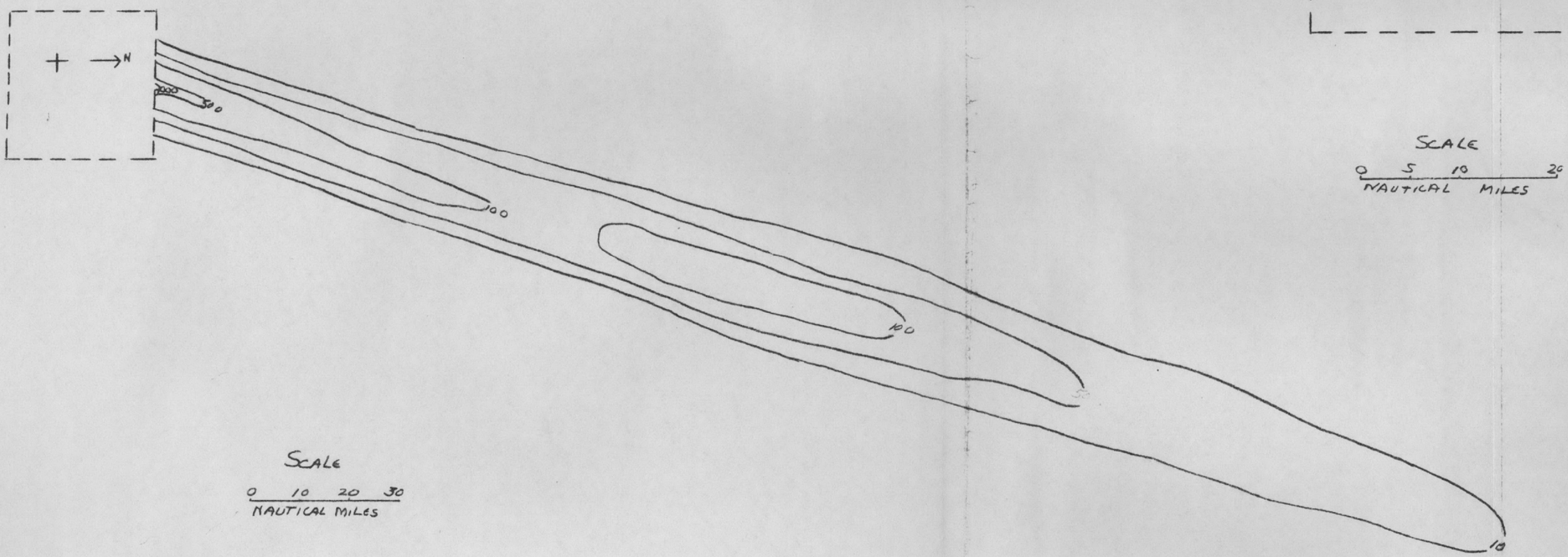

Fig. 10c Dosage from time of arrival to 24 hrs. due to a 1 MT device detonated at St. Louis, Missouri on June 15, 1954.

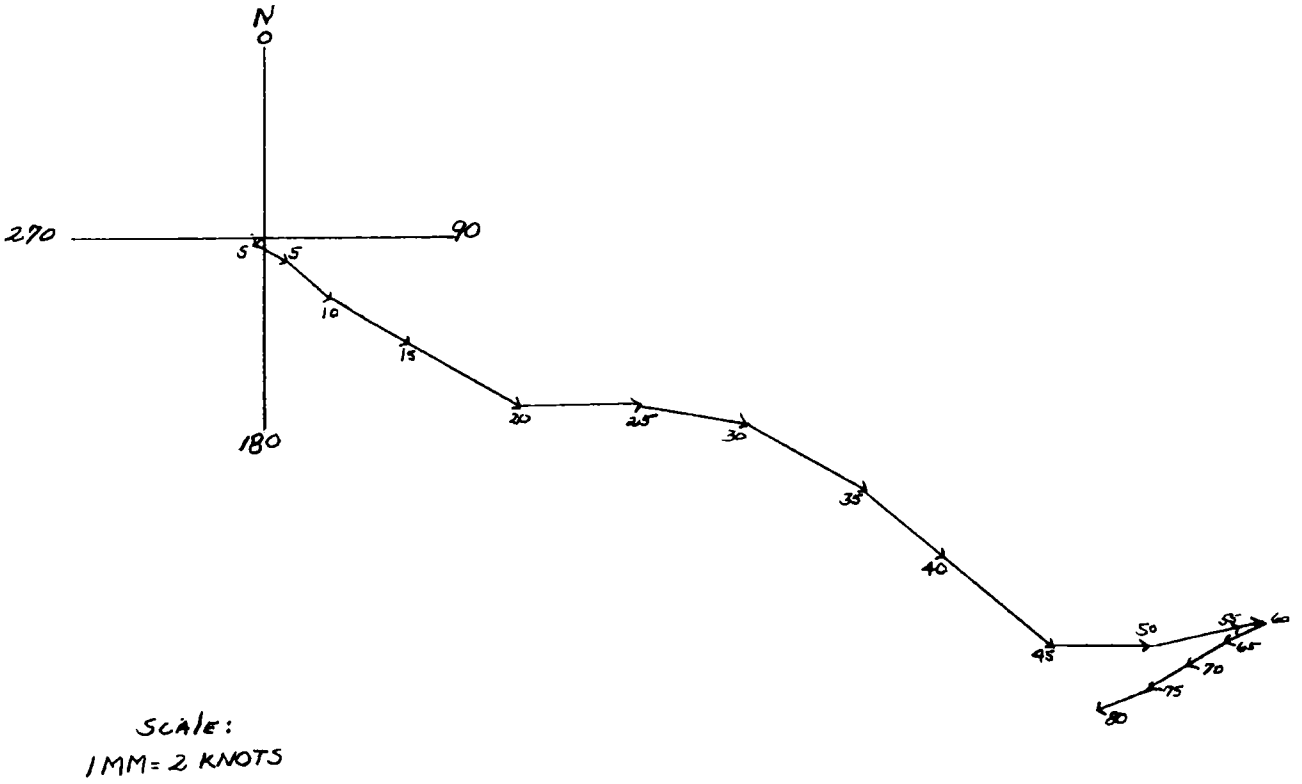

Fig. 11a Hodograph of winds at Los Angeles, California on June 15, 1954

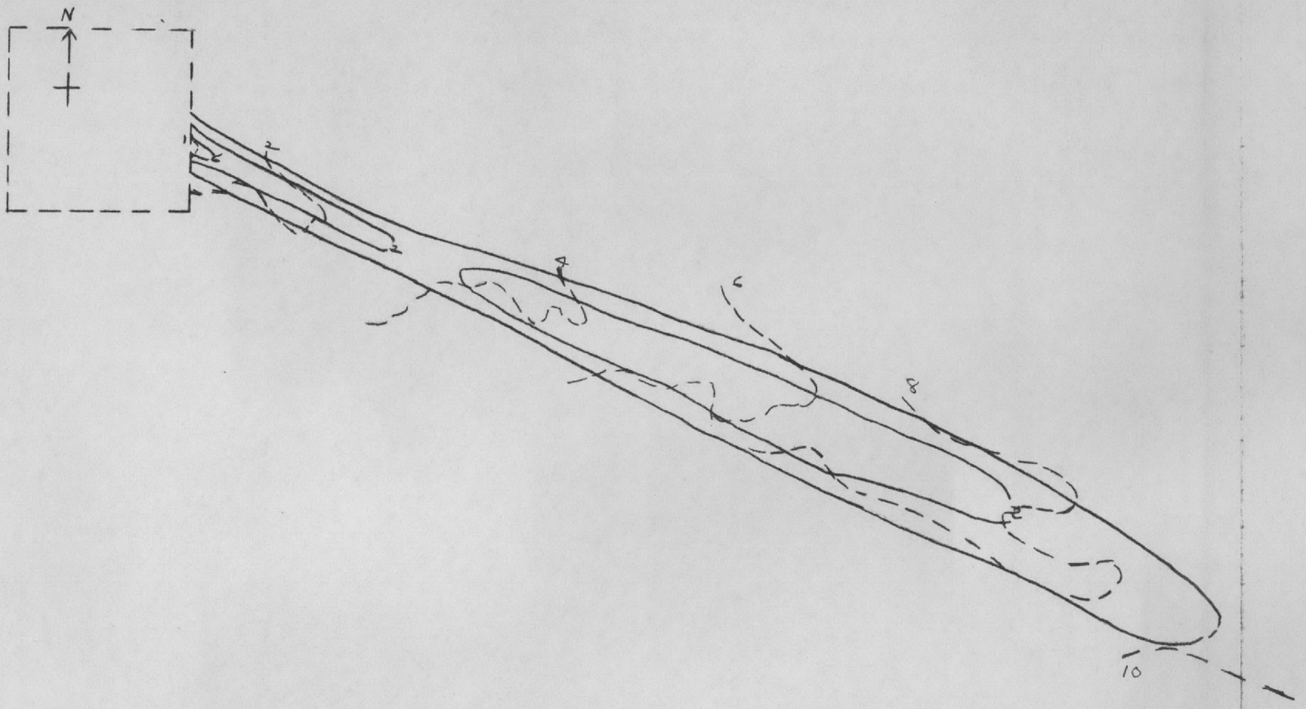

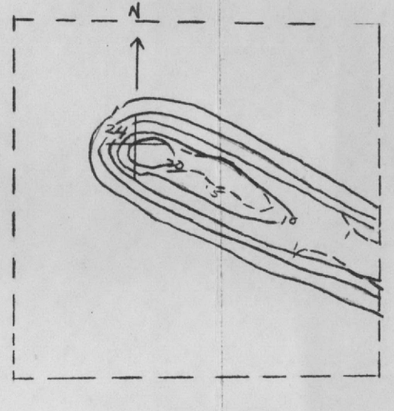

Fig. 11b Dose rate at 24 hours due to a 1 MT device detonated at Los Angeles, California on June 15, 1954 with approximate mean arrival times.

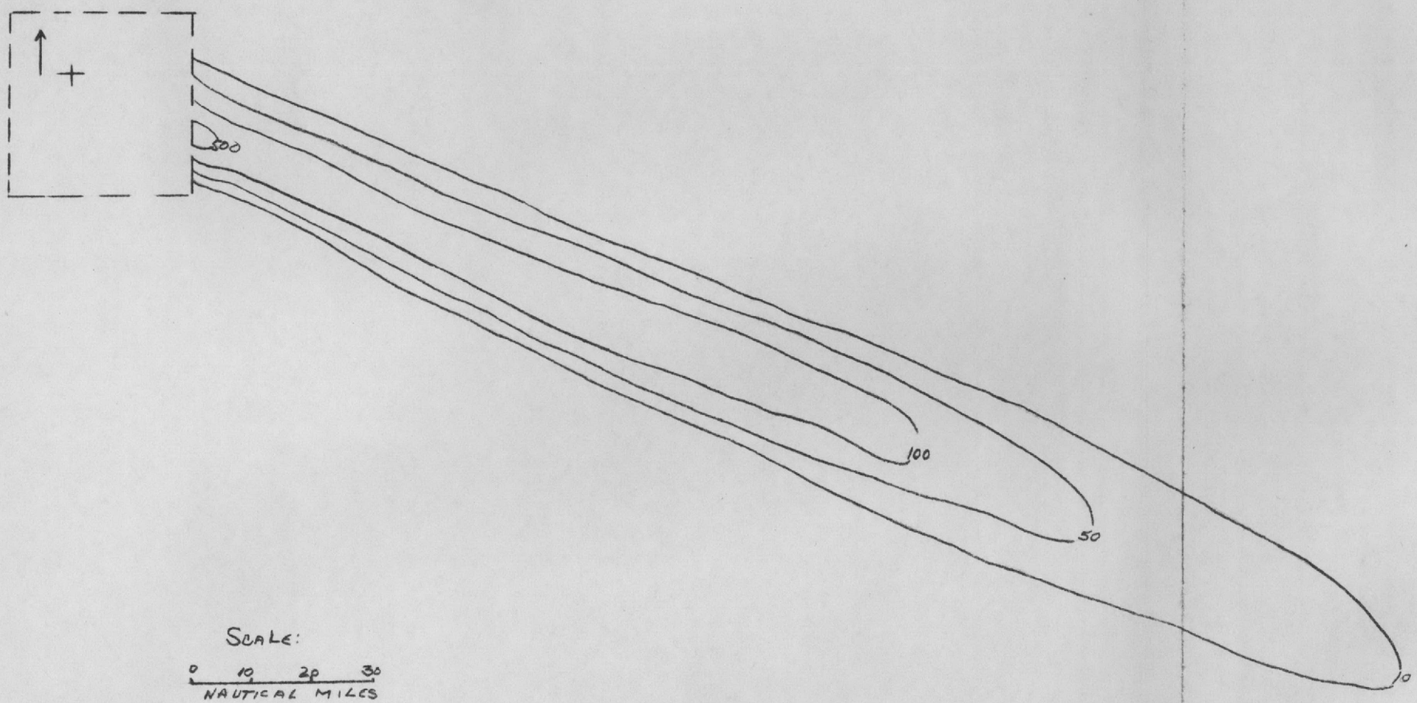

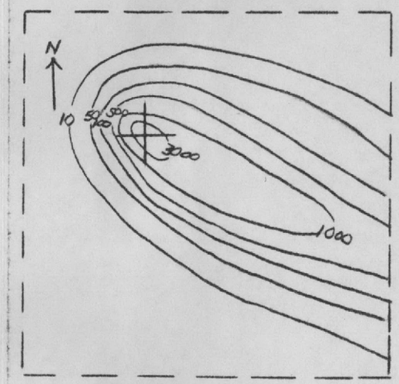

Fig. 11c Dosage from time of arrival to 24 hrs. due to a 1 MT device detonated at Los Angeles, California on June 15, 1954.

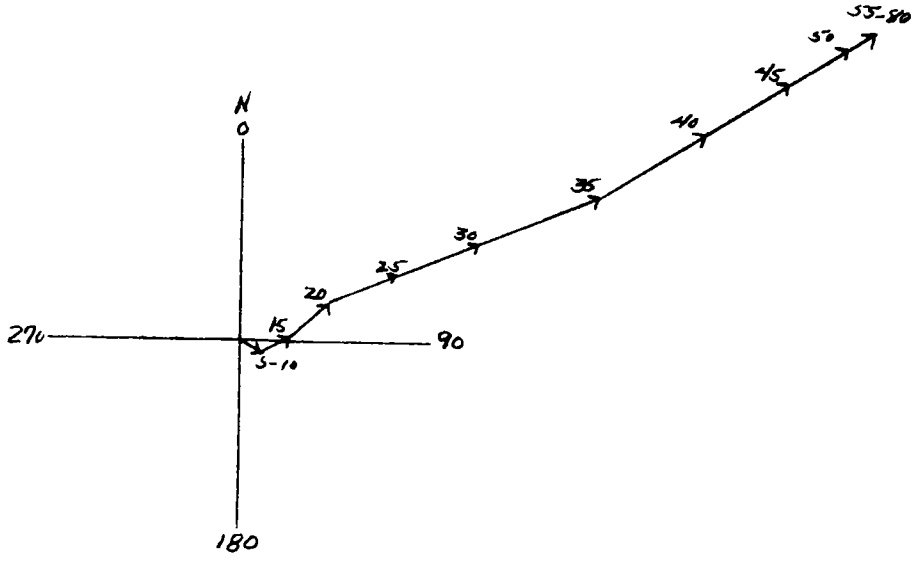

Scale:
1MM=2 KNOTS

Fig. 12a Hodograph of winds at Los Angeles, California on June 15, 1953.

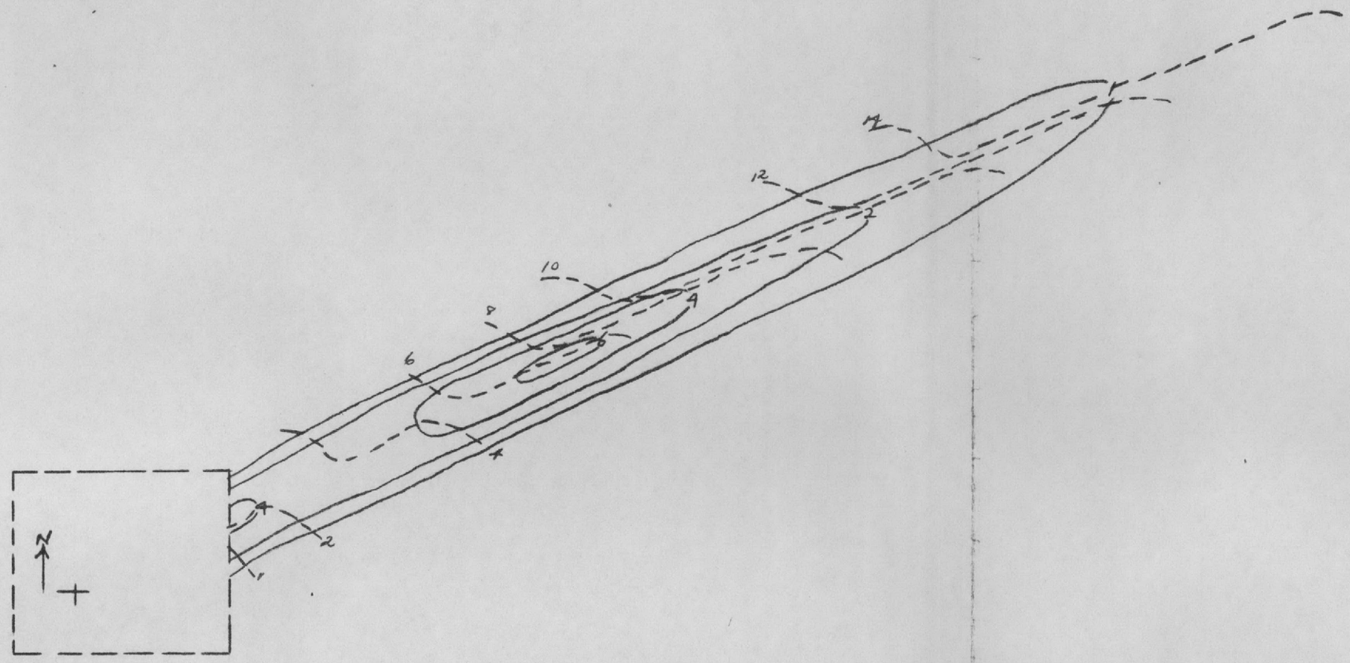

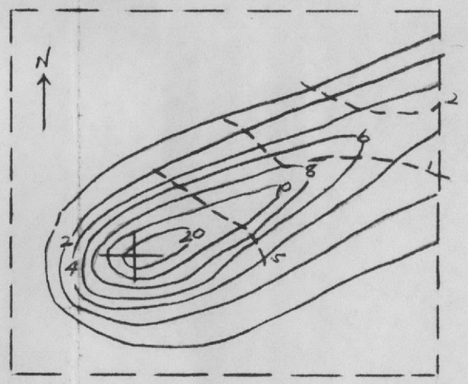

Fig. 12b Dose rate at 24 hours due to a 1 MT device detonated at Los Angeles, California on June 15, 1953 with approximate mean arrival times.

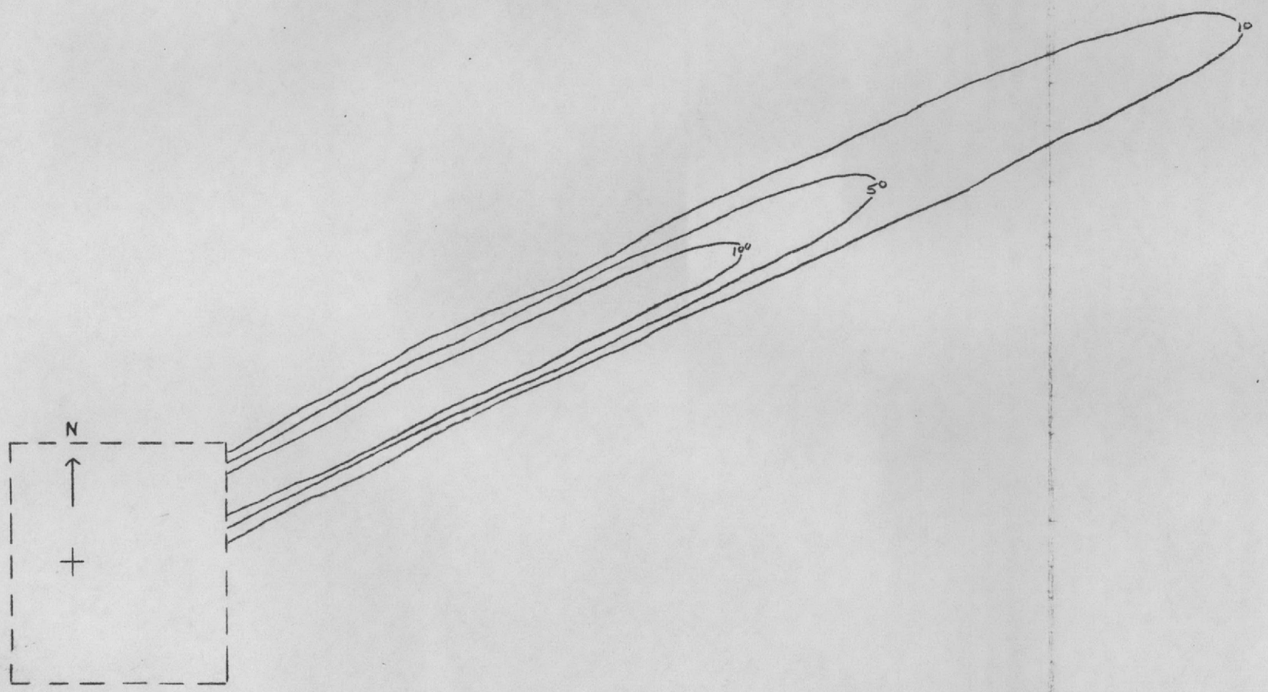

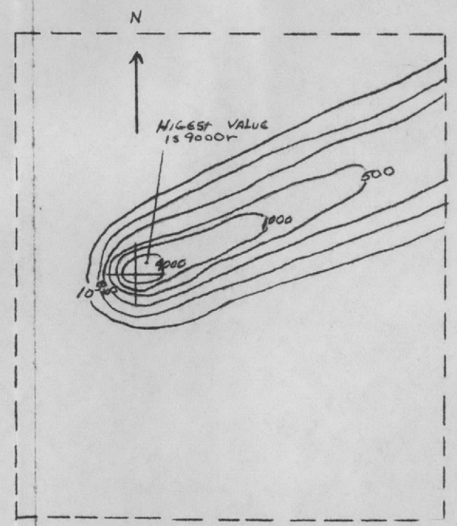

Fig. 12c Dosage from time of arrival to 24 hrs. due to a 1 MT device detonated at Los Angeles, California on June 15, 1953.

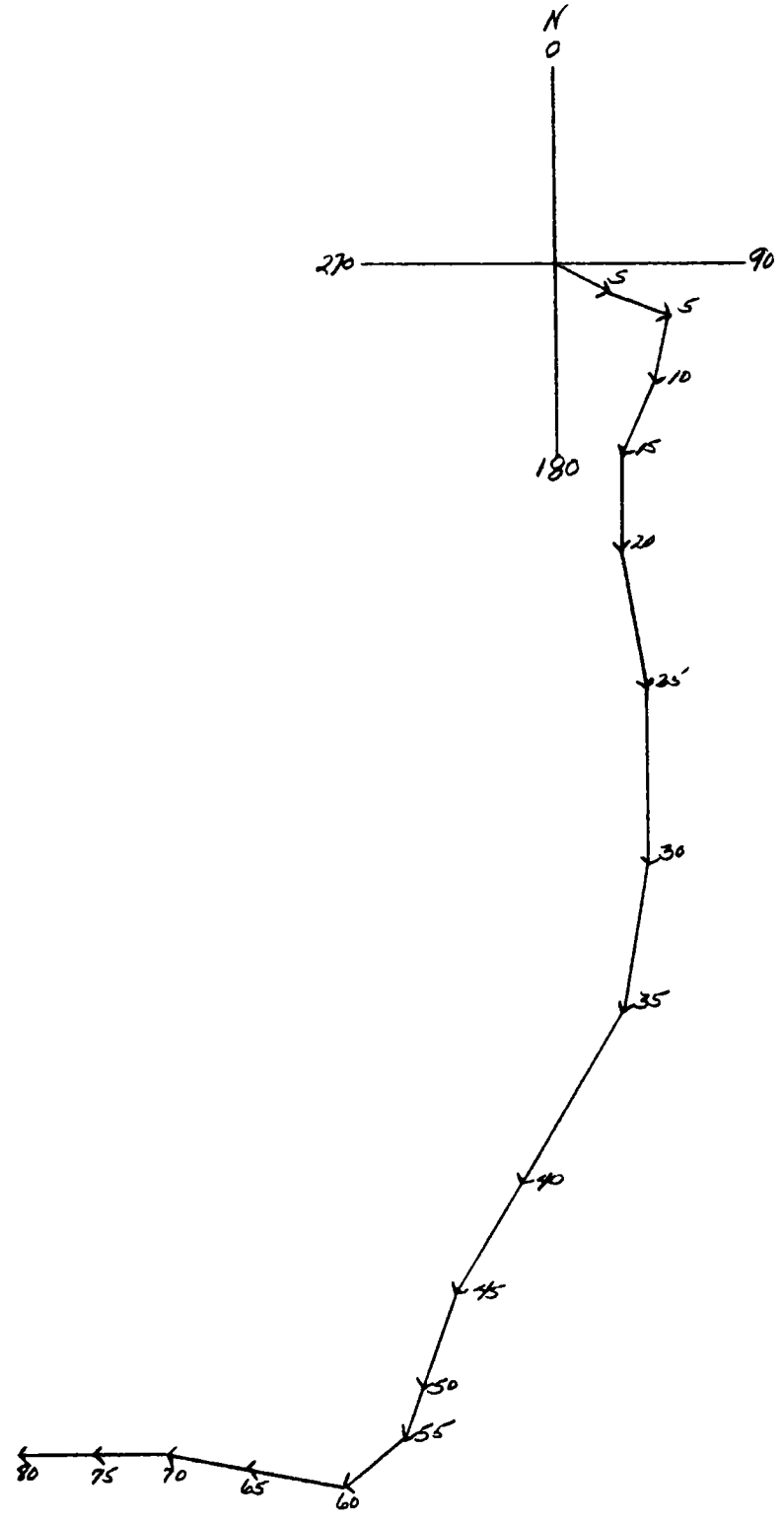

Fig. 13a Hodograph of winds at Atlanta, Georgia on June 15, 1953

Scale:
1mm = 2 knots

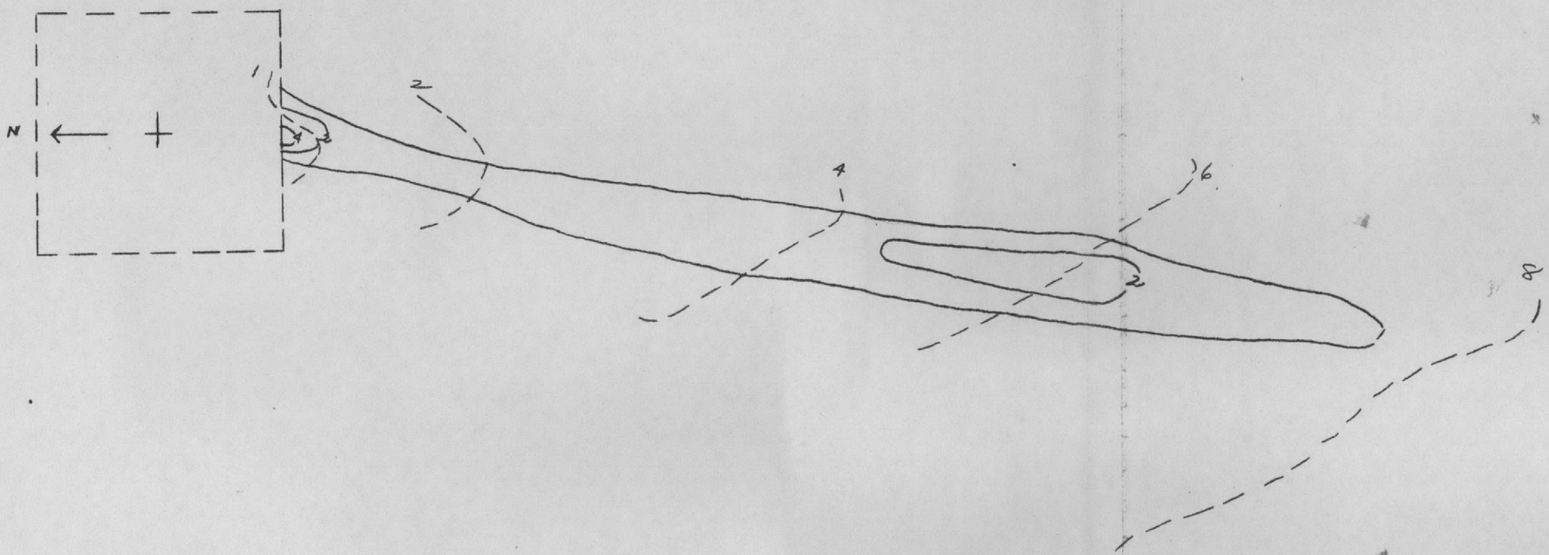

SCALE:
0 10 20 30
NAUTICAL MILES

SCALE:
0 5 10 20
NAUTICAL MILES

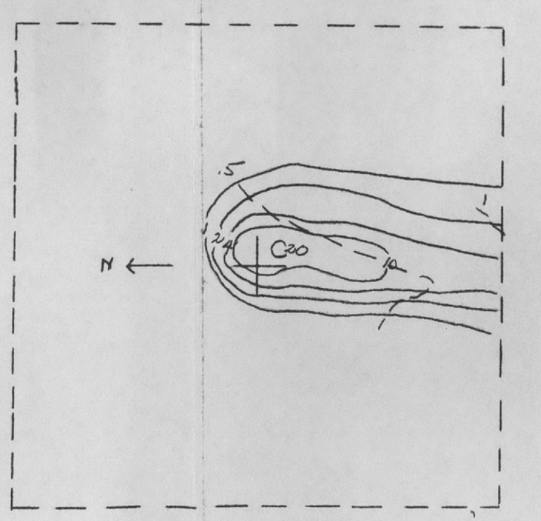

Fig. 13b Dose rate at 24 hours due to a 1 MT device detonated at Atlanta, Georgia on June 15, 1953 with approximate mean arrival times.

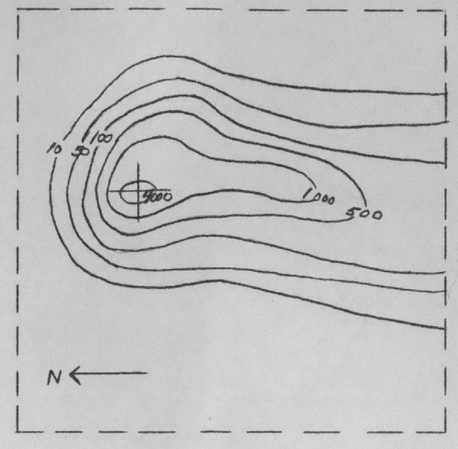

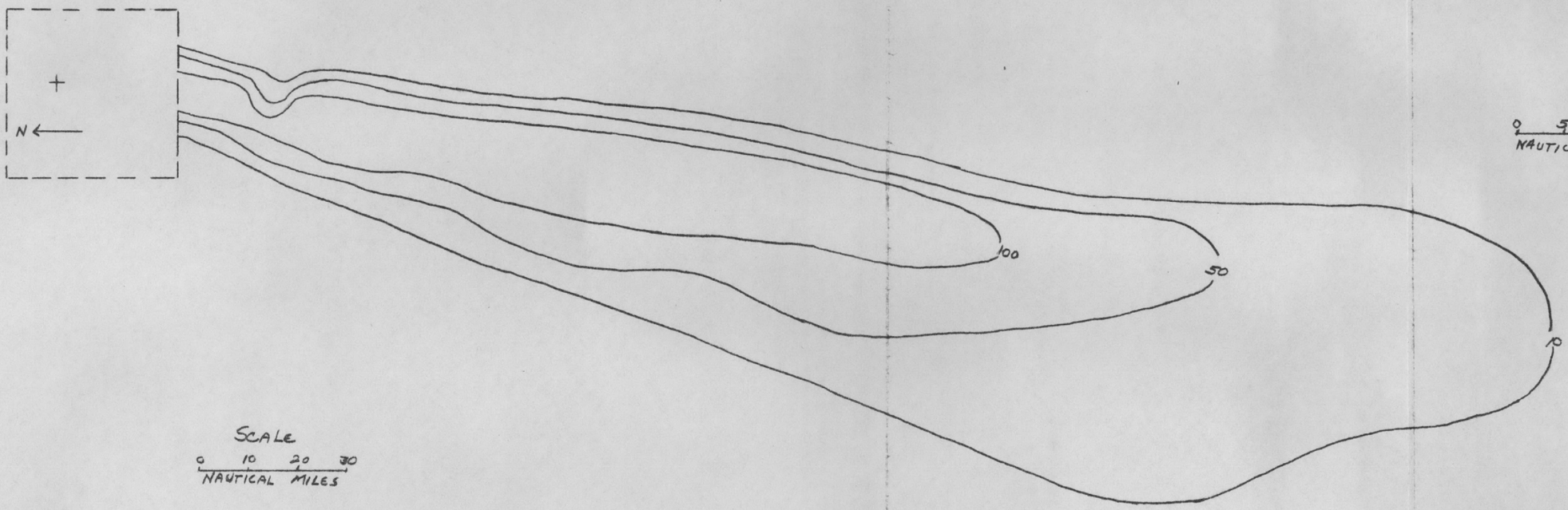

SCALE:
0 5 10 20
NAUTICAL MILES

Fig. 13e Dosage from time of arrival to 24 hrs. due to a 1 MT device detonated at Atlanta, Georgia on June 15, 1953.

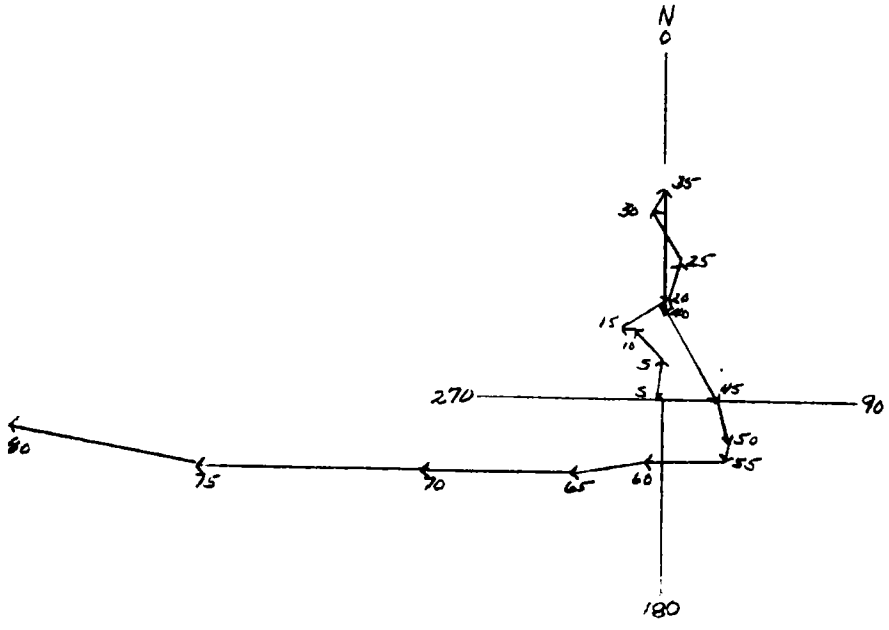

Fig. 14a Hodograph of winds at Atlanta, Georgia on June 15, 1954.

SCALE:
1MM = 1 KNOT

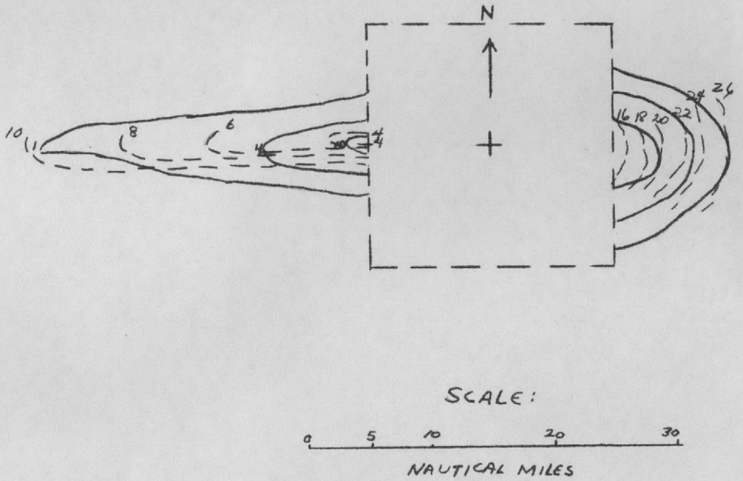

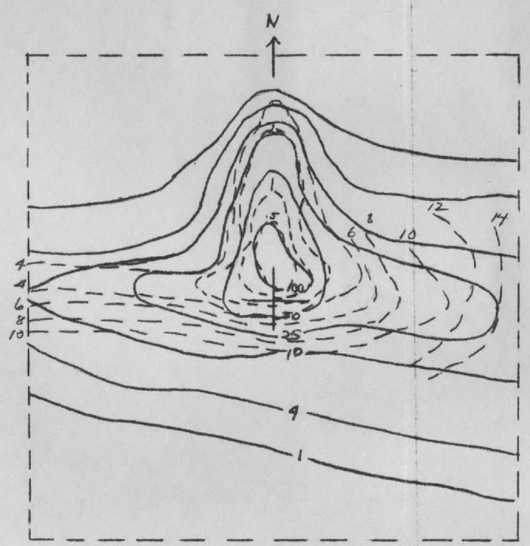

Fig. 14b Dose rate at 24 hours due to a 1 MT device detonated at Atlanta, Georgia on June 15, 1954 with approximate mean arrival times.

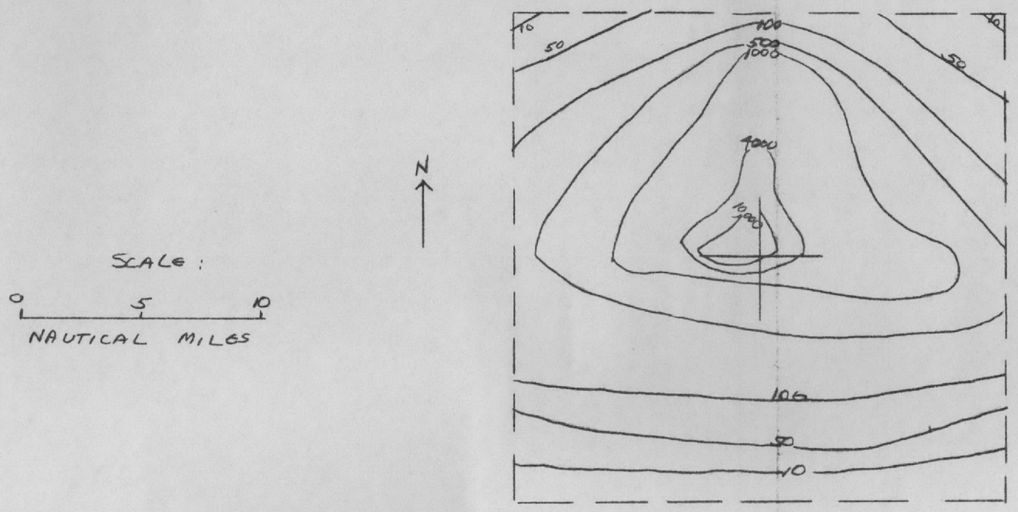

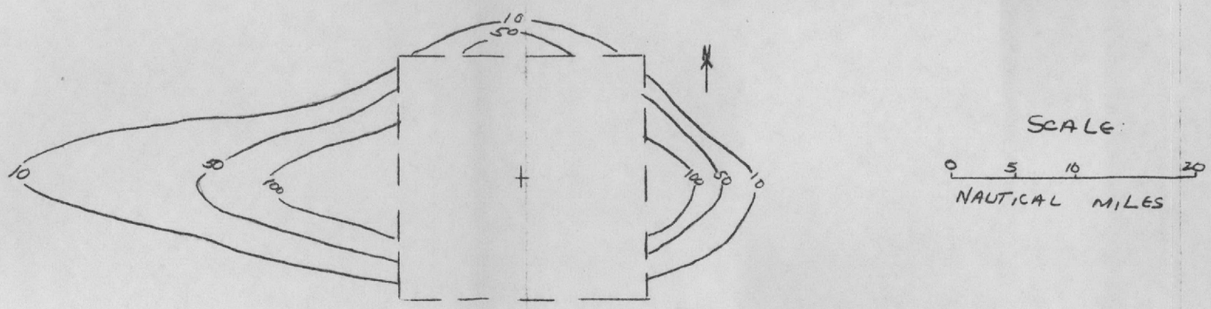

Fig. 14c Dosage from time of arrival to 24 hrs. due to a 1 MT device detonated at Atlanta, Georgia on June 15, 1954.

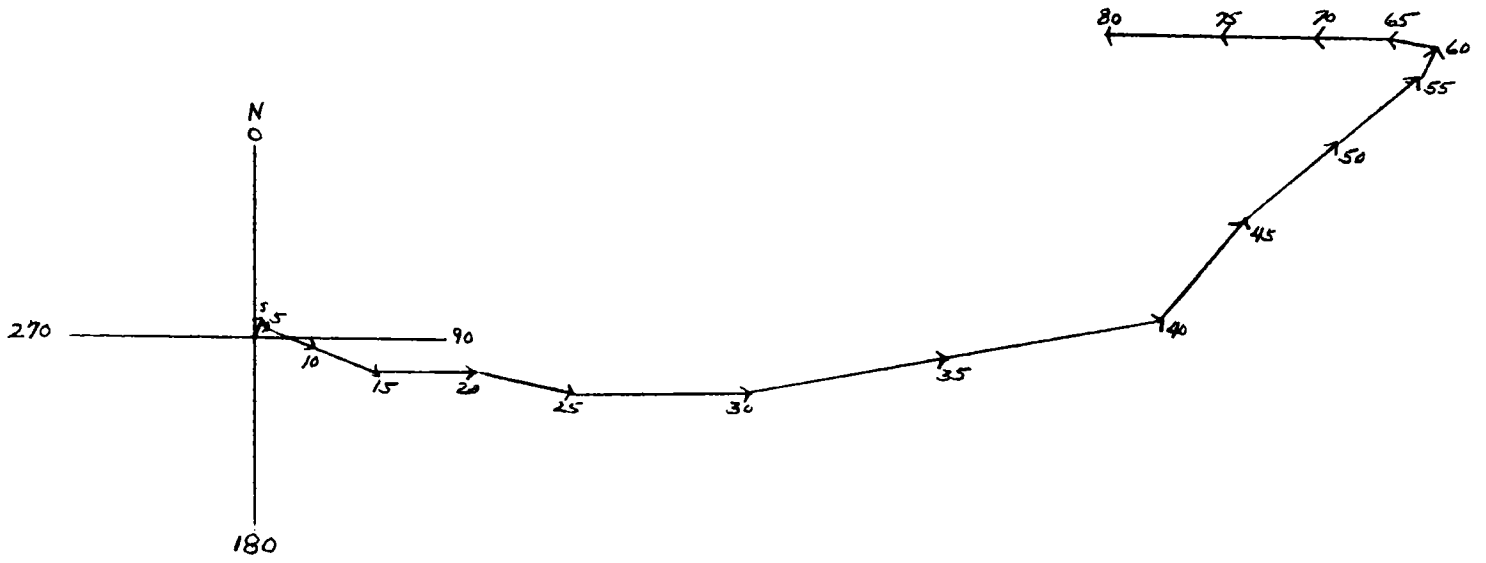

Fig. 15a Hodograph of winds at San Francisco, California on June 15, 1953

Scale:
1mm = 2 knots

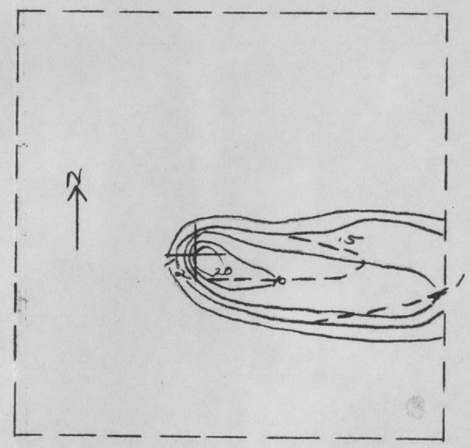

Fig. 15b Dose rate at 24 hours due to a 1 MT device detonated at San Francisco, California on June 15, 1953 with approximate mean arrival times.

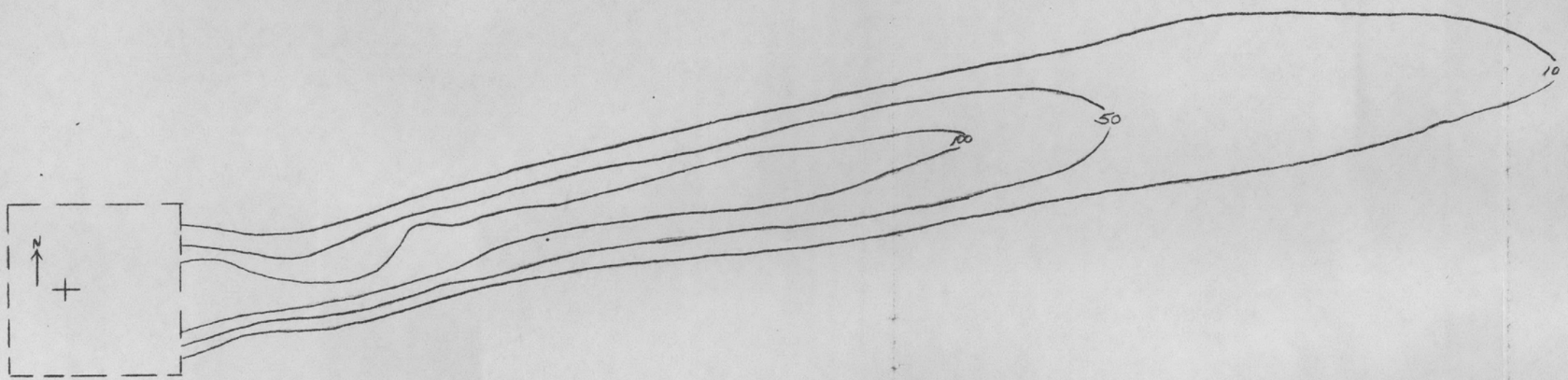

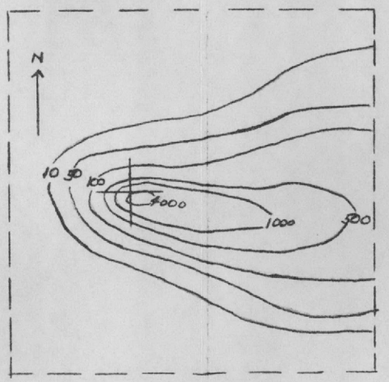

Fig. 15c Dosage from time of arrival to 24 hrs. due to a 1 MT device detonated at San Francisco, California on June 15, 1953.

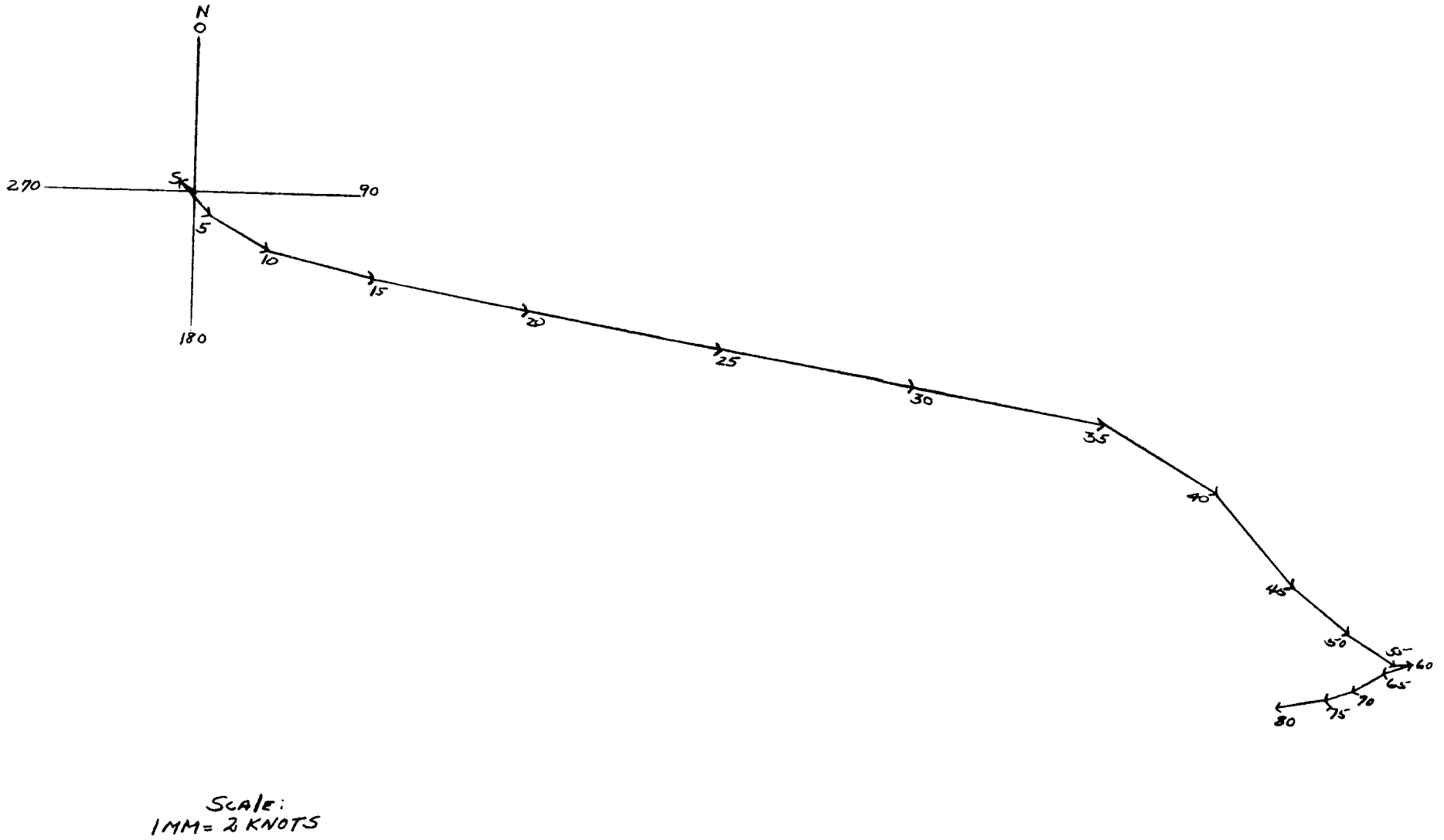

Fig. 16a Hodograph of winds at San Francisco, California on June 15, 1954

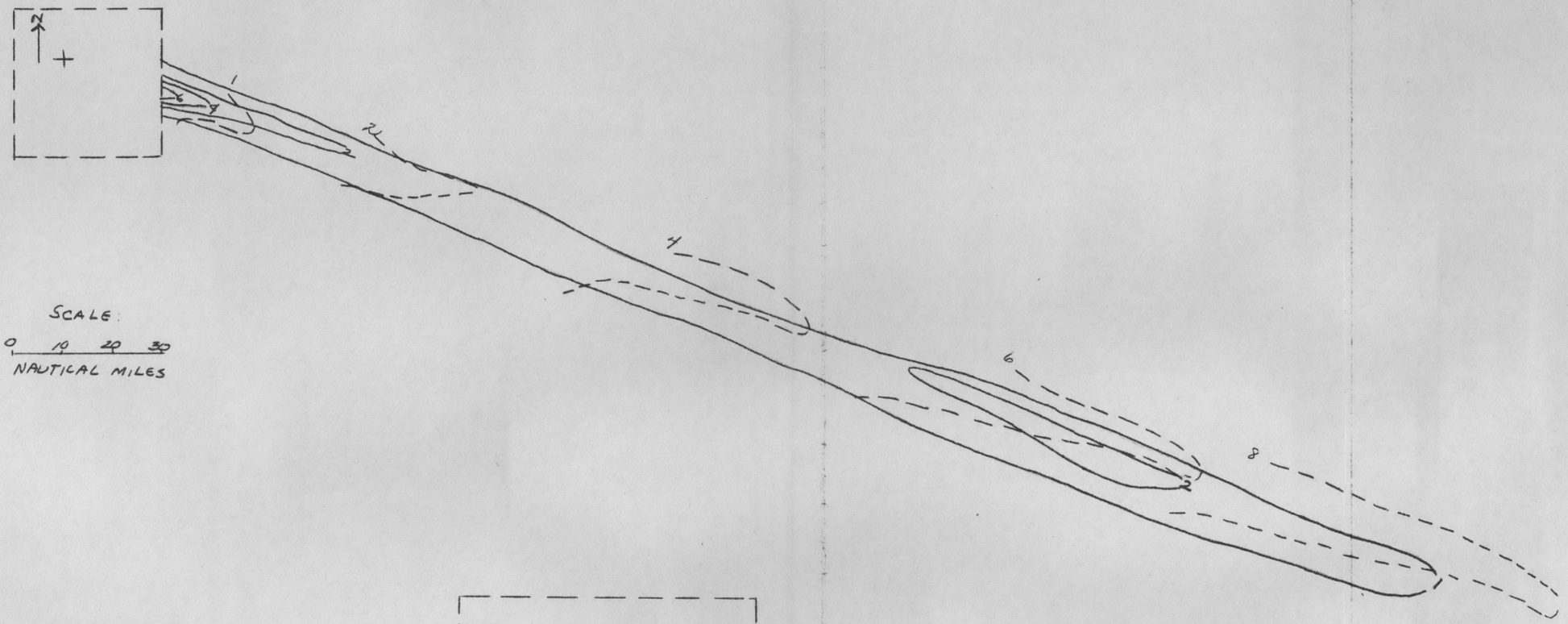

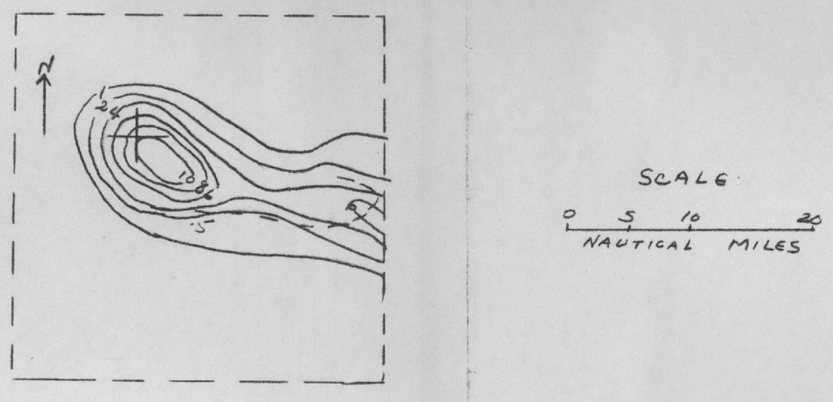

Fig. 16b Dose rate at 24 hours due to a 1 MT device detonated at San Francisco, California on June 15, 1954 with approximate mean arrival times.

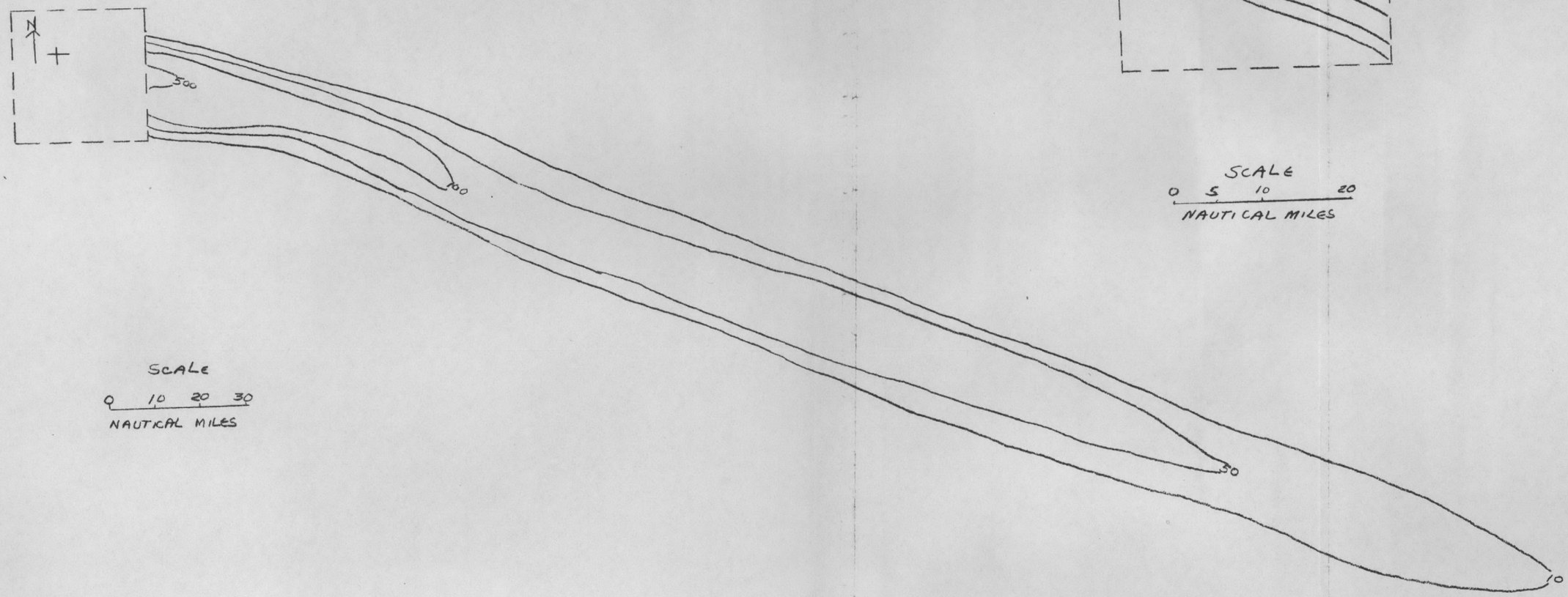

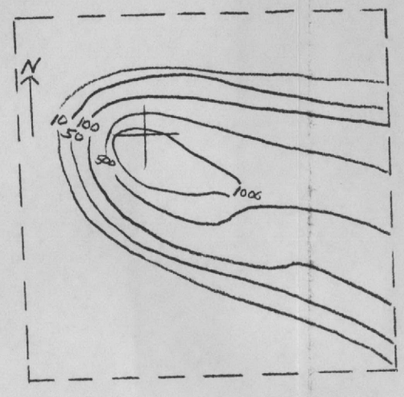

Fig. 16c Dosage from time of arrival to 24 hrs. due to a 1 MT device detonated at San Francisco, California on June 15, 1954.

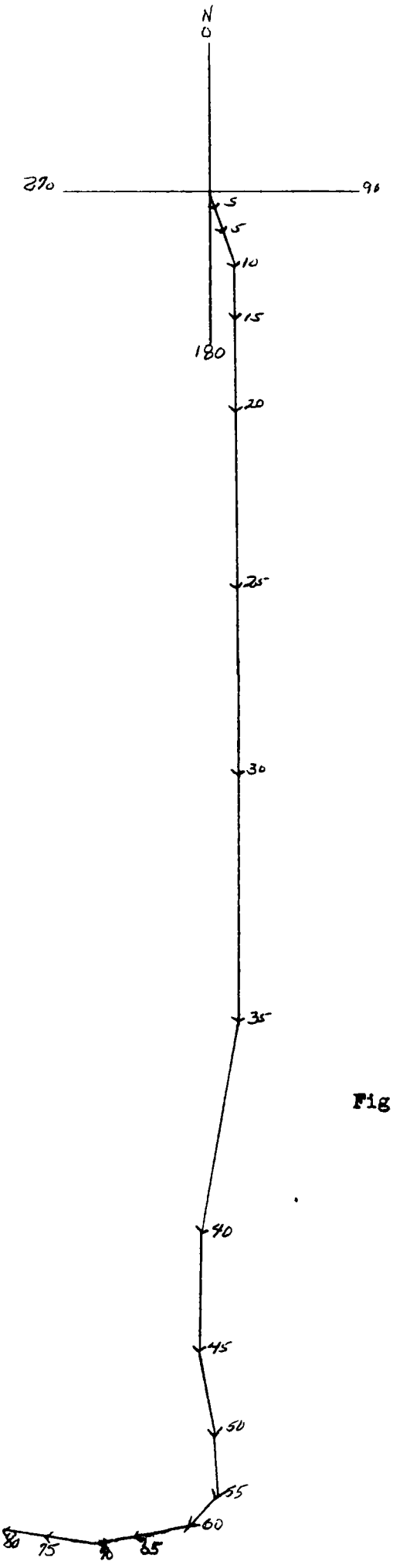

Fig. 17a Hodograph of winds at Philadelphia, Pennsylvania on June 15, 1953.

Scale:
1MM = 2 KNOTS

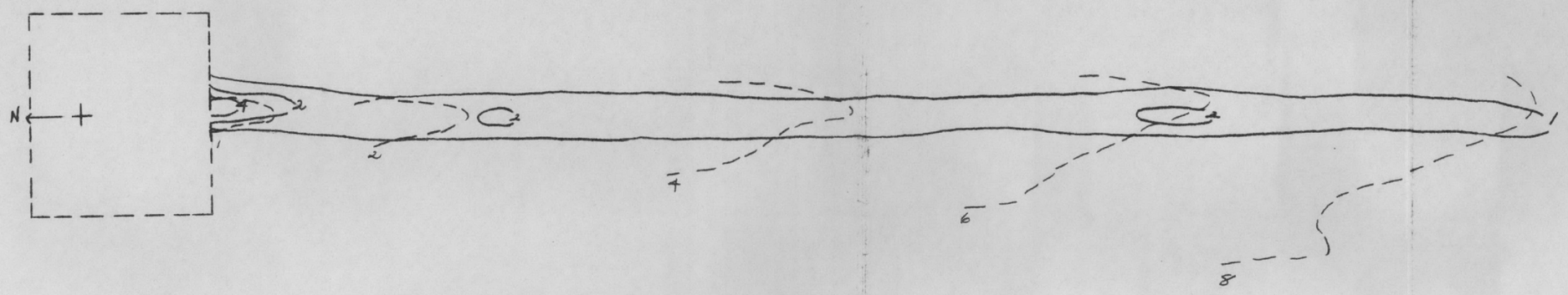

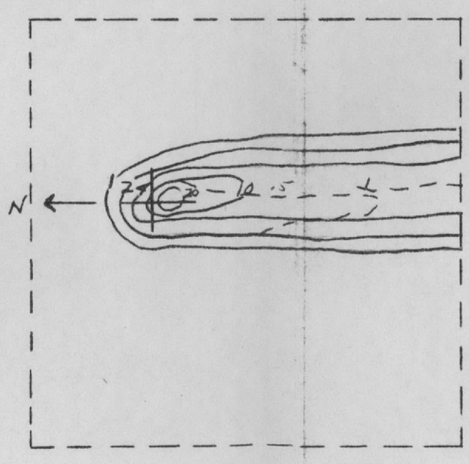

Fig. 17b Dose rate at 24 hours due to a 1 MT device detonated at Philadelphia, Pennsylvania on June 15, 1953 with approximate mean arrival times.

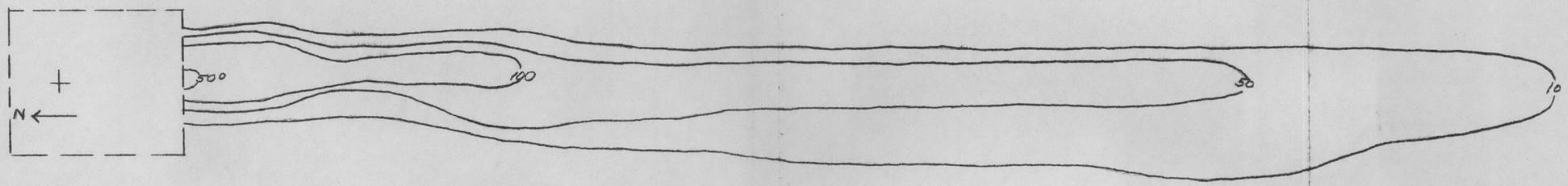

SCALE:
0 10 20 30
NAUTICAL MILES

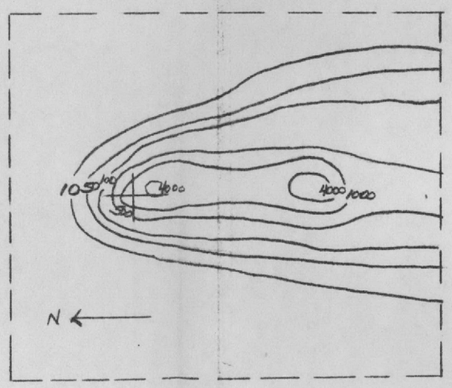

SCALE
0 5 10 30
NAUTICAL MILES

Fig. 17c Dosage from time of arrival to 24 hrs. due to a 1 MT device detonated at Philadelphia, Pennsylvania on June 15, 1953.

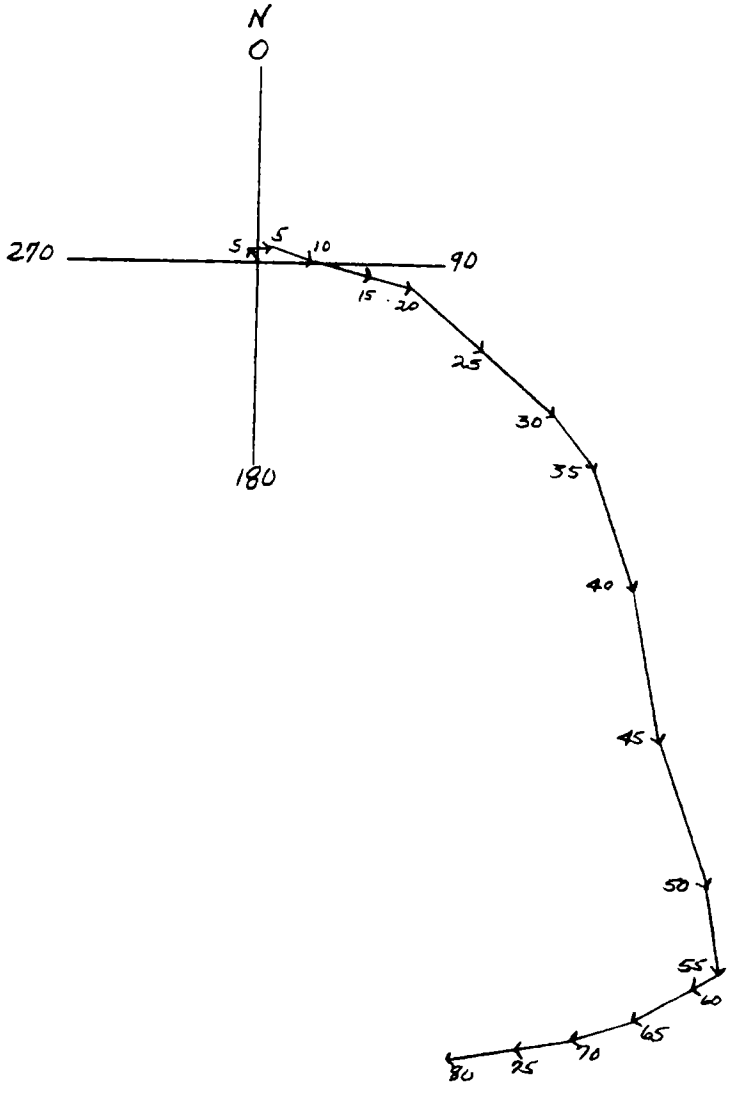

Fig. 18a Hodograph of winds at Philadelphia, Pennsylvania on June 15, 1954

Scale:
1MM = 2 KNOTS

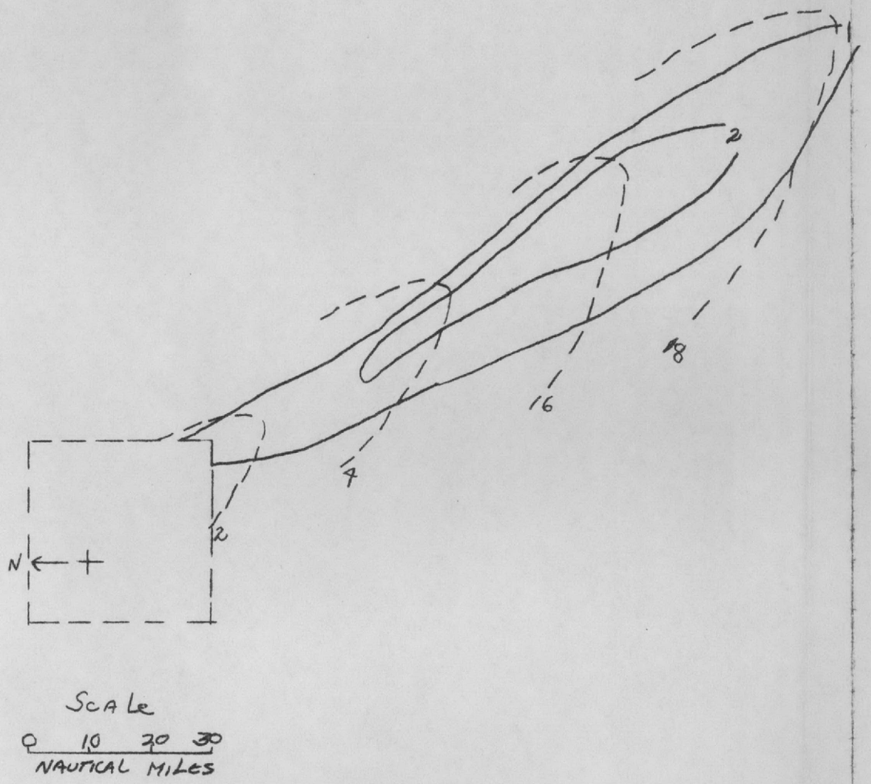

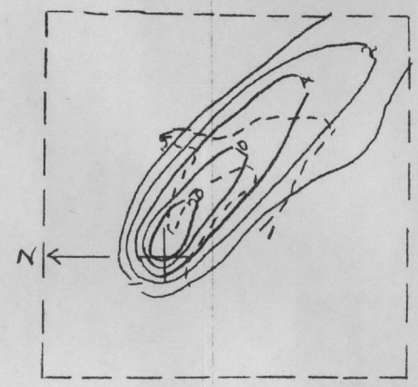

Fig. 18b Dose rate at 24 hours due to a 1 MT device detonated at Philadelphia, Pennsylvania on June 15, 1954 with approximate mean arrival times.

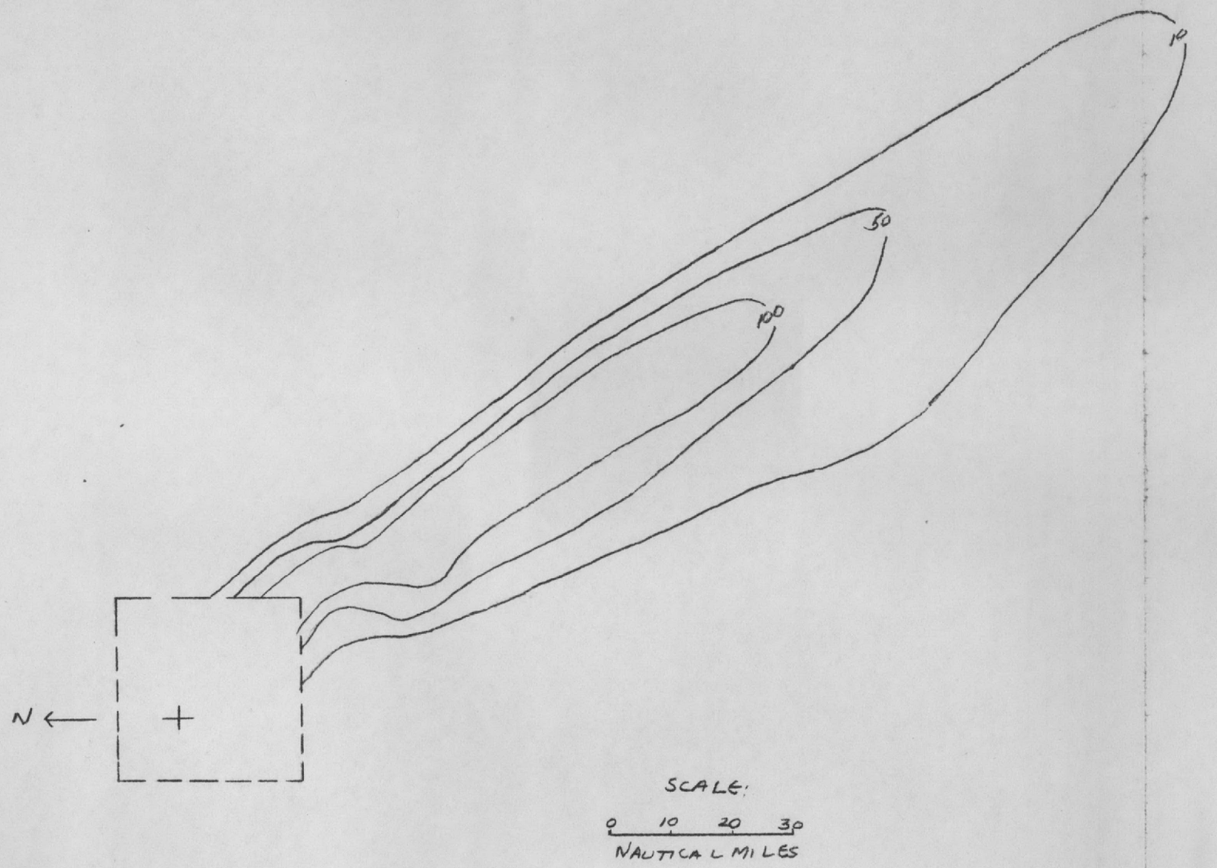

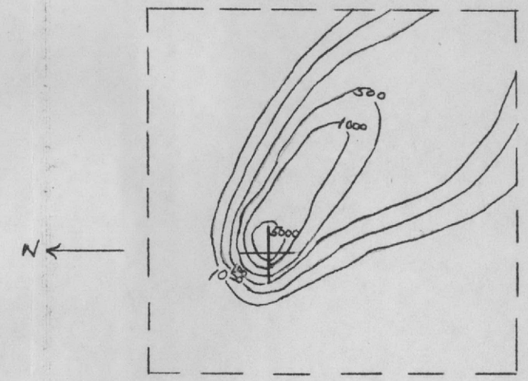

Fig. 18c Dosage from time of arrival to 24 hrs. due to a 1 MT device detonated at Philadelphia, Pennsylvania on June 15, 1954.

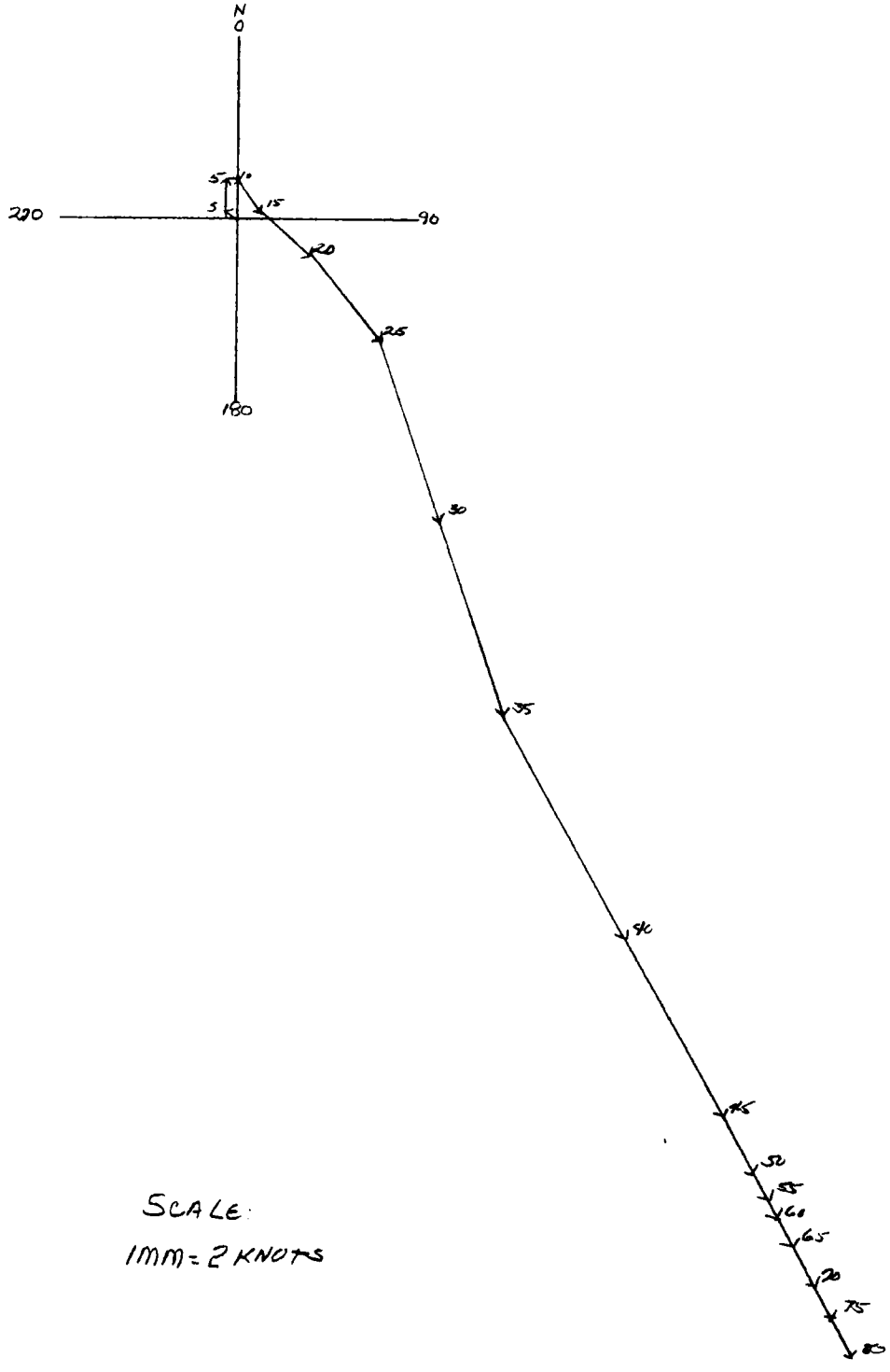

Fig. 19a Hodograph of winds at Detroit, Michigan on June 15, 1953.

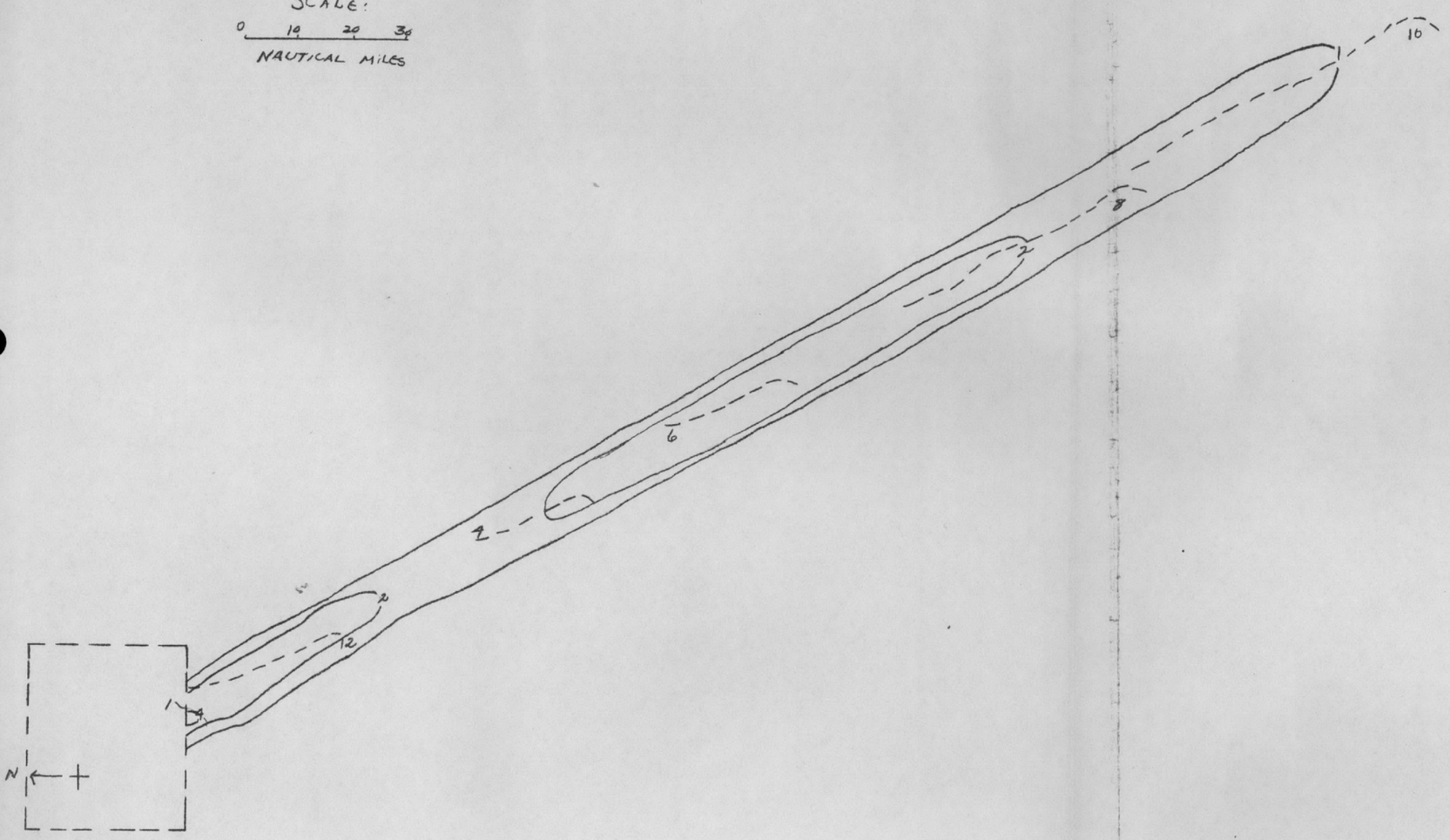

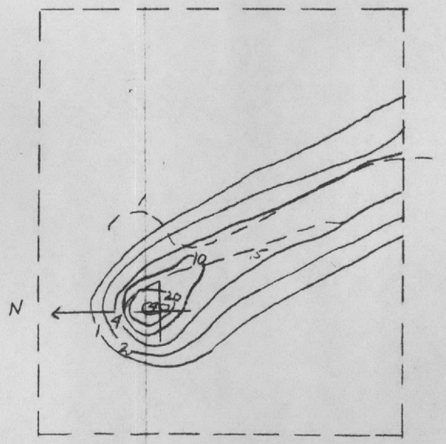

SCALE:
0 5 10 20
NAUTICAL MILES

Fig. 19b Dose rate at 24 hours due to a 1 MT device detonated at Detroit, Michigan on June 15, 1953 with approximate mean arrival times.

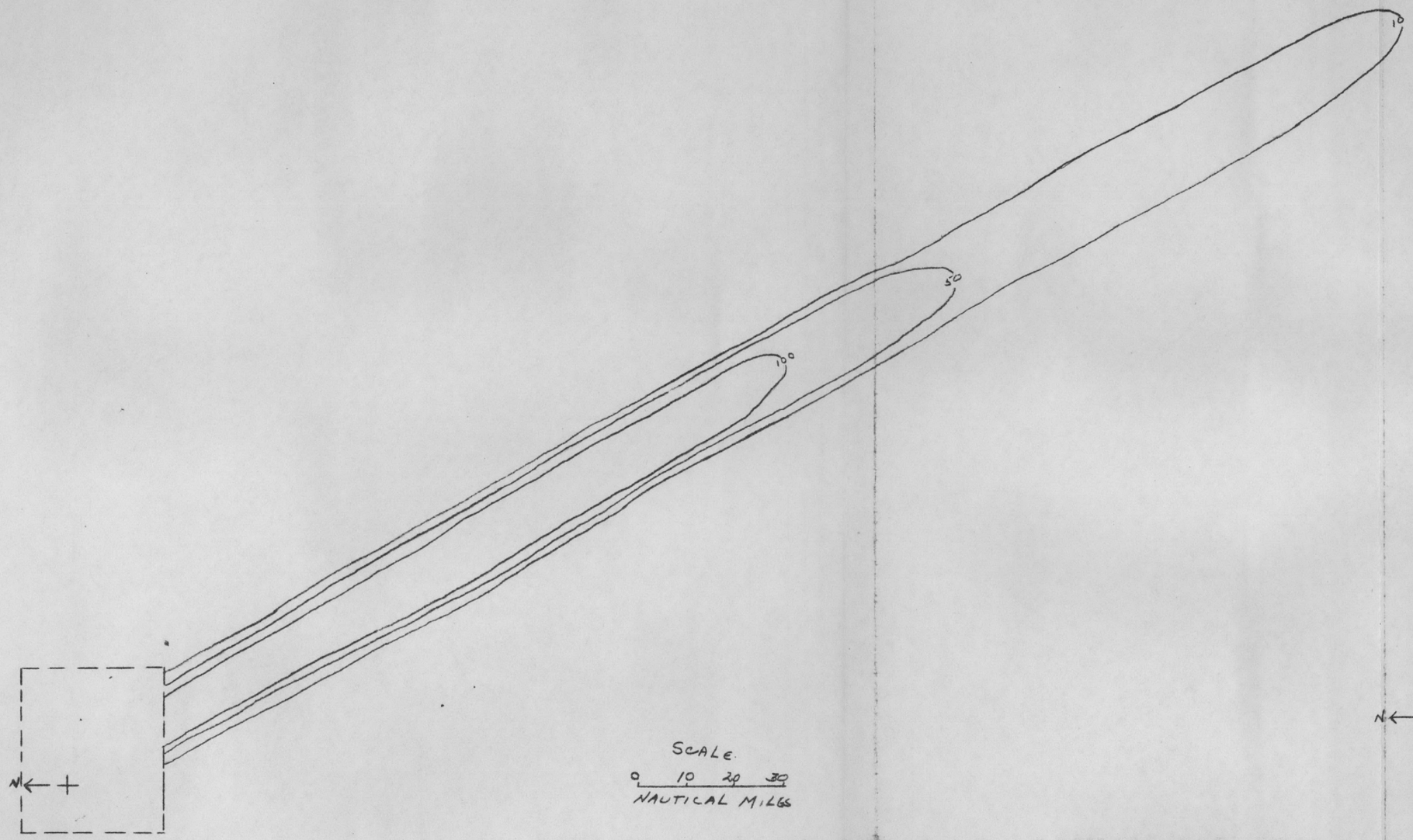

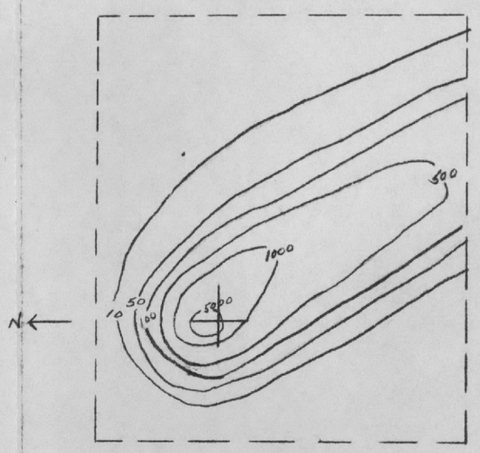

Fig. 19c Dosage from time of arrival to 24 hrs. due to a 1 MT device detonated at Detroit, Michigan on June 15, 1953.

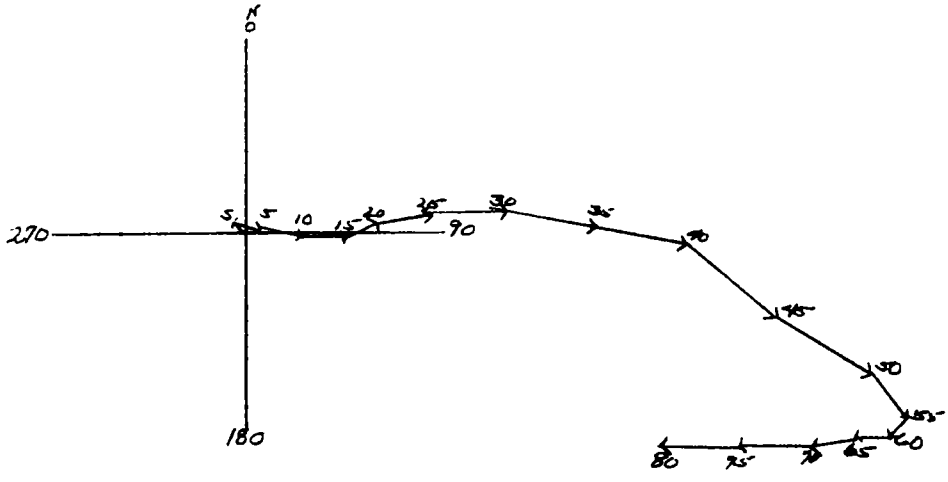

Scale:
1mm = 2 knots

Fig. 20a Hodograph of winds at Detroit, Michigan on June 15, 1954

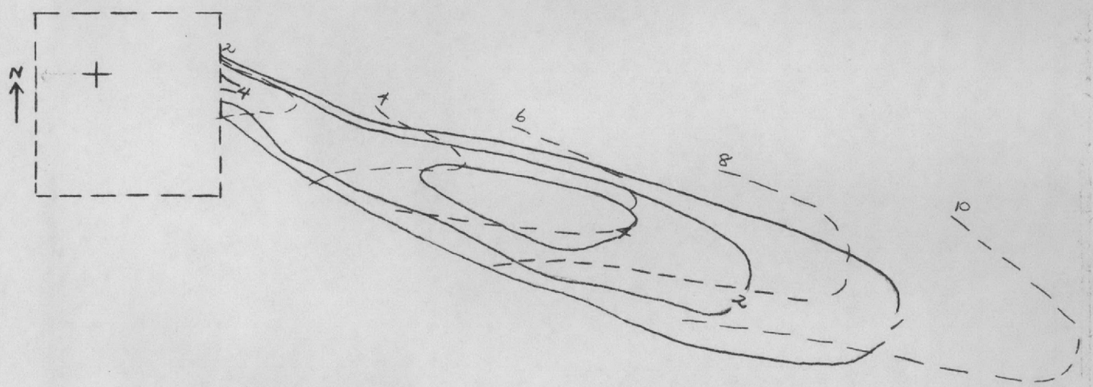

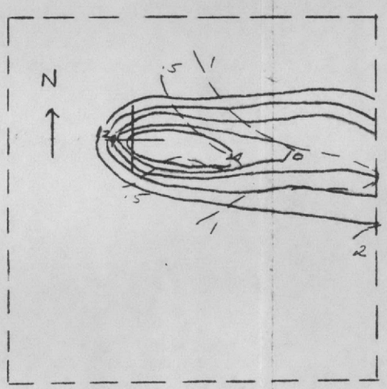

Fig. 20b Dose rate at 24 hours due to a 1 MT device detonated at Detroit, Michigan on June 15, 1954 with approximate mean arrival times.

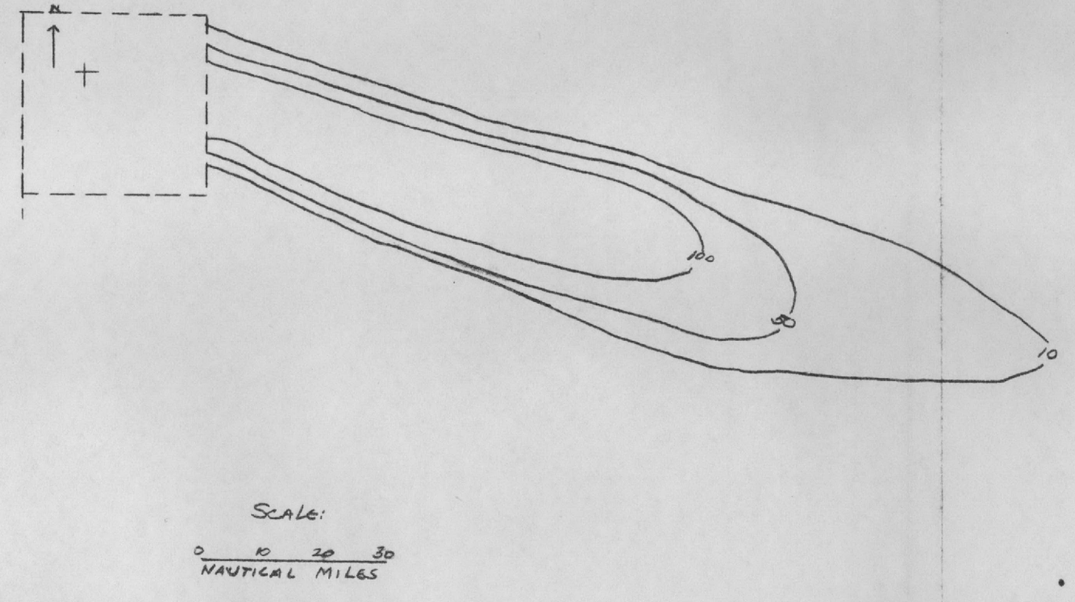

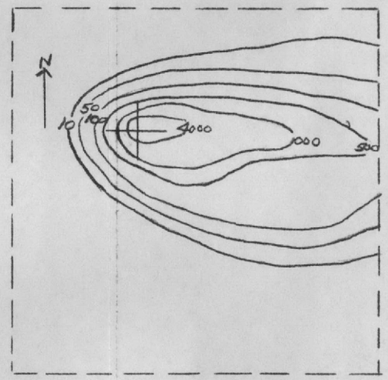

Fig. 20c Dosage from time of arrival to 24 hrs. due to a 1 MT device detonated at Detroit, Michigan on June 15, 1954.

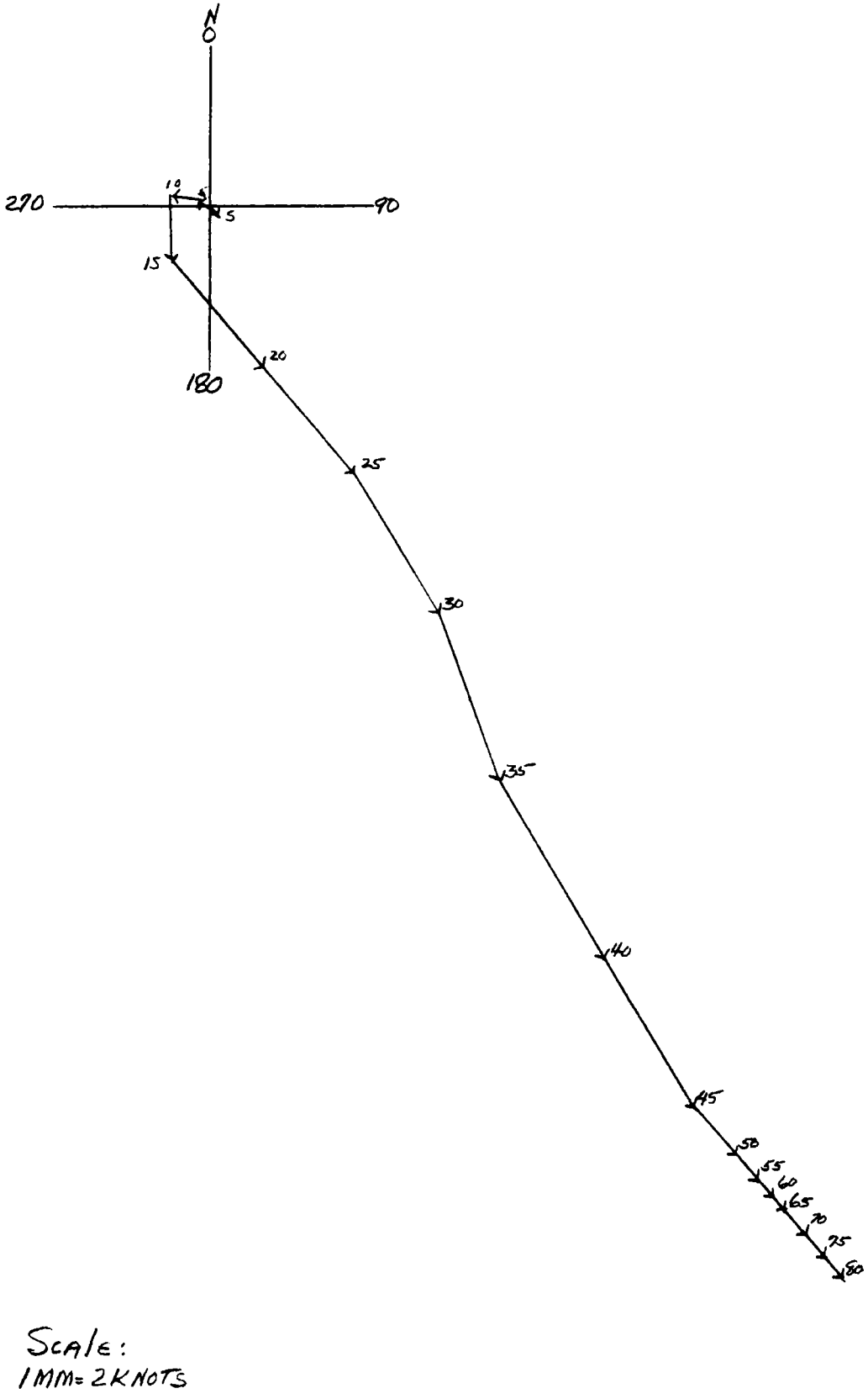

Fig. 21a Hodograph of winds at Buffalo, New York on June 15, 1953.

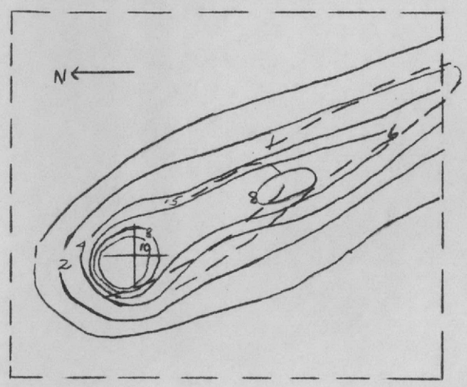

SCALE.
0 5 10 20
NAUTICAL MILES

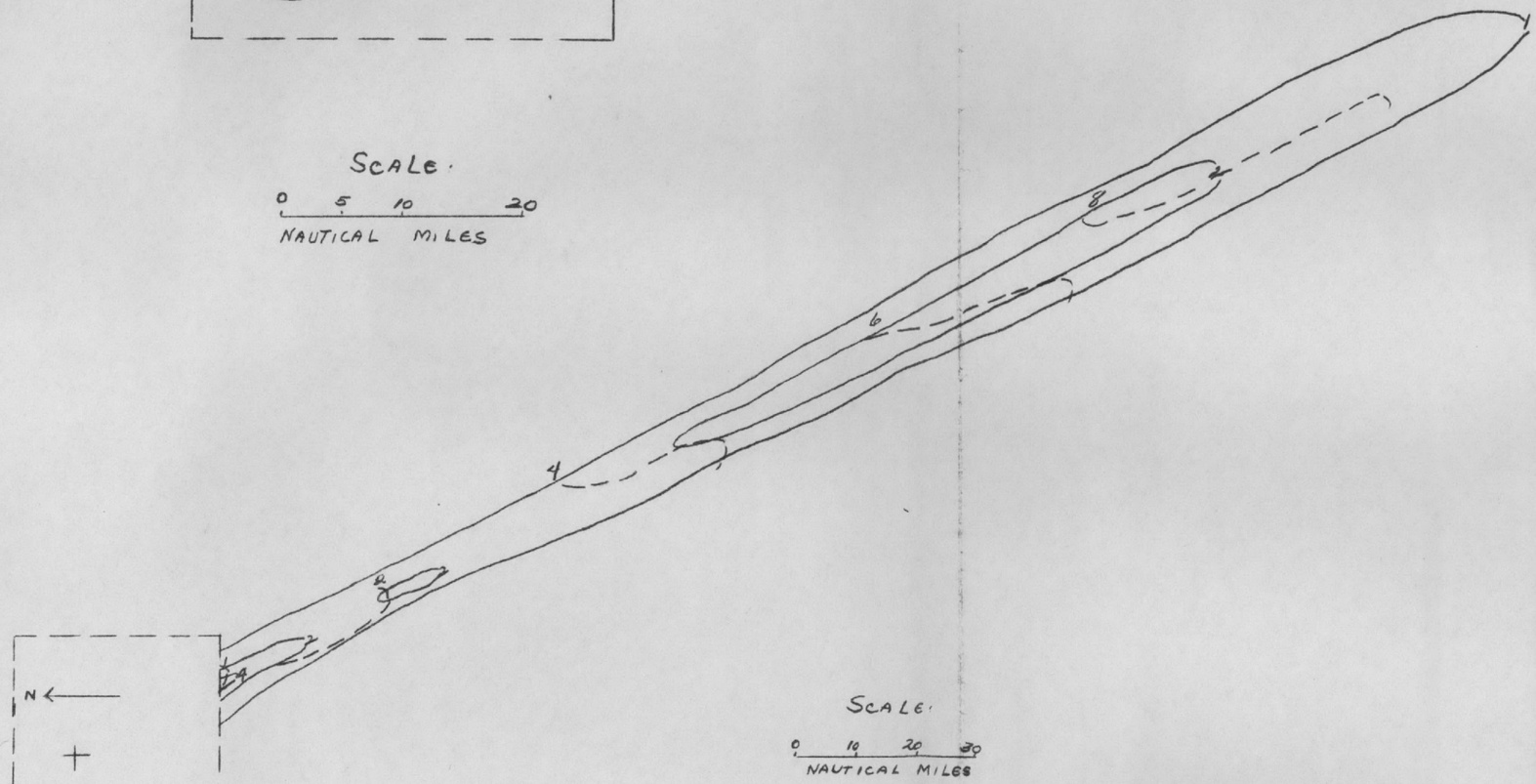

Fig. 21b Dose rate at 24 hours due to a 1 MT device detonated at Buffalo, New York on June 15, 1953 with approximate mean arrival times.

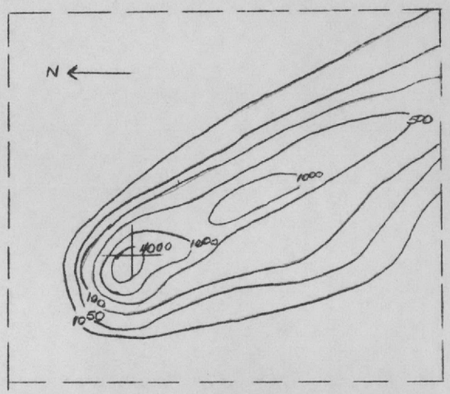

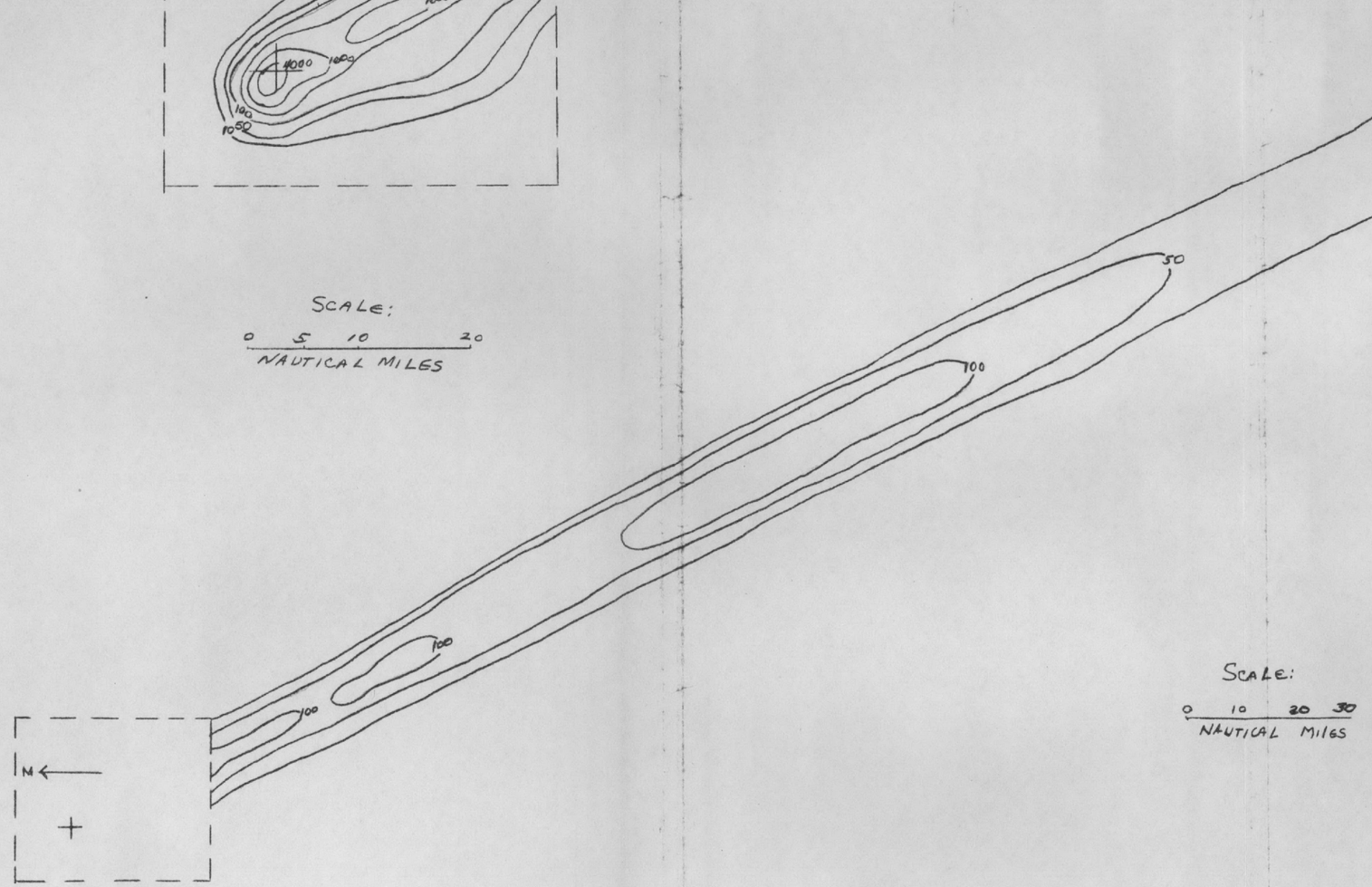

Fig. 21c Dosage from time of arrival to 24 hrs. due to a 1 MT device detonated at Buffalo, New York on June 15, 1953.

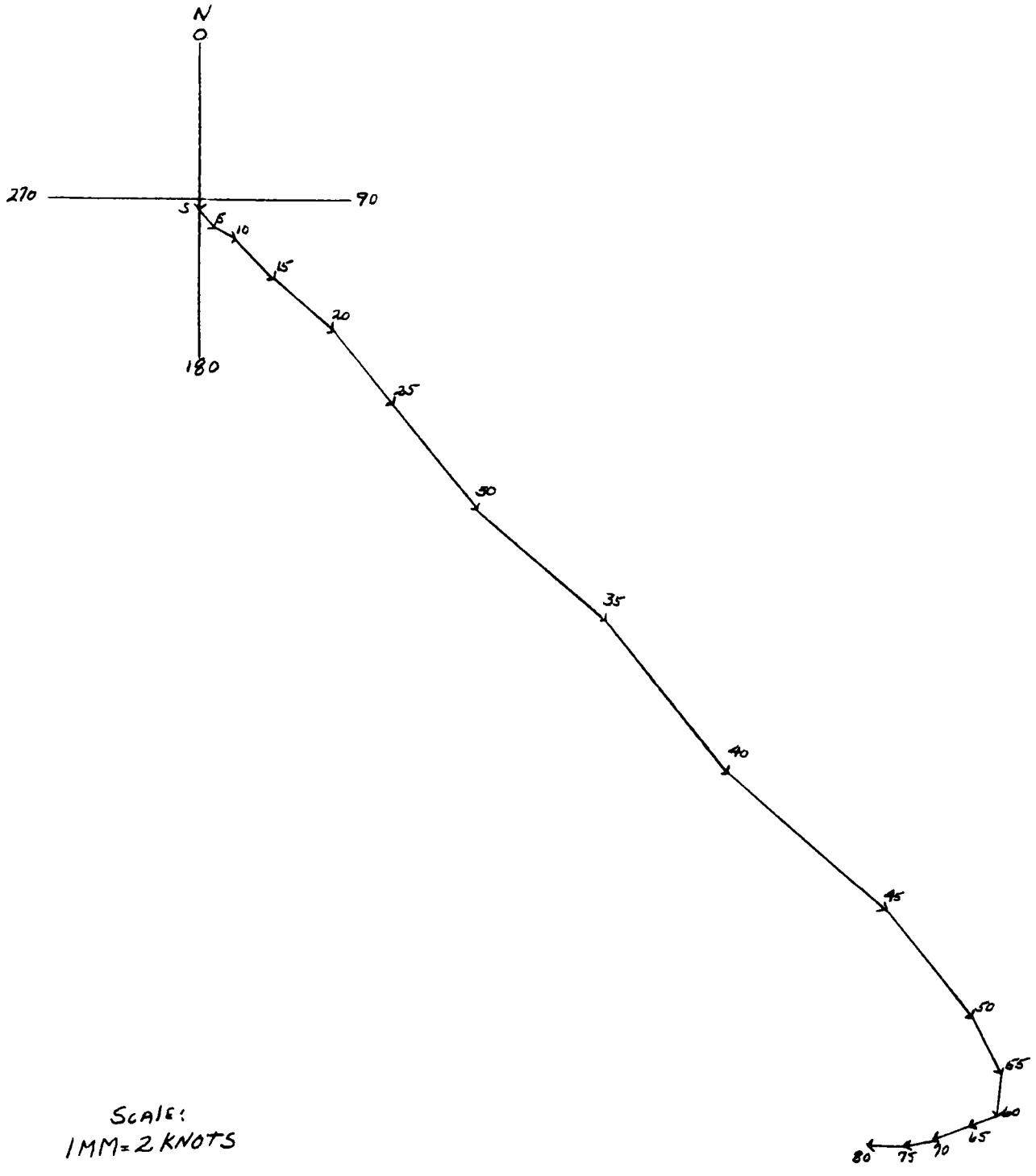

Fig. 22a Hodograph of winds at Buffalo, New York on June 15, 1954.

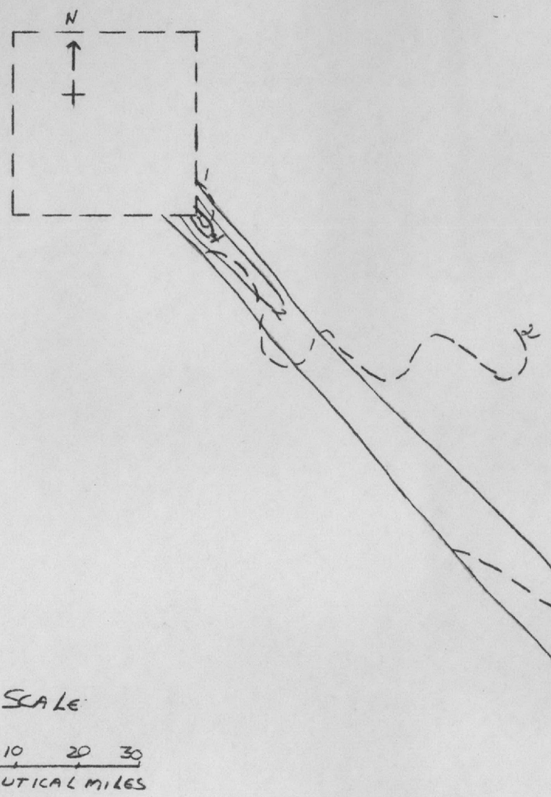

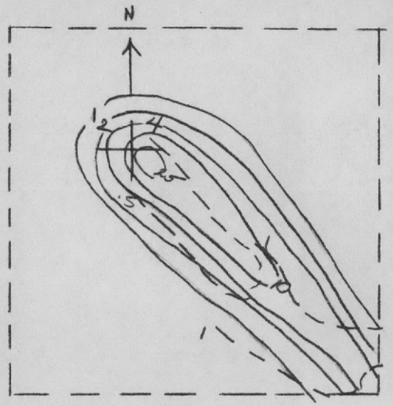

Fig. 22b Dose rate at 24 hours due to a 1 MT device detonated at Buffalo, New York on June 15, 1954 with approximate mean arrival times.

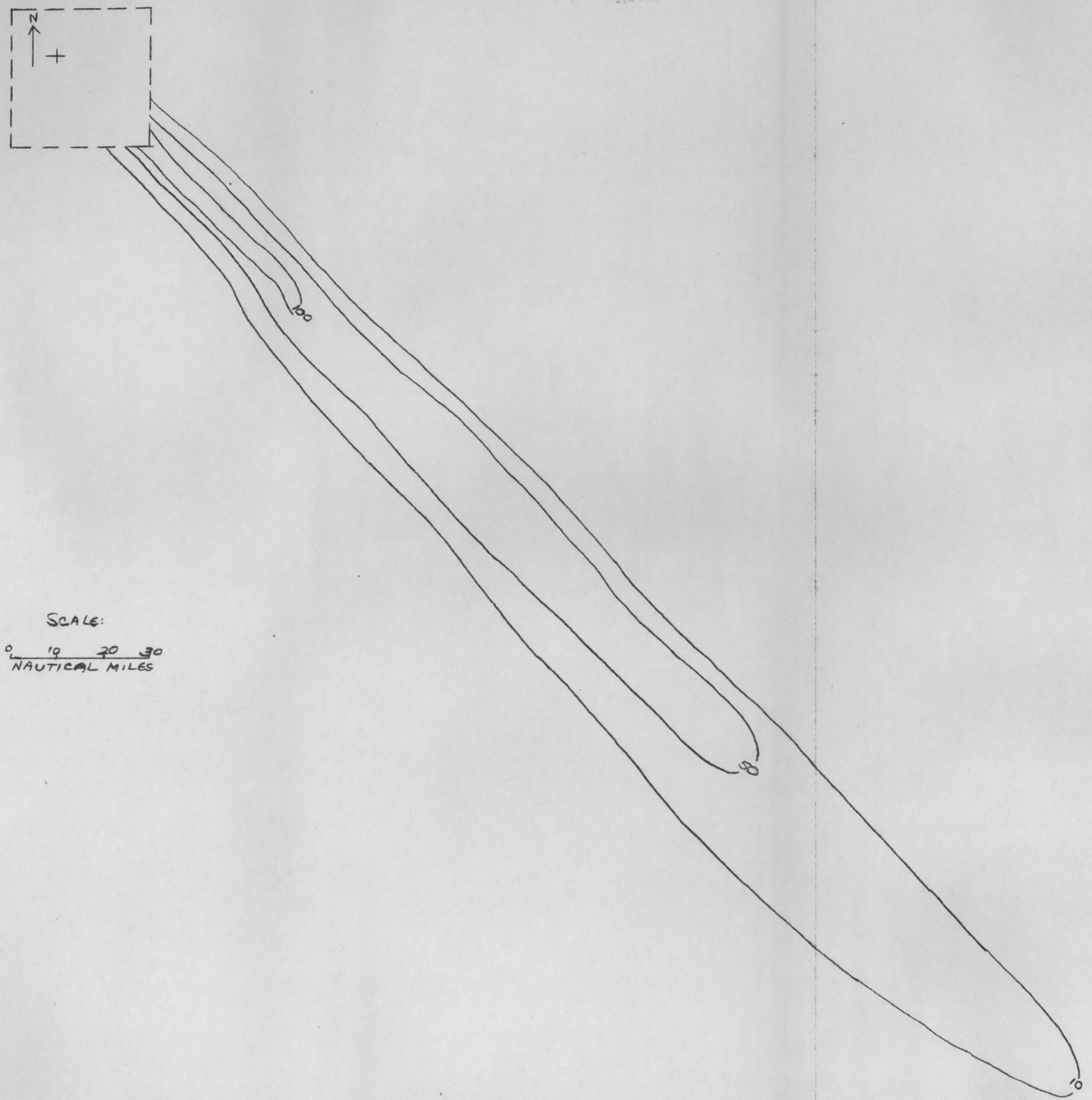

Fig. 22c Dosage from time of arrival to 24 hrs. due to a 1 MT device detonated at Buffalo, New York on June 15, 1954.

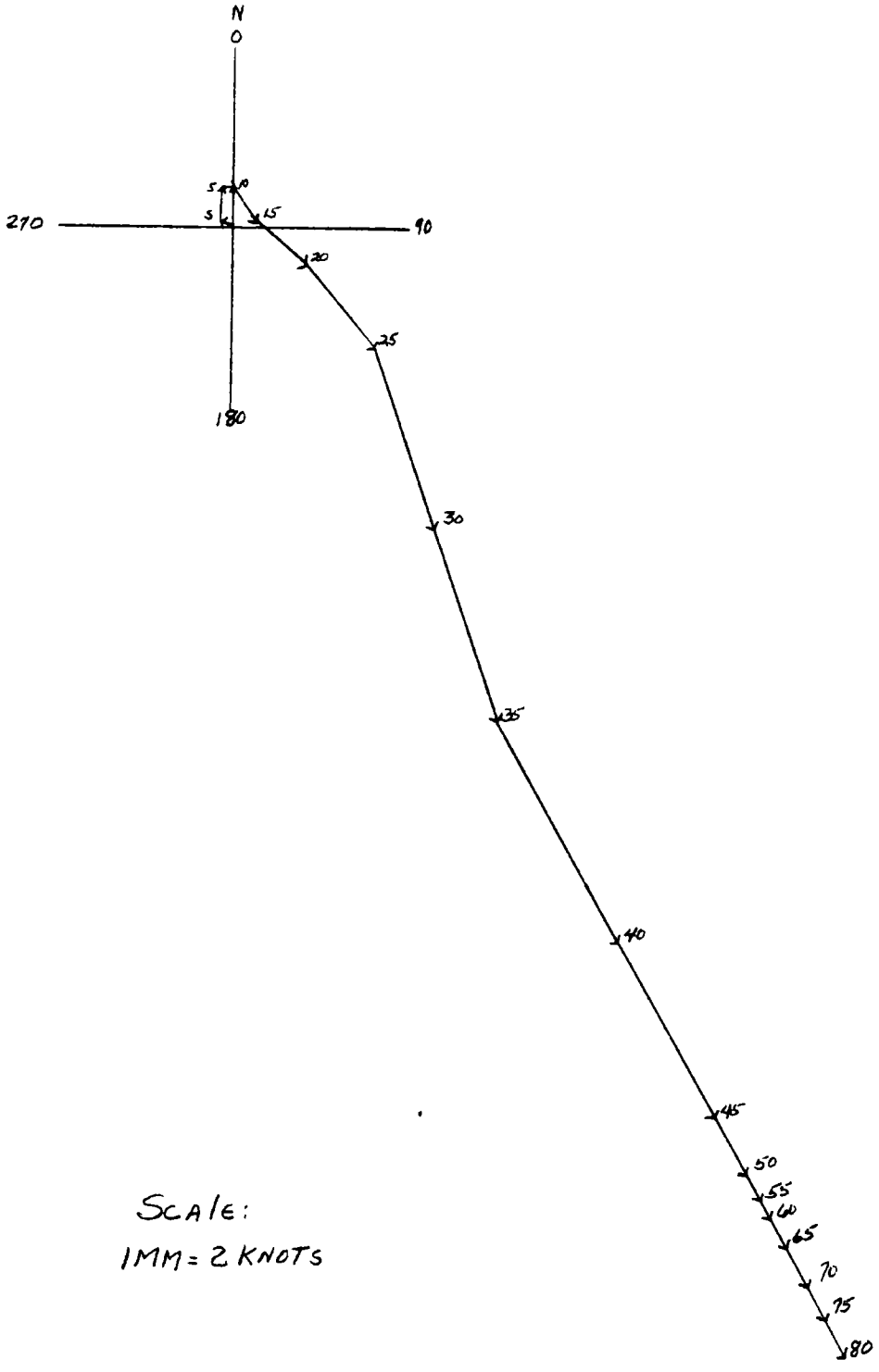

Fig. 23a Hodograph of winds at Cleveland, Ohio on June 15, 1953.

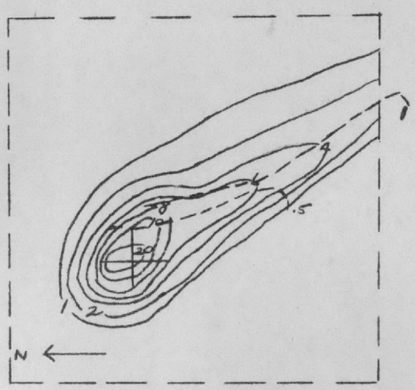

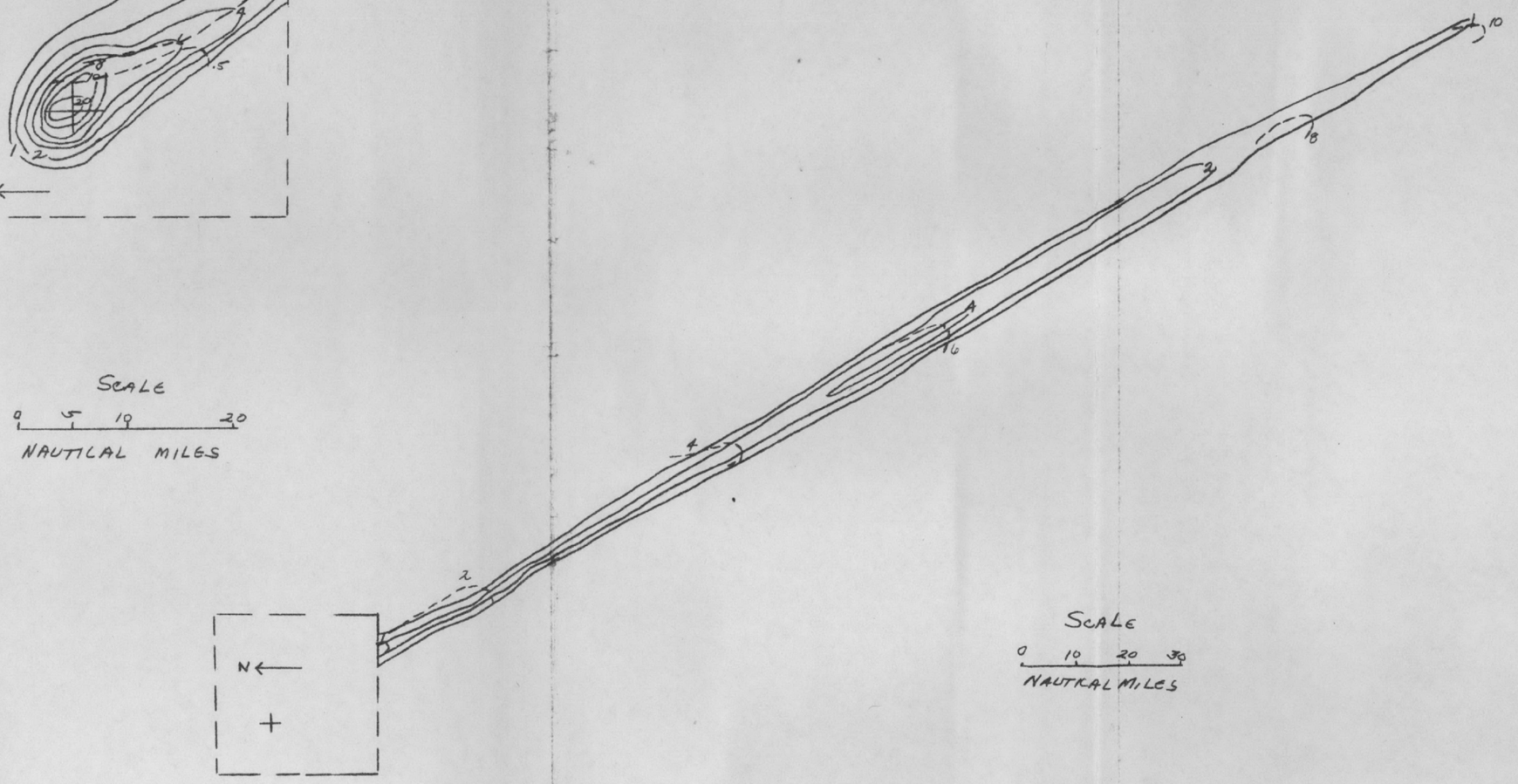

Fig. 23b Dose rate at 24 hours due to a 400 KT device detonated at Cleveland, Ohio on June 15, 1953 with approximate mean arrival times.

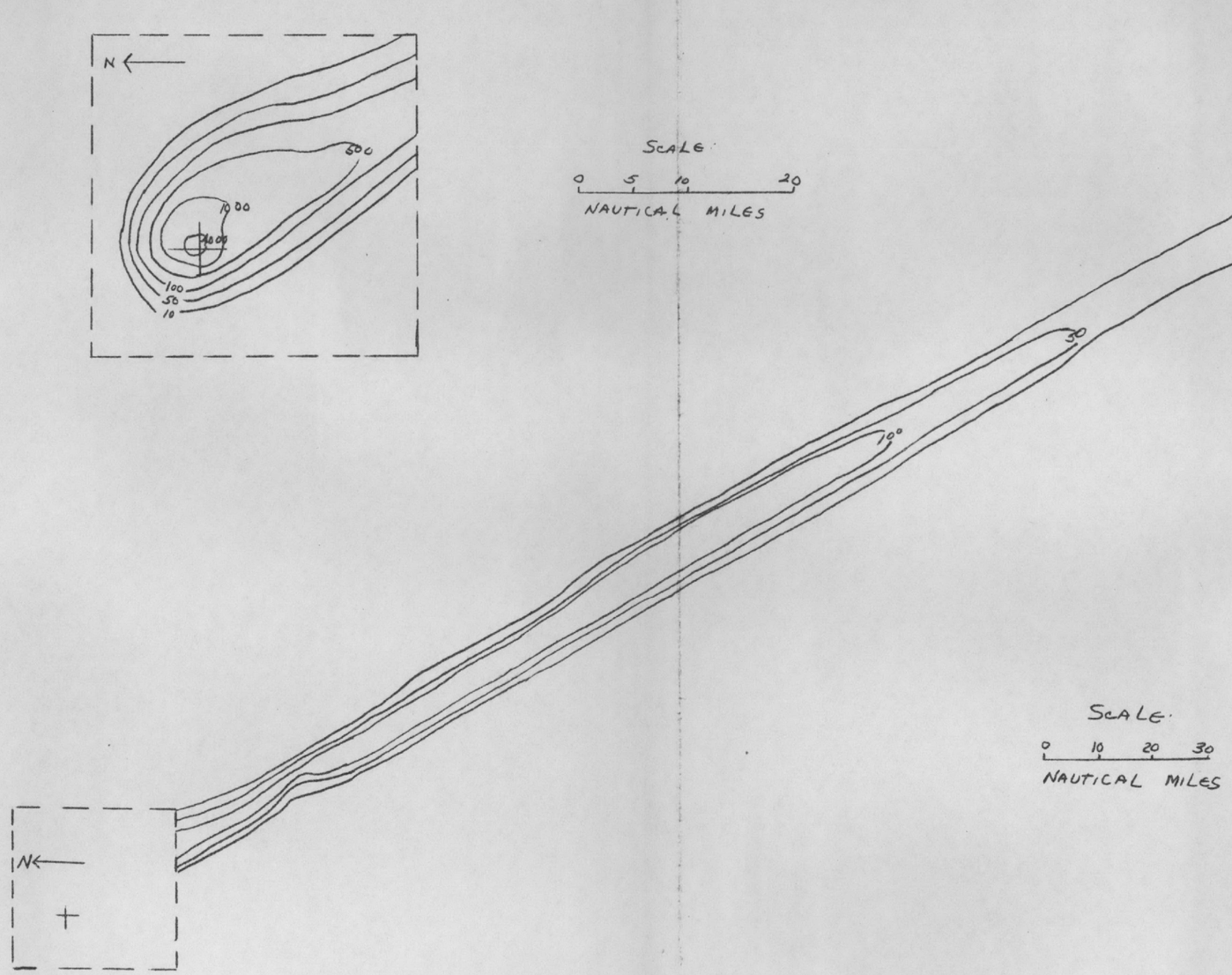

Fig. 23c Dosage from time of arrival to 24 hrs. due to a 400 KT device detonated at Cleveland, Ohio on June 15, 1953.

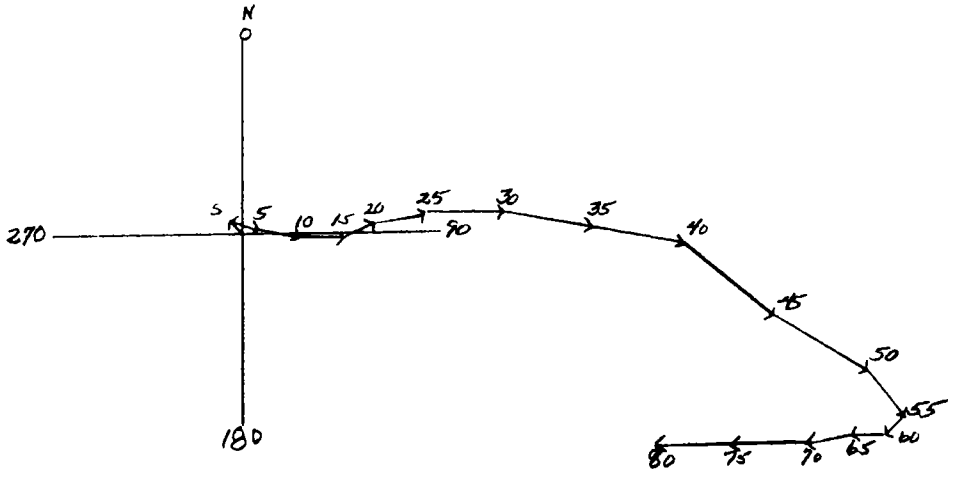

Scale:
1MM=2 KNOTS

Fig. 24a Hodograph of winds at Cleveland, Ohio on June 15, 1954.

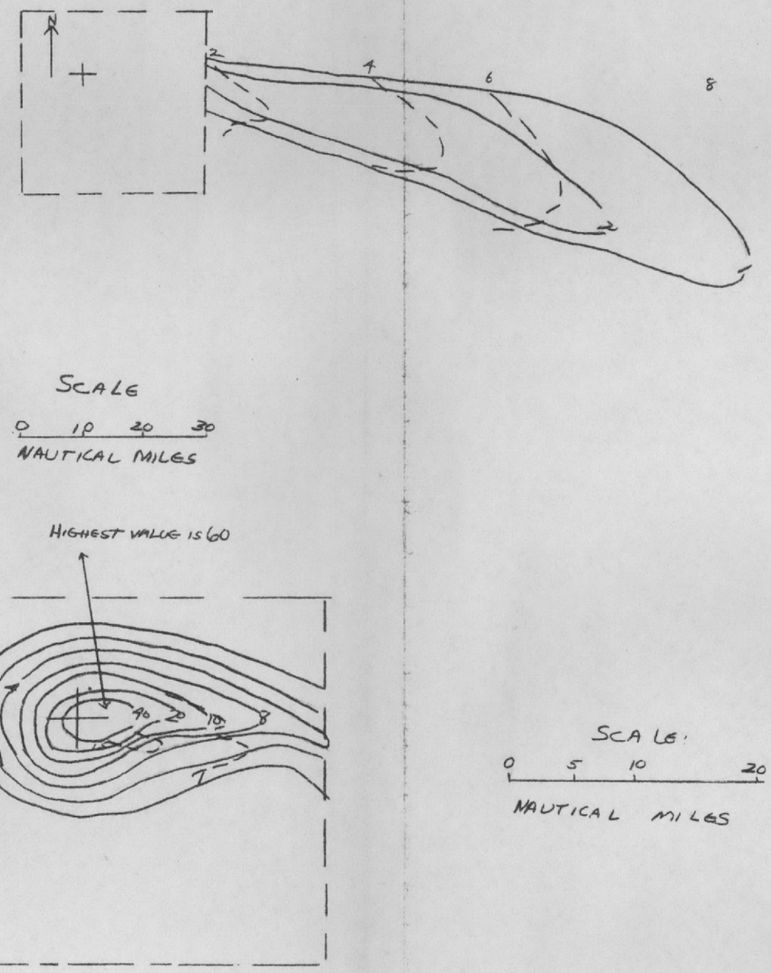

Fig. 24b Dose rate at 24 hours due to a 400KT device detonated at Cleveland, Ohio on June 15, 1954 with approximate mean arrival times.

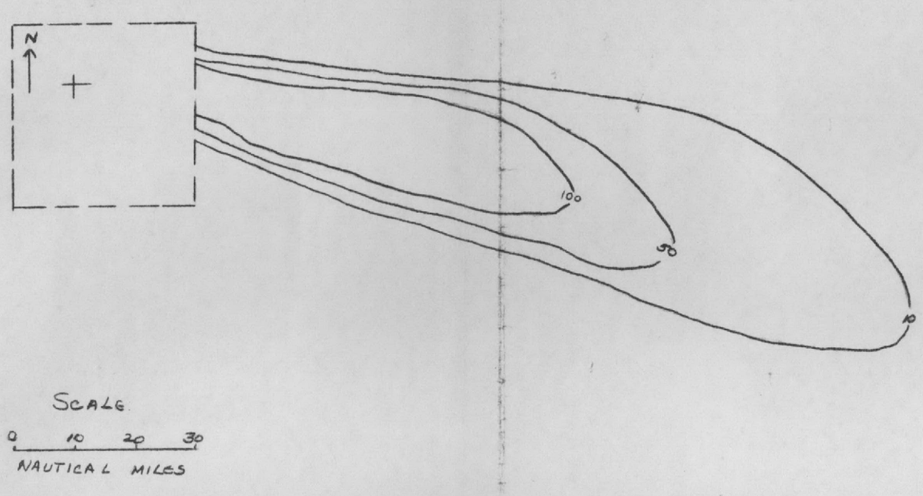

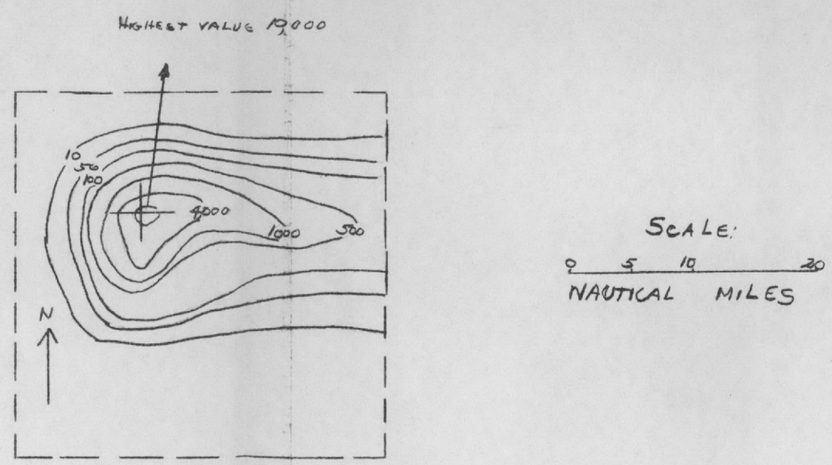

Fig. 24c Dosage from time of arrival to 24 hrs. due to a 400 KT device detonated at Cleveland, Ohio on June 15, 1954.

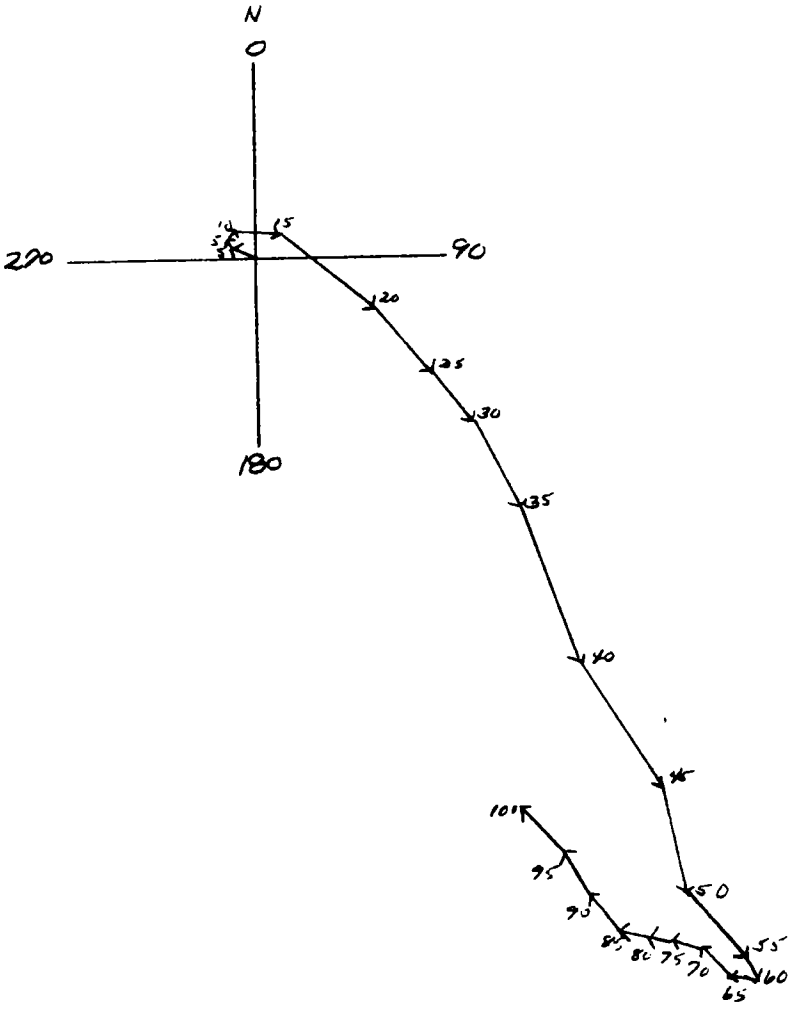

SCALE:

1MM = 2 KNOTS

Fig. 25a Hodograph of winds at Gary, Indiana on June 15, 1953.

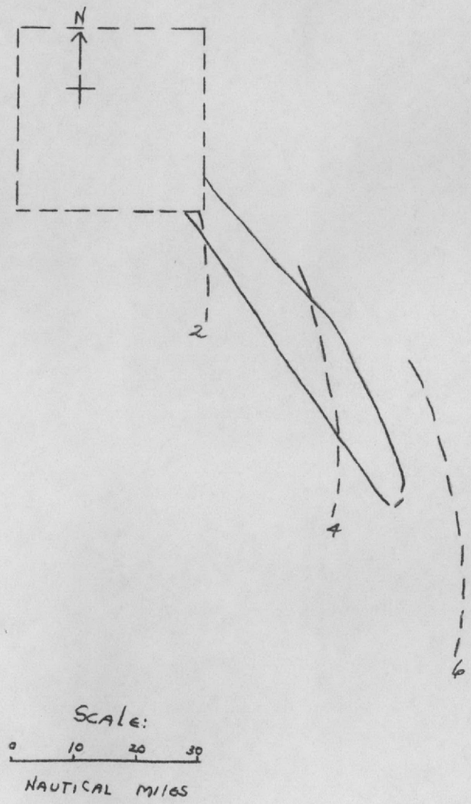

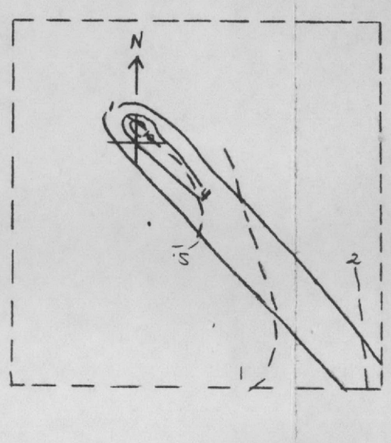

Fig. 25b Dose rate at 24 hours due to a 100 KT device detonated at Gary, Indiana on June 15, 1953 with approximate mean arrival times.

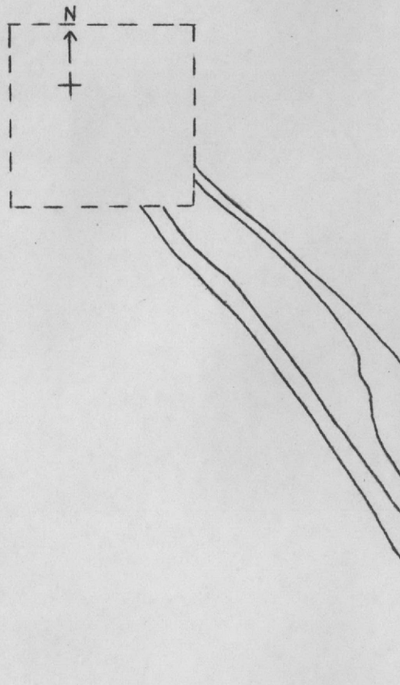

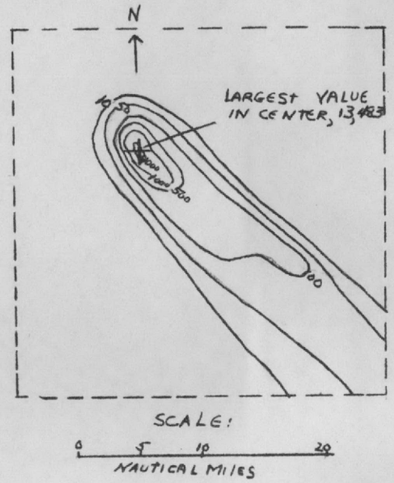

Fig. 25c Dosage from time of arrival to 24 hrs. due to a 100 KT device detonated at Gary, Indiana on June 15, 1953.

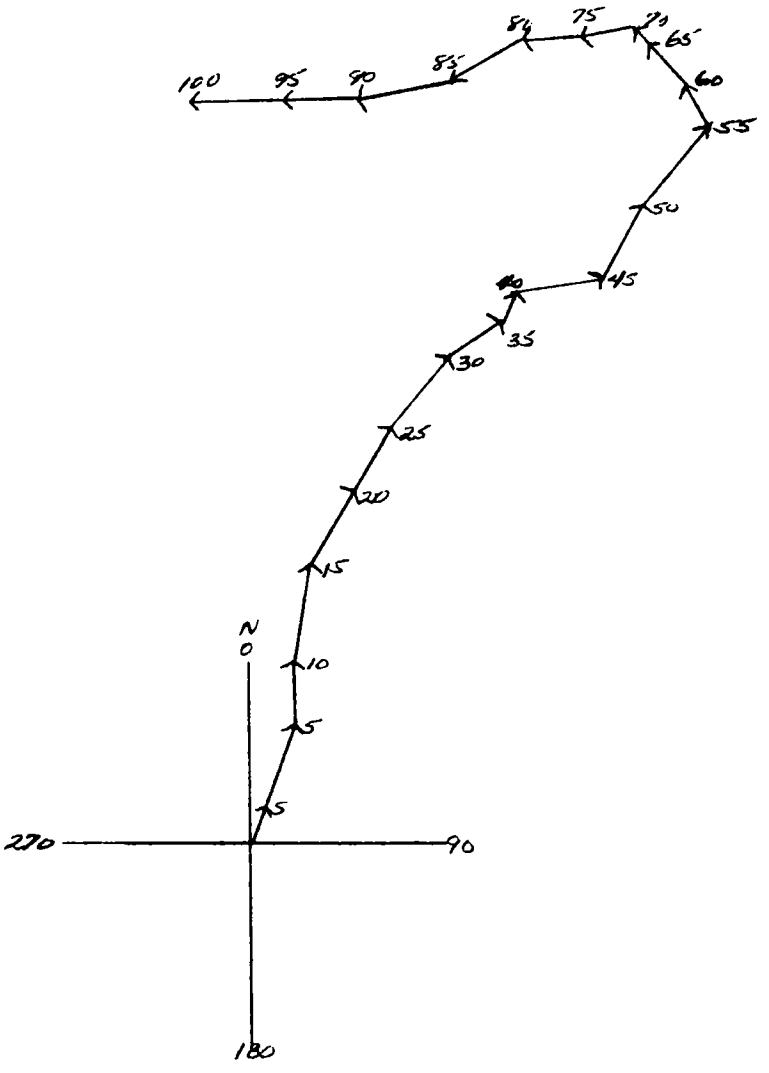

SCALE
1mm = 2 KNOTS

Fig. 26a Hodograph of winds at Gary, Indiana on June 15, 1954.

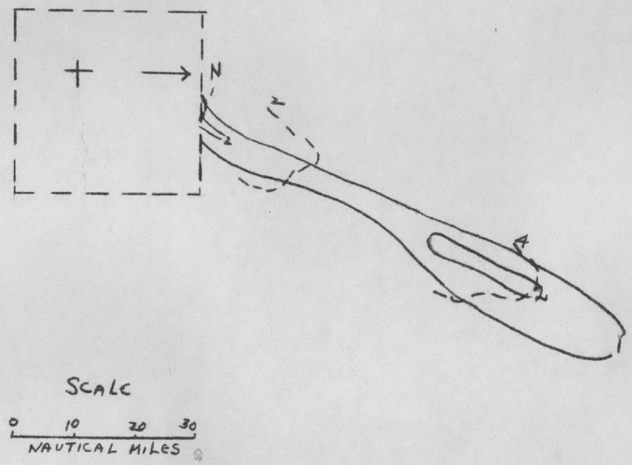

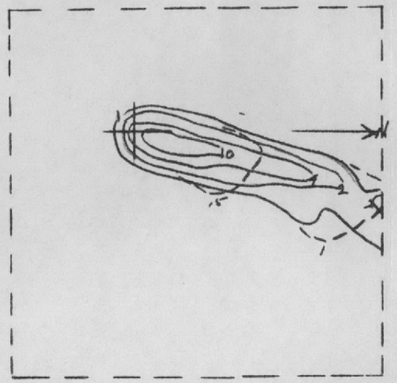

Fig. 26b Dose rate at 24 hours due to a 100 KT device detonated at Gary, Indiana on June 15, 1954 with approximate mean arrival times.

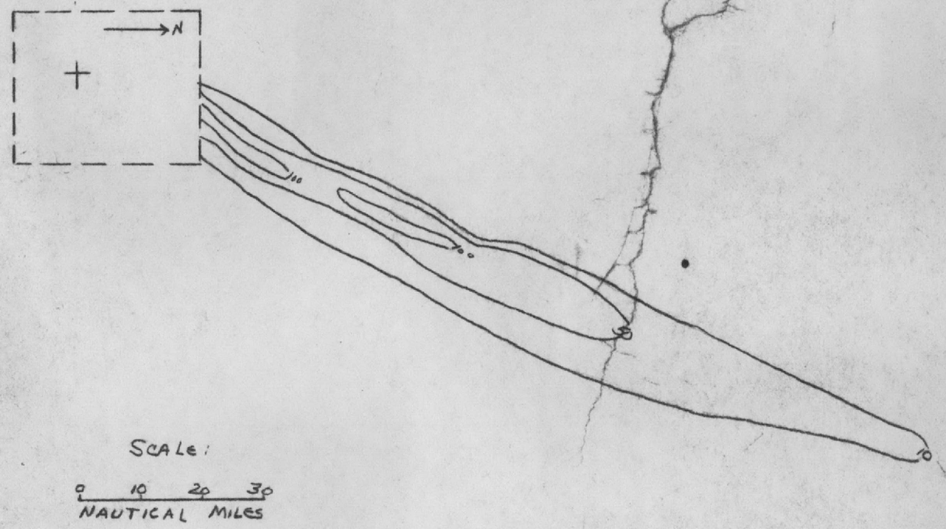

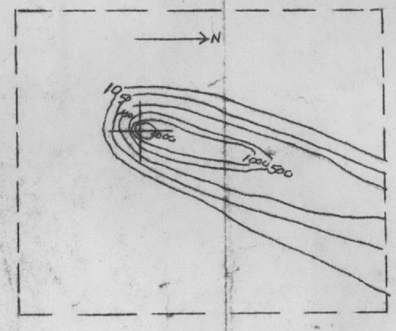

Fig. 26e Dosage from time of arrival to 24 hrs. due to a 100 KT device detonated at Gary, Indiana on June 15, 1954.

Index of wind-structure patterns

(approximately to scale)

Winds to 80,000 or 100,000 ft

N

5 MT yield

Fig. 1A - Page 15

Fig. 2A - Page 18

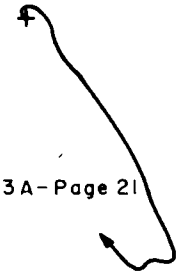

Fig. 3A - Page 21

Fig. 4A - Page 24

1 MT yield

Fig. 5A - Page 27

Fig. 6A - Page 30

Fig. 7A - Page 33

Fig. 8A - Page 36

Fig. 9A - Page 39

Fig. 10A - Page 42

Fig. 11A - Page 45

Fig. 12A - Page 48

Fig. 13A - Page 51

Fig. 14A - Page 54

Fig. 15A - Page 57

Fig. 16A - Page 60

Fig. 17A - Page 63

Fig. 18A - Page 66

Fig. 19A - Page 69

Fig. 20A - Page 72

Fig. 21A - Page 75

Fig. 22A - Page 78

400 KT yield

Fig. 23A - Page 81

Fig. 24A - Page 84

100 KT yield

Fig. 25A - Page 87

Fig. 26A - Page 90